



Durham E-Theses

Some aspects of the cosmic ray origin problem

Freedman, Immanuel

How to cite:

Freedman, Immanuel (1985) *Some aspects of the cosmic ray origin problem*, Durham theses, Durham University. Available at Durham E-Theses Online: <http://etheses.dur.ac.uk/7115/>

Use policy

The full-text may be used and/or reproduced, and given to third parties in any format or medium, without prior permission or charge, for personal research or study, educational, or not-for-profit purposes provided that:

- a full bibliographic reference is made to the original source
- a [link](#) is made to the metadata record in Durham E-Theses
- the full-text is not changed in any way

The full-text must not be sold in any format or medium without the formal permission of the copyright holders.

Please consult the [full Durham E-Theses policy](#) for further details.

SOME ASPECTS OF THE COSMIC RAY
ORIGIN PROBLEM

by

Immanuel Freedman B.Sc. (Hon.) Dunelm

The copyright of this thesis rests with the author.
No quotation from it should be published without
his prior written consent and information derived
from it should be acknowledged.

A thesis submitted for the Degree of
Doctor of Philosophy in the University of Durham
November 1985



15. APR. 1986

Theris
1985/FRE

To my parents

"After all, when the historians of science look back on our times with the perspective of the years, all that we do today will certainly be seen to have been wrong, or irrelevant, or obvious."

G.H. Herbig in Star Formation, I.A.U. Symp.
75, 289 (T. de Jong and A. Maeder , eds.)
(Reidel : Dordrecht 1977).

ABSTRACT

The central contribution of this thesis is a detailed study of cosmic ray acceleration in collapsing gas clouds. The conditions for cosmic ray enhancement in collapsing rotating magnetised clouds during Galaxy formation, cloud formation and subsequent star formation are assessed. The thesis continues with a critical review of antiproton origin models, together with an assessment of the extragalactic origin model in terms of the putative Galactic Wind. The thesis finishes with an assessment (and dismissal) of the Galactic Wind terminal shock hypothesis for the origin of the highest energy cosmic rays.

The principal conclusion is that the collapse of a gas cloud can yield enhanced cosmic ray flux up to the highest observed enhancement (Carina Nebula). Up to a few percent of Galactic or extragalactic cosmic rays below 10^{15} eV/nucleon may originate this way (a firm upper limit is $\sim 10^{21}$ eV/nucleon). The new model helps to explain the paucity of short pathlengths and somewhat increases the maximum accelerated cosmic ray energy during Supernova shock acceleration of ambient cosmic rays. The model predicts that the luminosity maximum should be from the molecular cloud (not HII region) in the Carina Nebula (for > 100 MeV gamma rays) and that there may be regions of reduced luminosity in the gamma ray sky observable with detectors planned for the future Gamma Ray Observatory.

PREFACE

The work performed in this thesis is primarily my original research. After an Introductory Chapter (1), there follows a detailed study of fast particle acceleration in collapsing gas clouds. This study was suggested and supervised by Prof. A.W. Wolfendale. Starting from his initial idea, I searched for and developed a model which adequately explains the enhancement of Cosmic Ray flux above 1 GeV/nucleon observed in some gas clouds. This work comprises Chapters (2) and (3). The effects of time-dependence, adiabatic and shock acceleration, energy-loss, cloud gravitation and rotation, Cosmic Ray scattering, pressure and magnetic pinch-effect escape time-scale are explicitly evaluated, together with the energy budget for adequate Cosmic Ray confinement. A simple model of a collapsing cloud is used to evaluate the hydrodynamical effects. These results are then applied to Galactic and protogalactic phenomena and checked against available satellite data. The application to Supernova-shock acceleration of cosmic rays in a cloudy interstellar medium is outlined.

Chapter (4) is partly review, partly original research. Some previous models of antiproton origin are critically discussed, an extragalactic version of the neutron-oscillation antiproton origin scenario assessed (and dismissed) and the effects of a putative Galactic Wind on the supposed extragalactic antiproton spectrum observed at earth evaluated and discussed. This chapter finishes with a detailed assessment of the Galactic terminal shock scenario for the acceleration of highest energy Cosmic Rays.

This thesis is not substantially the same as any other one I have submitted to any other University.

	<u>CONTENTS</u>	Page
Abstract		i
Preface		ii
1. INTRODUCTION		1
1.1 General description of cosmic rays		1
1.1.1 Discovery		1
1.1.2 Mass composition		1
1.1.3 Anisotropy		10
1.2 General remarks about the origin problem		13
1.2.1 Basic Galactic vs. Extragalactic p origin		13
1.2.2 Acceleration mechanisms		20
1.3 Format of the thesis		21
1.4 Summary and Conclusions		21
2. CAN COSMIC RAYS BE ACCELERATED IN COLLAPSING MOLECULAR CLOUDS? (PART I)		22
2.1 Introduction		22
2.2 Models of a Collapsing Cloud		25
2.2.1 Cold spherical cloud in free fall		25
2.2.2 Cold spherical imploding cloud		36
2.3 Escape of Cosmic Rays from the Cloud		39
2.3.1 Confinement by straight-line transit time		39
2.3.2 Confinement by magnetic scattering on resonant Alfven waves		39
2.3.3 Cold spherical magnetized rotating cloud		48
2.3.4 Is there any evidence for enhanced magnetic fields in clouds?		58
2.3.5 Cooling of external ambient cosmic rays		60
2.4 Summary and Conclusions		63
3. CAN COSMIC RAYS BE ACCELERATED IN COLLAPSING MOLECULAR CLOUDS? (PART II)		64
3.1 Introduction		64
3.2 Shock Acceleration of Cosmic Rays trapped inside the cloud		64
3.2.1 The effect of proton pressure on the collapse		77
3.3 Comparison of Model Predictions with Gamma- Ray observations		79

	Page
3.3.1 Comparison of Model Predictions with Gamma-Ray Observations	79
3.3.2 Are there point-like regions of reduced cosmic ray intensity?	82
3.4 Implications for Galactic and Proto-galactic Proton Origin	84
3.5 Summary and Conclusions	87
4. ANTIPROTON ORIGIN MODELS	88
4.1 Introduction	88
4.2 Brief Summary of Experimental Situation	88
4.3 Solar Modulation	90
4.4 Previous Origin Models	92
4.4.1 What is the secondary \bar{p} production cross-section?	93
4.4.2 Shrouded CR source models	93
4.4.3 Stochastic acceleration models	95
4.4.4 Non-annihilation inelasticity deceleration models	96
4.4.5 Secondary \bar{p} origin, cosmological deceleration models	96
4.4.6 Galactic Centre (GC) explosion models	98
4.4.7 Non-uniform Galactic disc models	98
4.4.8 Exotic models	98
4.5 Modulation of Extragalactic Spectra by Galactic Wind	103
4.5.1 Solution of the transport equation	106
4.5.2 Escape of \bar{p} from anti-galaxies	107
4.5.3 Constraints on q	110
4.6 Modulation of Galactic Spectra by Galactic Wind	116
4.7 Acceleration of High Energy Particles at Galactic Wind Terminal Shock?	121
4.7.1 Implications for Extragalactic \bar{p} Origin	127
4.7.2 Implications for the model of the Galactic Wind	127
4.8 Summary and Conclusions	127

	Page
5. SUMMARY AND CONCLUSIONS	129
5.1 Suggested Future Work	130
Appendix A	
Release of Gravitational Energy During Cloud Contraction	131
Appendix B	
Solution of the time-dependent transport equation	132
Appendix C	
When does magnetic flux-freezing hold?	133
Acknowledgements	135
References	136
List of Publications	147
Papers	

LIST OF ILLUSTRATIONS

Figure

- 1.1 Summary integral high-energy cosmic ray spectrum presented by Linsley (1980).
- 1.2 The elemental abundance distribution of the cosmic radiation.
- 1.3 Amplitude and phase of the first harmonic anisotropy of cosmic rays.
- 2.1 Gamma-ray fluxes above 100 MeV from local giant molecular clouds divided by our predicted fluxes.
- 2.2 The fraction of total mass contained in Giant Molecular Cloud complexes of mass m per logarithmic interval.
- 2.3 Cosmic ray enhancement v. Cloud density.
- 2.4 Cosmic ray enhancement v. Time.
- 2.5 Cosmic ray enhancement v. Cloud density.
- 2.6 Cloud density v. Time.
- 2.7 The run of energy at which CR protons become inertially confined.
- 2.8 Diffusion escape time-scale and remaining time to complete collapse v. Cloud density.
- 2.9 Collapse of a magnetized cloud.
- 2.10 Pinch effect escape timescale and remaining time to complete collapse v. Cloud density.
- 2.11 Ratio of acceleration to loss or (pinch-effect) escape rate.
- 2.12 Upper limit to Cosmic Ray energy density v. Cloud density.
- 2.13 Magnetic field v. HI density.
- 2.14 Schematic gas density distribution for a collapsing gas cloud.
- 3.1 Enhancement of cosmic ray intensity v. Cloud density.
- 3.2 Density and velocity distributions shortly after the formation of a stellar core.
- 3.3 Collapse of a magnetized cloud core.
- 3.4 Upper limit the enhancement of cosmic ray intensity v. Cloud density.

- 3.5 Enhancement of cosmic ray intensity v. Cloud density.
- 3.6 Enhancement factors for some nearby clouds, organized by cloud total mass.
- 4.1 Secondary antiproton flux predictions.
- 4.2 Comparison of various predicted \bar{p} fluxes with experimental data.
- 4.3(a) The nonuniform Galactic disc model
(b) The predicted \bar{p} fluxes for that model.
- 4.4 The effect of extragalactic primary protons and antiprotons on the total cosmic ray spectrum.
- 4.5 The simple model of the Galaxy.
- 4.6 Predictions of \bar{p} intensity v. \bar{p} kinetic energy.
- 4.7 Escaping antiproton spectra for various conditions.
- 4.8 Predictions of \bar{p} intensity v. \bar{p} kinetic energy.
- 4.9 Gravitational acceleration perpendicular to the Galactic plane.
- 4.10 Adiabatic deceleration/acceleration of Galactic secondary \bar{p} by Galactic Winds.
- 4.11 Modulation of Galactic protons by Galactic winds.
- 4.12 Adiabatic deceleration/acceleration of Galactic secondary electrons by Galactic winds.
- 4.13 Adiabatic deceleration/acceleration of Galactic secondary positrons by Galactic winds.
- 4.14 The Galactic Halo model of Jokipii and Morfill (1985).

LIST OF TABLES

Table

- 1.1 Energy Densities of 'Cosmic' Components near the Earth.
- 1.2 Table of Source Models.

CHAPTER 1

1. Introduction

1.1 General description of cosmic rays

1.1.1 Discovery. Cosmic Rays (CR) are penetrating charged particles of kinetic energy greater than 100 MeV, raining down on the earth.

CR were discovered in balloon experiments with electroscope ionisation chambers; a decrease in dark-current being observed up to 1 km above the earth's surface followed by an increase with height between 1 and 5 km (Hess 1912). The (zinc) chambers were sufficiently thick to exclude alpha and beta-radiation from the atmosphere, and the gamma-radiation from radioactivity in the earth's crust should have been attenuated considerably (attenuation grammage $\sim 50\text{g cm}^{-2}$). After analysing carefully the natural sources of ionisation in air and the balloon environment, and checking the gamma-ray attenuation grammage in air, Hess (1912) concluded that a penetrating 'radiation' was coming through the atmosphere from above (Hillas 1972, monograph). Many other experiments (e.g. Millikan and Bowen 1926, Millikan and Otis 1926, Millikan and Cameron 1926) confirmed these results.

1.1.2 Mass composition. We do not consider, in detail, those components of terrestrial ('Secondary CR') or Solar origin (particles from Solar flares or Solar wind). The 'Secondary CR' result from nuclear interactions between the Primary CR (those observed at



the top of the earth's atmosphere or above) and nuclei of the earth's atmosphere. The PCR were initially identified with ultra hard gamma-rays produced above the atmosphere. The discovery that the paths of CR were affected by the earth's magnetic field (Clay 1932, experiments from 1927 to 1932) showed the bulk of the incident radiation to be charged. The small ($\approx 10\%$) excess of particles from West over East of zenith at $\sim 45^\circ\text{N}$ latitude, observed by several workers, indicated that the majority of particles were positive and not secondary to gamma-ray materializations in the magnetic field of nuclei of atoms of the earth's atmosphere. The discovery of a very small flux (2×10^{-6} of total) of genuine gamma-rays above 100 MeV awaited the satellite experiments of OSO-III (Kraushaar et al. 1972), SAS-II (Fichtel et al. 1975; other papers) and COS-B (e.g. Bennett et al. 1977). The topic of gamma-ray astronomy includes low-energy (keV band), nuclear lines, e^+e^- annihilation radiation, the medium-to-high energy (35 to 100 MeV band, electron-bremsstrahlung and some π^0 -decays contribute), high-energy (100 to 500 MeV band, π^0 -decay and pulsar radiation ...) and ultra-high energy ($> 10^{12}$ eV band, Gibson et al. 1982, γ 's from Cyg X-3; 10^{15} - 10^{16} eV sections of the electromagnetic spectrum).

Gamma-ray astronomy is reviewed by e.g. Hillier (1984), and Wolfendale (1983).

Many experiments have gradually revealed the CR mass composition. Balloons, rockets, satellites and particle-counting arrays (Extensive Air Shower arrays,

EAS) have all contributed, at various energies.

Figure 1.1 shows a summary integral energy spectrum of high-energy Cosmic Rays presented by Linsley (1980, review). The (approximate) range of energy in which each technique just mentioned appears useful is: 10^8 to 10^{11} eV (Satellites), 10^8 to 10^{12} eV (Balloons), 10^8 to 10^{14} eV (Indirect methods, EAS, muons), 10^{14} eV onwards (EAS). Note that EAS experiments determine the total energy of the primary, not energy/nucleon. The spectral index at $\sim 10^8$ eV is $\gamma = -2.6$, steepening to ~ -3.0 at $\sim 10^{14.5}$ eV (Nagano et al. 1984).

The power-law spectrum (energy or rigidity) of CR protons may continue in interstellar space below $\sim 10^8$ eV/nucleon to ~ 40 MeV/nucleon (not known experimentally) where ionisation losses become important.

The non-thermal spectrum includes ionising ~ 1 MeV/nucleon particles: but their penetration into (or origin in) gas clouds is uncertain. The ionisation rate spatially averaged over a cloud has been measured in a few cases, and depends on ion-molecule chemistry. Analyses of HD in diffuse clouds suggest rates $\dot{\gamma} \sim 10^{-17} n_H \text{ cm}^{-3} \text{ s}^{-1}$ for clouds with column density $N_H \sim 10^{21} \text{ cm}^{-2}$ (Hartquist et al. 1980) or $\dot{\gamma} \sim 10^{-18} n_H \text{ cm}^{-3} \text{ s}^{-1}$ for the dense clouds with $n_H \sim 10^6 \text{ cm}^{-3}$ (Hartquist and Dalgarno 1980).

If that ionisation is entirely due to ~ 1 MeV CR protons in partly-ionised hydrogen, their rate of energy loss would be

$$-\left(\frac{d\bar{E}}{dt}\right)_i = 7.62 \times 10^{-9} Z^2 n_e \sqrt{\frac{Mc^2}{2E_k}} \left\{ 11.8 + \ln\left(\frac{E_k}{Mc^2}\right) \right\} \text{ eV/sec.}$$

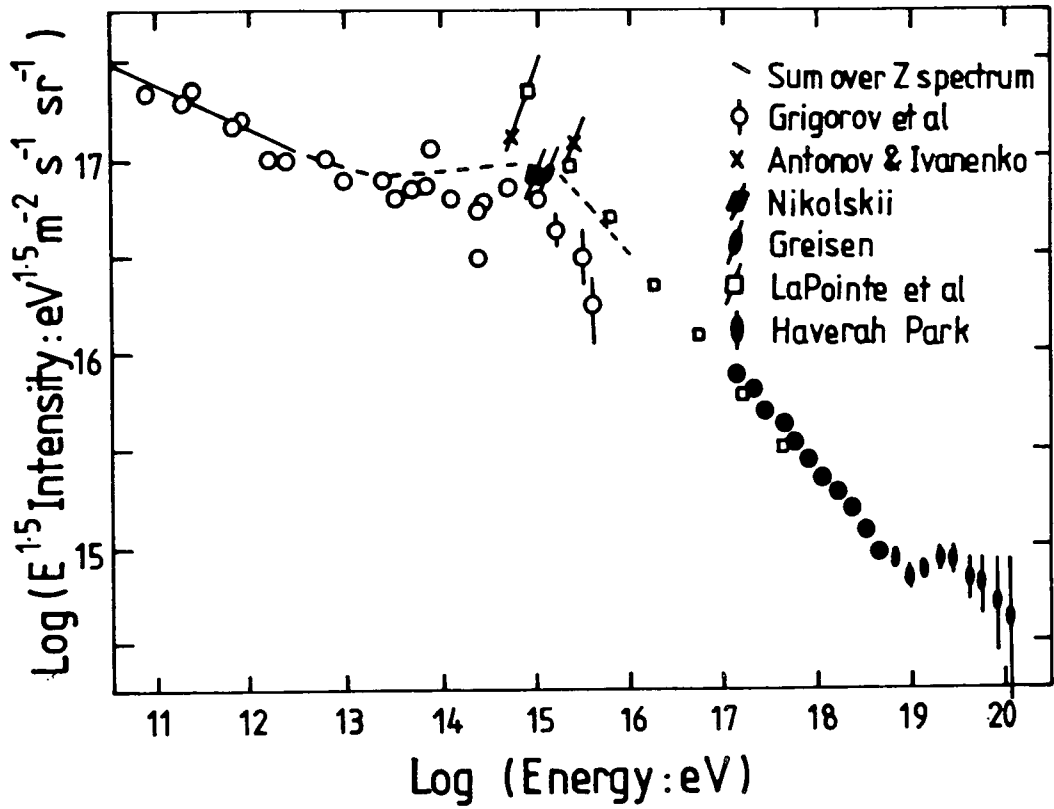


Fig. 1.1 Summary integral high-energy cosmic ray spectrum presented by Linsley (1980).

(Ginzburg and Syrovatskii 1969, p.122) ($E_k \ll Mc^2$)
 $Z = 1$, M = proton mass, E_k = proton energy/eV, n_e is the
thermalelectron concentration in the cloud; the geometric
mean ionisation potential is $\sim 15\text{eV}$. The density effect
(Cerenkov emission of plasma waves) is negligible at low
energies $E_k < 10^{11} / \sqrt{n_e}$ eV.

Hence a 1 MeV p in partly-ionised hydrogen generates
 $\sim 5 \times 10^{-10} n_H \text{ ions cm}^{-3} \text{ s}^{-1}$. So upper limits to
the energy density of ~ 1 MeV p averaged over some clouds
are $\sim 2 \text{ eV cm}^{-3}$ ($n_H \sim 10^6$) or $\lesssim 0.2 \text{ eV cm}^{-3}$ ($N_H \sim 10^{21}$).
Table 1.1 shows the energy density at the top of the
atmosphere for all primary CR confirmed to date.

The nuclear component dominates ($\sim 99\%$ of total),
the remaining $\sim 1\%$ being made up of relativistic electrons
(e.g. Cummings et al. 1975, Meegan and Earl 1976), positrons
(Buffington et al. 1974), and antiprotons (Golden et
al. 1979, Bogomolov et al. 1979, Buffington et al. 1981a,
1981b). The ratio of directly detected positrons to that
of both electrons and positrons is about 0.3 at 0.1 GeV
and again at 10 GeV, with a broad (~ 1 GeV) minimum
of $\lesssim 0.01$ at total energy $E \sim 9$ GeV (Buffington et al.
1974).

Recently, the relative abundance of elements in
the CR has become clear (Meyer 1978, 1980, reviews) at
low energies, at least, and all elements from ^1H to ^{92}U
have been observed. The mass and energy resolution of
the particle-counting telescopes has improved steadily
(cf. University of Chicago IMP series, ISEE-3 and Danish-
French HEAO-3 satellites), but isotope separation beyond

TABLE 1.1

Component		Energy Density (eV cm ⁻³)
Charged primaries (from summary by Wolfendale, 1973)	above 10 ⁹ eV	5.10 ⁻¹
	10 ¹² eV	2.10 ⁻²
	10 ¹⁵ eV	10 ⁻⁴
	10 ¹⁸ eV	10 ⁻⁸
Electrons and positrons (from summary spec- trum of Meyer, 1971)	above 10 ⁹ eV	4.10 ⁻³
	10 ¹⁰ eV	1.10 ⁻³
	10 ¹¹ eV	2.10 ⁻⁴
γ-rays, diffuse background (from summary by Strong et al., 1974)	above 10 ⁷ eV	1.10 ⁻⁵
	above 10 ⁸ eV	2.10 ⁻⁶
Starlight (from Allen, 1973)		4.10 ⁻¹
2.7K Black body radiation		2.4.10 ⁻¹

Energy Densities of 'Cosmic' Components near the
Earth calculated from the expression

$$\epsilon = \frac{4\pi}{c} \int j(E) E dE, \text{ where } j(E) \text{ is the differential}$$

energy spectrum of the appropriate component.
By 'charged primaries' is meant protons and heavier
nuclei.

(Taken from Wolfendale, 1974 ;references therein)

^{56}Fe is still difficult. Figure 1.2 shows the observed abundance of elements $Z \geq 1$ from the IMP4 and 5 experiments relative to standard Solar-system abundances (typical of the earth's crust and Solar photosphere) (Cameron, 1973), normalised to ^{12}C . Earlier work on balloon flights (e.g. Webber et al. 1972, 250 to 850 MeV/nucleon) and IMP-series results (e.g. Garcia-Munoz et al. 1975, 100 to 300 MeV/nucleon; many other papers) is reviewed by Meyer (1978).

It is important to remember that these measurements refer only to quite low kinetic energies at earth (~ 1 GeV/nucleon interstellar) and there is no direct information to date about the CR composition at much higher energies (e.g. $> 10^{12}$ eV/nucleon) where anisotropy measurements are significant. The various nuclide groups are given by Ginzburg and Syrovatskii (1969); p, α , L (Li, Be, B), M (C, N, O, F), H ($Z \geq 10$), VH ($Z \geq 20$).

The L-group nuclides are grossly excessive in the CR by Solar-system standards. Rapidly destroyed in nucleosynthesis (e.g. Clayton 1968), the conclusion is that they are secondary to spallation of primary M group nuclides.

The L/M ratio falls steadily with increasing energy, roughly as $E^{-0.5}$ over the range 1-100 GeV (Meyer 1980).

The meaning of this relation is not so clear: the manner of propagation of the particles and confinement region are uncertain (Wolfendale 1982). It is often taken to suggest that either (1) all CR nuclides are rapidly accelerated before much matter is traversed, or (2) stochastic acceleration and reacceleration through-

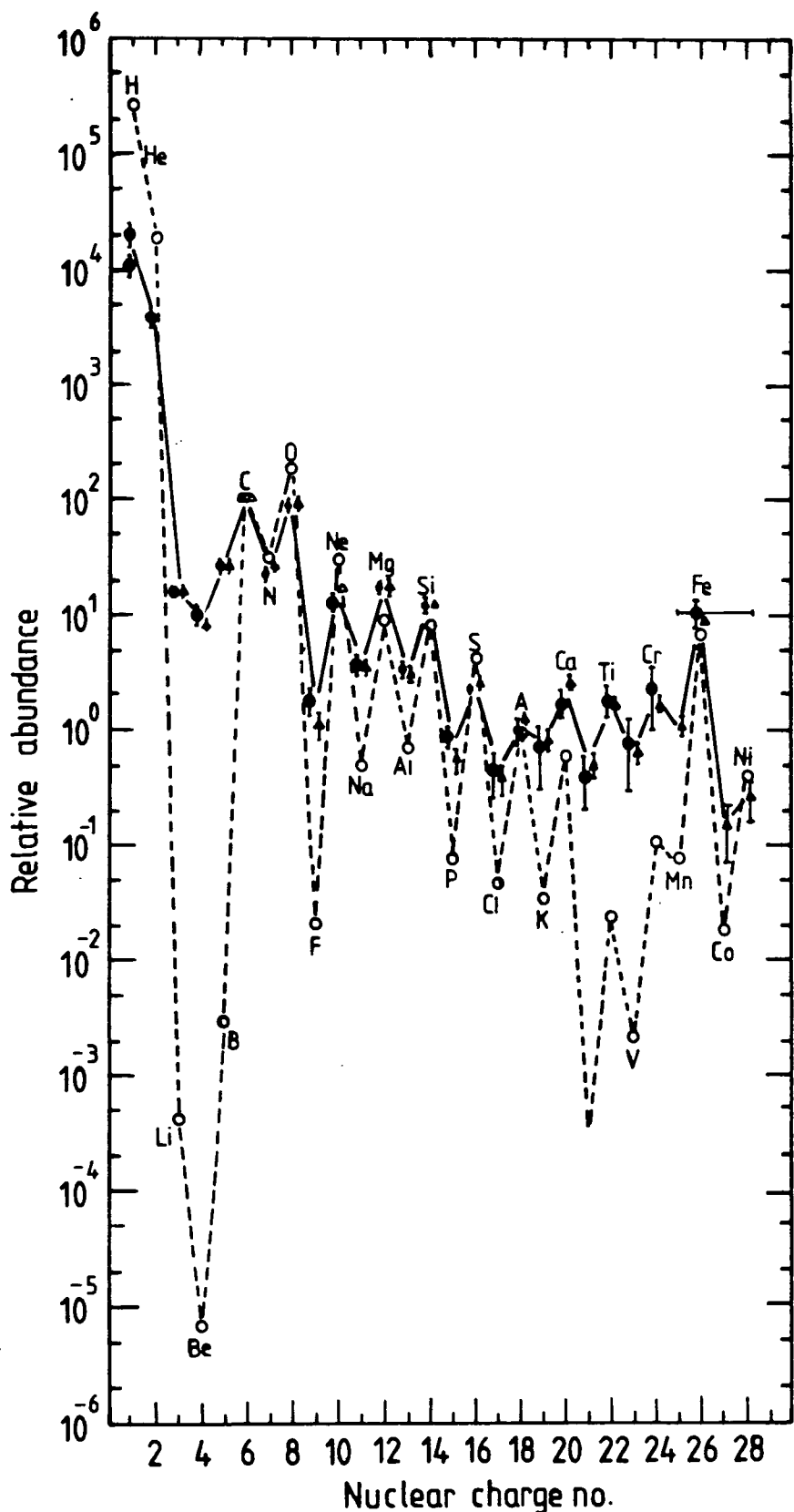


Fig. 1.2 The elemental abundance distribution of the cosmic radiation and the Solar System abundances, normalised to C. ●, Measured by University of Chicago cosmic-ray telescope on board the IMP-4 and IMP-5 satellites from 100 to 300 MeV per nucleon; Δ, Webber et al. from 250 to 850 MeV per nucleon; ○, Solar System of 'universal' abundances (after Meyer 1978).

out the ISM are not significant, as the oldest particles (which have traced most matter) would have the highest energies before escape. In this connection, acceleration at a single shock in the ISM is a case (1) situation; acceleration in the halo of the Galaxy (matter only being traversed in rare entries of CR into the Galaxy, Schlickeiser 1983) falls in case (2) .

Transuranides and islands of stability (e.g. $Z = 126$) have occasionally been claimed, although the results are not clear. The genuine detection of a surprisingly large flux of antiprotons in the primary CR (referred to earlier) is important for understanding of proton origin and propagation : see Chapter 4.

Exotic particles (e.g. relativistic dust grains (Alfvén 1939, Hayakawa 1972), nuclearites and monopoles have sometimes been claimed. The anti-triton reported by Apparao et al. (1983) remains to be confirmed. It is very likely that significant fluxes of neutrons and neutrinos exist in the primary CR, but only Solar neutrinos appear to have been detected to date. Supersymmetry theory predicts new particles in the CR flux ($E > 10^{25}$ eV) - this is open to conjecture and experimentation. The search for tachyons has so far yielded negative results, as has that for free quarks.

CR isotope ratios (e.g. $^{10}\text{Be}/^{7+9}\text{Be}$, Garcia-Munoz et al. 1975, 1977) have proved useful, in that they probe (a) The escape lifetime ($t_{\text{esc}} \gtrsim 10^8$ years at ~ 1 GeV/nucleon interstellar, model dependent) of CR nuclei (e.g. Jones 1979, Freedman et al. 1979, 1980).

(b) The CR source composition via anomalies: studies of the $^{22}\text{Ne}/^{20}\text{Ne}$, $^{26}\text{Mg}/^{24}\text{Mg}$ excess over system abundances (the consensus of opinion is that the CR sources have Solar-system abundances with some notable exceptions). The $^{22}\text{Ne}/^{20}\text{Ne}$ excess has been ascribed to injection of $\sim 1\text{MeV}$ stellar wind particles from Wolf-Rayet star atmospheres (Cassé et al. 1980). See also reviews by Meyer (1980) and Reeves (1980). We now move on to the topic of CR arrival-direction anisotropy.

1.1.3 Anisotropy.

(a) Observations

The search for anisotropies in CR arrival directions plays a key role in the question of CR origin. Anisotropies have been recorded for all energies but only measurements above $\sim 10^{12}\text{eV}$ are unaffected by the smearing due to the Solar magnetic field.

Such measurements have been carried out up to 10^{20}eV , the highest observed (Suga 1971 reports 10^{21}eV but core position of EAS uncertain, see Garmston and Watson 1972), by sidereal phase analysis of air shower data (cf. Gombosi et al. 1975, Wdowczyk and Wolfendale 1984a,b).

Figure 1.3 shows the results of the first harmonic analysis characterising the 'vector' anisotropy (δ, ϕ).

$$\delta = \frac{I_{\max} - I_{\min}}{I_{\max} + I_{\min}}, \quad \phi = \text{phase of } I_{\max} \quad (1)$$

These results show a constancy of amplitude and phase up to $\sim 10^{14}\text{eV}$. The amplitude then increases with energy, but so does the noise, as the frequency of air showers

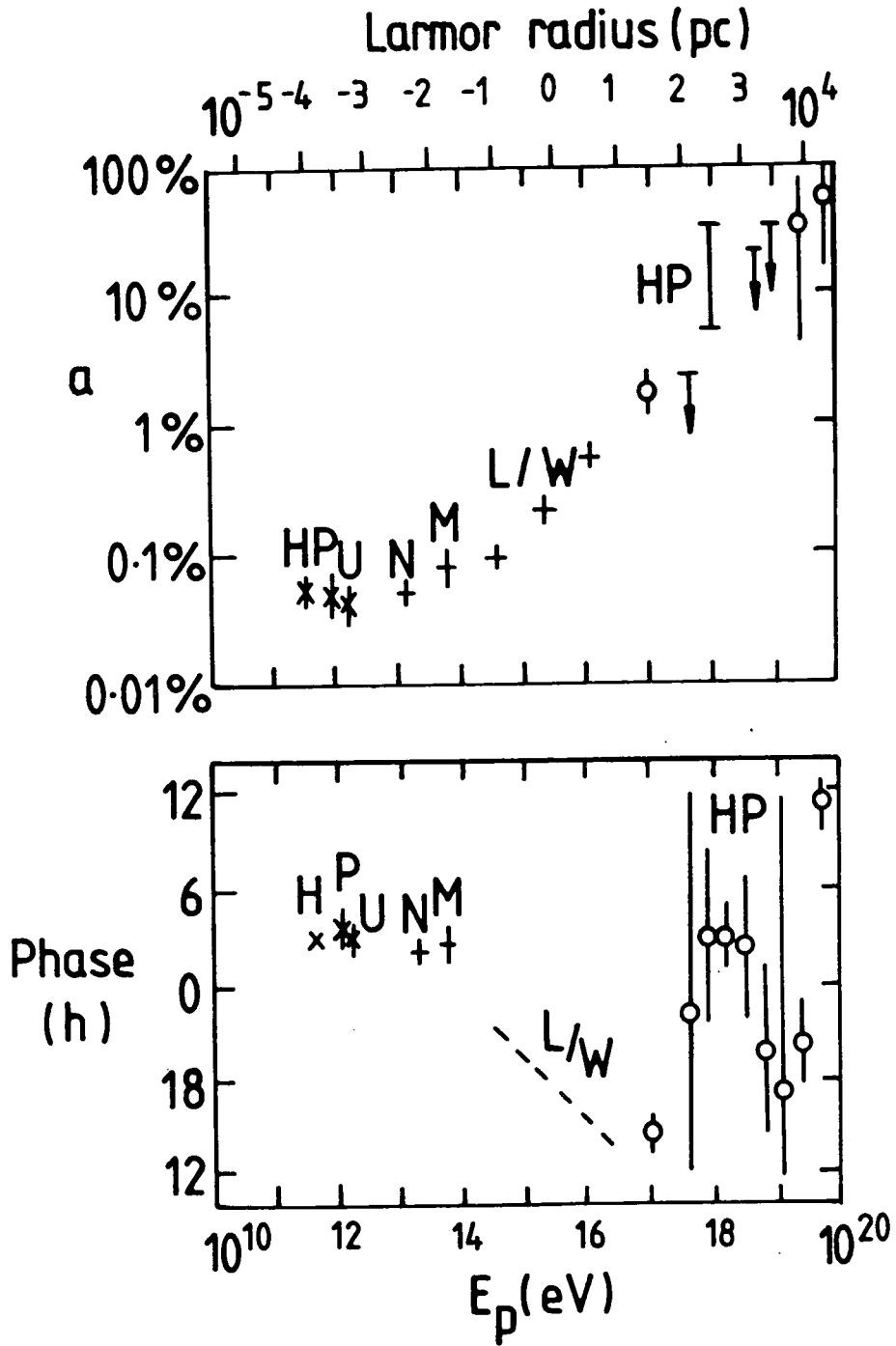


Fig. 1.3 Amplitude and phase of the first harmonic anisotropy of cosmic rays. The near constancy of amplitude and phase below 10^{14} eV is marked. The Larmor radius in a typical interstellar magnetic field of $3 \mu\text{G}$ is indicated (after Wolfendale 1983, where the symbols are described).

falls. Wdowczyk and Wolfendale (1984a,b) have also carried out a second harmonic analysis (sensitive e.g. to zenith directions). They update the summary by Linsley and Watson (1983), show that the apparent N-S excess may be due to the asymmetric coverage of the Galactic plane by EAS arrays, and interpret the results.

(b) Implications

1. $10^{12} < E < 10^{14}$ eV : simple drift of particles (\emptyset is close to the local magnetic field direction defined over ~ 100 pc, $l^{II} \sim 90^\circ$, by optical polarisation and also over 300 to 4000 pc by Faraday rotation of pulsars (Lequeux 1974). Vela SNR lies close to this direction ($l^{II} = 264^\circ$, $b^{II} = -5.6^\circ$) (Compton-Getting ('windshield') effect : $\delta = u/c (\gamma + 2)$, u = drift speed, γ = spectral index).
2. $10^{16} < E < \text{few} \times 10^{16}$ eV : although protons may escape the Galaxy, leaving heavy primaries to provide the 'bump', evidence is accumulating that there may be an upturn in the photon spectrum near 10^{15} eV in which case the bump might then have an excess of photons.
3. $\text{Few} \times 10^{16} < E < 22 \times 10^{19}$ eV : Galactic plane excess - CR trajectories spread out by field irregularities. Rapid change of phase with energy suggests pure composition (consistent with p or p and \bar{p}).
4. $E > 22 \times 10^{19}$ eV : Larmor radius (pc/300 BZ) \gtrsim Galaxy radius (15 kpc) for typical $B = 2 \mu\text{G}$, $Z = 1$. Pure composition?

A celestial plot of source directions shows a wide range of possibilities.

1.2 General remarks about the origin problem

1.2.1 Basic Galactic vs. Extragalactic p origin.

As usually stated, the Cosmic Ray (CR) proton origin problem is to find the source of the CR protons incident on the top of the earth's atmosphere, together with some indication of the region in which the CR energy density is nearly the local value, $\sim 1 \text{ eV cm}^{-3}$.

Guides to the solution are:

- (a) The long-term near constancy of CR flux (variation $\lesssim 40\%$ over $\sim 10^6$ years : Tokar and Povinec (1983) via lunar rock samples; less than a factor of two over $\sim 10^9$ years (e.g. Raisbeck and Yiou 1977) via Be^{10} concentration in marine sediments.
- (b) The local energy density (see Table 1.1).
- (c) The supposed CR gradient in the Galaxy from gamma-ray data (see Dodds et al. 1975, Issa et al. 1981a,b Bloemen et al. 1984a,b; Houston and Wolfendale 1984, Bhat et al. 1984, Wolfendale 1985 (review)).
- (d) The Halo of the Galaxy as a storage volume for (at least) the electron component of the CR (e.g. Meyer 1974 , review) also evidence for the steepening of the synchrotron spectrum in external spiral galaxies seen edge-on cf. Strong (1981), Lerche and Schlickeiser (1981a).
- (e) Anisotropy data (see section 1.1.3).
- (f) The detailed CR source-composition deduced (especially) from secondary components of the CR flux, e.g. Li, Be, B, Sc, V, Al, Mg - see Reeves (1974, review) and their isotope ratios; also e^+ spectrum which

can be predicted from the p spectrum ($\pi^+ \rightarrow \mu^+ \rightarrow e^+$ chain).

- (g) The antiproton spectrum (see Chapter 4).
- (h) The gamma-ray data mentioned (principally SAS-II and COS-B) were once hoped to show the characteristic signal of proton acceleration, namely a bump in the gamma-ray spectrum at $\frac{1}{2} m (\pi^0)c^2 = 67$ MeV, corresponding to the decay ($\pi^0 \rightarrow \gamma + \gamma$) of π^0 particles produced by CR-ISM collisions.

This hope has not (so far) been fulfilled; many workers believe that the gamma-ray quanta produced by CR-electron Bremsstrahlung in the ISM fills this in in the 35 to 100 MeV gamma-ray band (e.g. Morfill 1982).

A number of 'Gamma Ray Sources (GRS)' have been discovered (Swanenburg et al. 1981, Hermsen 1981), some later confirmed in SAS II data (Houston and Wolfendale 1982) - two pulsars and some sources (possibly time-variable) had been previously seen by SAS-II as 'significant' excesses over background data. Their presence both gives hope for the detection of genuine Cosmic Ray sources and contaminates the overall gamma-ray gradient signal.

The clearest signal for a Galactic origin of p at perhaps 1 to 10 GeV comes from the reported Loop I excess in gamma rays above 100 MeV (Bhat et al. 1984).

Gamma-ray data do not preclude an Extragalactic p origin Model (e.g. Hillas 1968, Rana and Wolfendale 1984), at the highest energies.

Inclusion of a metallicity gradient in the Inner Galaxy, with consequent decrease of n_{H_2} (Bhat et al.

1984) restores a CR gradient, supporting a Galactic Model.

Anisotropy data support, but do not prove, a Galactic Model up to $\sim 2Z \times 10^{19}$ eV, where a Metagalactic or Extragalactic model seems appropriate. The remaining arguments are concerned with the feasibility of likely Galactic CR sources. We may quote Galactic energy densities from Wolfendale (1983) for possible sources:

- (1) Rest energy of total mass $\sim 10^9 \text{ eV cm}^{-3}$
 Efficiency $\eta \lesssim 10^{-5}$ leading
 to $\epsilon_1 \approx 10^4 \text{ eV cm}^{-3}$
 - (2) Gravitational potential
 energy of Galaxy as a
 whole $\sim 3 \times 10^3 \text{ eV cm}^{-3}$
 A few percent may have
 gone into CR when the
 Galaxy formed (Chapter 3) $\epsilon_2 \approx 30 \text{ eV cm}^{-3}$
 - (3) Gravitational energy of
 stars in the Galaxy. $\sim 2 \times 10^4 \text{ eV cm}^{-3}$
 Situation as for (2) $\epsilon_3 \approx 2 \times 10^2 \text{ eV cm}^{-3}$
- For (1), (2) and (3) we assume that most of the CR are still in the Galaxy.
- (4) Magnetic field in Galaxy
 $(B^2/8\pi)$ $\sim 1 \text{ eV cm}^{-3}$.
 Equipartition (e.g. reconnection)
 could result and so $\eta \simeq 1$, $\epsilon_4 \simeq 1 \text{ eV cm}^{-3}$.
 - (5) Kinetic energy of gas motion
 $(\frac{1}{2} \rho v^2)$ $\sim 1 \text{ eV cm}^{-3}$
 Equipartition (e.g. shocks)
 could result and $\eta \simeq 1$, $\epsilon_5 \simeq 1 \text{ eV cm}^{-3}$.

(6) Starlight ($\int I_{\nu} d\nu$) $\sim 1 \text{ eV cm}^{-3}$

Hard to find a specific model
for equipartition.

Extragalactic energy densities can now be considered.

(1) Rest energy of total mass

(i.e. mc^2 , assuming $\Omega = 0.1$) $\sim 10^3 \text{ eV cm}^{-3}$

cf. Black Holes (Active Galactic
Nuclei)

$$\epsilon'_1 \approx 10^2 \text{ eV cm}^{-3}$$

$\eta \sim 1$ (but radio-lobes favoured
on loss grounds).

(2) Energy of 3K radiation ($h\nu$)

$$\epsilon'_2 \approx 0.24 \text{ eV cm}^{-3}$$

Hard to find a specific model.

(3) Energy of intergalactic starlight

($h\nu$)

$$\sim 10^{-2} \text{ eV cm}^{-3}$$

Hard to find a specific model to
give equipartition with EG
starlight.

(4) Gravitational P.E. of galaxies

$$\sim 10^{-4} \text{ eV cm}^{-3}$$

A few per cent of this energy may
have gone into CR when galaxies
formed, the CR then escaping (see
Chapter 3).

$$\epsilon'_4 \approx 10^{-5} \text{ eV cm}^{-3}$$

If CR are confined to clusters of galaxies this value
can be raised considerably.

A model in which Extragalactic CR enter the Galaxy (e.g.
from Virgo A) and are re-accelerated in e.g. the Halo
or clouds of our Galaxy is not ruled out.

Further to the discussion of likely CR sources, we should mention the excess in 10^{15} - 10^{16} eV gamma-rays, attributed to a cascade initiated by monoenergetic 10^{17} eV CR particles accelerated by Cyg X-3 (Hillas 1984).

The positron and antiproton spectra are sensitive to the Cosmic Ray source and propagation models, the latter especially so (see Chapter 4).

It has long been suspected - at least on energetics grounds - that the most violent (10^{52} ergs) frequent (1/26 years, e.g. Tamman 1977) Type II Supernova outbursts are major contributors to the Galactic Cosmic Ray proton pool, as are the putative Type III (10^{53} ergs) outbursts (Loop I?) and the Galactic pulsars. Evidence for the pulsar origin is that the Vela PSR 0833 - 45 and Crab PSR 0531 + 21 pulsars shine brightly in medium and high energy gamma-rays, with some DC flux surrounding them. Attributing all the pulsed flux to electron interactions with the magnetic field, and considering the total rate of energy loss derived from spindown observations, we arrive at a proton/electron ratio at 1 GeV of at most 7 for Vela, 3 for the Crab. Vela, particularly, is energetically capable of supplying some of the local CR flux, and the direction of the local CR streaming is close to that of the magnetic field lines connecting Vela to us.

We could proceed generally, choosing an alternative, plausible on energetics grounds, then attempting (using a propagation model) to satisfy other available constraints - still a difficult problem 73 years after the discovery

of CR.

It seems reasonable to start by listing in Table 1.2 several Galactic p origin models and consider their feasibility on energetics grounds.

The clearest evidence that CR protons fill the Galaxy is the close equality in the > 100 MeV energy band between the gamma ray flux deduced by (passive) CR irradiation of the (total) Galactic gas and observation (Black and Fazio 1973, Wolfendale 1981, Bignami 1984).

That the same is true for several nearby Giant Molecular Cloud complexes was shown by Issa et al. (1981a) and also Wolfendale (1984).

Indirect evidence that there are relativistic protons anywhere but locally is given by the suggestion of Dennison (1980) that the electrons, filling the Halo of the Coma cluster of galaxies, are secondary to CR protons accelerated in the central galaxy(ies). These electrons could not fill out the Halo if their outwards streaming were limited to little more than the Alfvén speed in the ionised part of the Inter-Galactic Medium (IGM). Excessive heating (caused by wave growth when the particle pressure overwhelms the magnetic pressure of the plasma, Holman et al. 1979) is not observed, neither does that Halo shrink with increasing radio frequency. Other explanations are possible (e.g. Valtaoja 1984, review) but if Dennison's model holds, the required proton/electron ratio would be ~ 100 (similar to local) for charge-neutrality, using a very simple propagation model.

TABLE 1.2

Table of Source Models

Supernovae:	<p>Max. Energy 10^{13} to 10^{14} eV/n; Spectrum: $\gamma \simeq -2.0$ or -2.2, (time-dependence, diffusion, unsteady flow, shock structure etc.)</p> <p>Shrouded by up to 20 g cm^{-2}, 1/26 years for antiproton spectrum.</p> <p>Energy input $\sim 6 \times 10^{40} \text{ erg s}^{-1}$</p> <p>VELA close; LOOP I a good example?</p> <p>May heat Halo (re-acceleration, pseudo-continuous)</p> <p>Distributed like Kodaira function, peaking in GMC ring at 4 kpc.</p>
Pulsars:	<p>Wind models, electrons (+ and -) only; \dot{p} up to 10^{16} eV?</p> <p>Steep spectrum, -3.0 (bump).</p> <p>Not generally detected in 100 MeV gamma-rays (only VELA and CRAB)</p>
Active Galaxies :	<p>not OK for $> 10^{19}$ eV? photon-photon collisions important.</p> <p>Black Hole - accretion powered?</p>
Accretion shocks :	<p>GMC collapse, star formation, buried (defunct) neutron stars ...</p> <p>Infalling Galactic streams. Galaxy formation(s).</p>
Exotic :	<p>Escaping neutrons from Active Galaxies.</p> <p>Stochastic electrodynamic model.</p> <p>Electron-proton charge deficiency model (up to 10^{19} eV, less than 10^{-21} deficiency).</p>

We now move on to discuss the topic of CR p acceleration mechanisms.

1.2.2. Acceleration mechanisms. Baade and Zwicky (1934) suggested that Supernovae were the main CR source. The (incompletely-sampled) objects are distributed over the Galactic plane somewhat like the Kodaira source function (the resulting Cosmic Ray gradients as the CR's diffuse away from their sources need careful analysis).

The magnetic field present (Alfvén 1954) sets a limit to the magnetic rigidity (momentum per unit charge) of the particles contained by an object, assuming magnetic confinement.

The basic acceleration mechanisms are of several types.

(1) Regular (Fermi 1949) magnetic acceleration by head-on collisions with magnetic inhomogeneities - most effective when the inhomogeneities are of small length scale and the energy transfer large.

(2) Stochastic acceleration (e.g. Betatron or magnetic pumping mechanisms which rely on transfer of energy to the component of momentum perpendicular to the magnetic field, followed by scattering to transfer the momentum irreversibly to the other components).

These mechanisms produce secondary particles whose age increases with time - apparently contrary to observation of the primary to secondary ratio (e.g. Ormes and Protheroe, 1983, Axford 1981 a,b,c; others).

(3) Electrostatic acceleration - effective only if there is a large potential difference across an insulating gap.

(4) Mechanical acceleration mechanisms where gas atoms directly transfer hydrodynamic flow energy to Cosmic Ray protons.

(5) Exotic mechanisms where other particles are accelerated and subsequently produce protons by decay or a secondary mechanism.

1.3 Format of the Thesis

The central contribution to knowledge of this thesis is a set of models for the acceleration of Cosmic Rays in cloud collapse, developed in Chapters 2 and 3. Chapter 4 reviews antiproton origin models and develops new ones, assessing also the validity of the Galactic and Extragalactic scenarios in the interpretation of the \bar{p} flux observed at earth. Finally, Chapter 5 is a summary of the whole work, together with conclusions and suggestions for future work in this field. Appendices (A,B,C) contain additional material not central to the argument.

1.4 Summary and Conclusions

* The Galactic Origin model is consistent with all data, up to 22×10^{19} eV primaries. An extragalactic model is preferred above these energies.

* Energetics grounds suggest a variety of possible models, no one model dominating.

* Collapsing clouds might provide up to a few per cent of the ambient CR flux - galaxy formation likewise - up to 10^{15} eV/nucleon and need detailed study.

CHAPTER 2

2. Can Cosmic Rays be Accelerated in Collapsing Molecular Clouds?(Part 1)

2.1 Introduction

The gravitational energy liberated in the collapse of a typical cloud, of mass $5 \times 10^5 M_\odot$, to molecular cloud densities ($\sim 300 \text{ H}_2 \text{ molecules} = 600 \text{ H-atoms cm}^{-3}$) is $\sim 6.4 \times 10^{50} \text{ erg}$; the cloud radius would be $\sim 20 \text{ parsec}$ and the freefall collapse timescale $\sim 5.1 \times 10^7 \text{ years}$ giving an energy release rate of $\sim 3.9 \times 10^{35} \text{ erg s}^{-1}$ per cloud (see Appendix A).

According to the (heavily undersampled) radio survey in CO of a narrow strip along the Galactic plane undertaken by Gordon and Burton (1980) there are ~ 4000 Giant Molecular Clouds (GMC's) in the Galaxy in a molecular ring between Galactocentric radii of 4 and 6 kpc. The corresponding rate of energy release amounts to $\sim 1.6 \times 10^{39} \text{ erg s}^{-1}$ and is only a factor of (6-30) below the usual estimate of $(1-6) \times 10^{40} \text{ erg s}^{-1}$ (e.g. Blandford and Ostriker 1980, Freedman et al. 1980, this thesis) needed to supply the entire (ambient) interstellar flux of cosmic rays above 1 GeV/nucleon. Thus, in principle at least, collapsing GMC could provide a significant fraction of the ambient cosmic ray flux (it should be noted, however, that Bhat et al. (1984) prefer somewhat less massive clouds).

A further topic of relevance is the existence of a number of GMC's which appear to have cosmic ray (CR) intensities higher than locally. The minimum requirement in energy for a gamma ray 'point' source observable by

Cosmic ray enhancement v Time

Model 2: Freefall, losses 3: Kiraly flow, losses

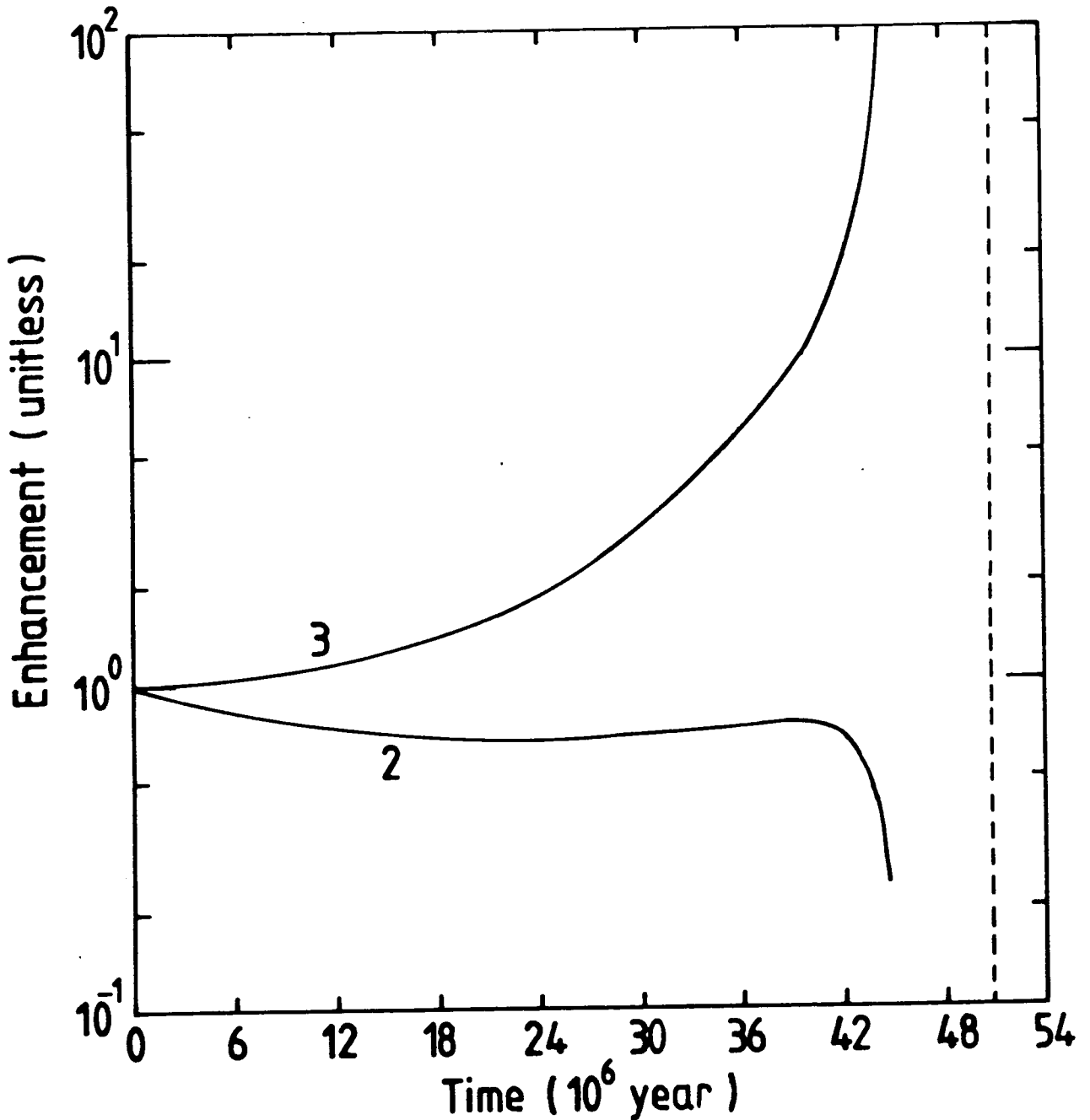


Fig. 2.4 Cosmic ray enhancement v Time for two models of the collapse of a gas cloud (initial density 1 H-atom cm^{-3}) permeated by test particle cosmic rays. The dashed line represents the time to total collapse of the cloud.

the COS B satellite at a distance of d kiloparsec in the presence of confusion by background or other sources is 1.0×10^{-6} photon (> 100 MeV) $\text{cm}^{-2}\text{s}^{-1}$, an energy requirement of $2 \times 10^{34} d^2 \text{erg s}^{-1}$, less than given out in collapse by a factor of up to 100, so some of the 'sources' might result from the process under consideration.

If the ultra-relativistic cosmic ray gas (a fluid with specific heat ratio $4/3$) were to be compressed adiabatically by a factor 600 (say), corresponding to a 'collapse' from a mean density of 1 H-atom cm^{-3} in the interstellar medium (ISM) to typical molecular cloud densities, without any energy loss, an enhancement of cosmic ray intensity by a factor F of $(600)^{4/3} = 5060$ would result. Figure 2.1 shows the observed enhancement factors for some nearby molecular clouds (Issa and Wolfendale 1981a,b, Wolfendale 1984). Since the highest observed enhancement factor detected to date is ~ 16 , the value ~ 5000 must be modified in the real world. Furthermore, statistical studies of the emission of high energy (> 100 MeV) gamma-radiation from simulated molecular clouds demonstrate that 40-60% of the famous 2CG catalogue (Hermsen 1981) of discrete gamma-ray sources may be explained by the irradiation of the clouds by the ambient interstellar flux of cosmic rays (CRI) (Li and Wolfendale 1981, Bignami 1984), i.e. without any enhancement of cosmic ray intensity at all.

In perspective, it would be reasonable to develop the hypothesis that some of the remaining sources (others are known to be due to discrete objects such as pulsars)

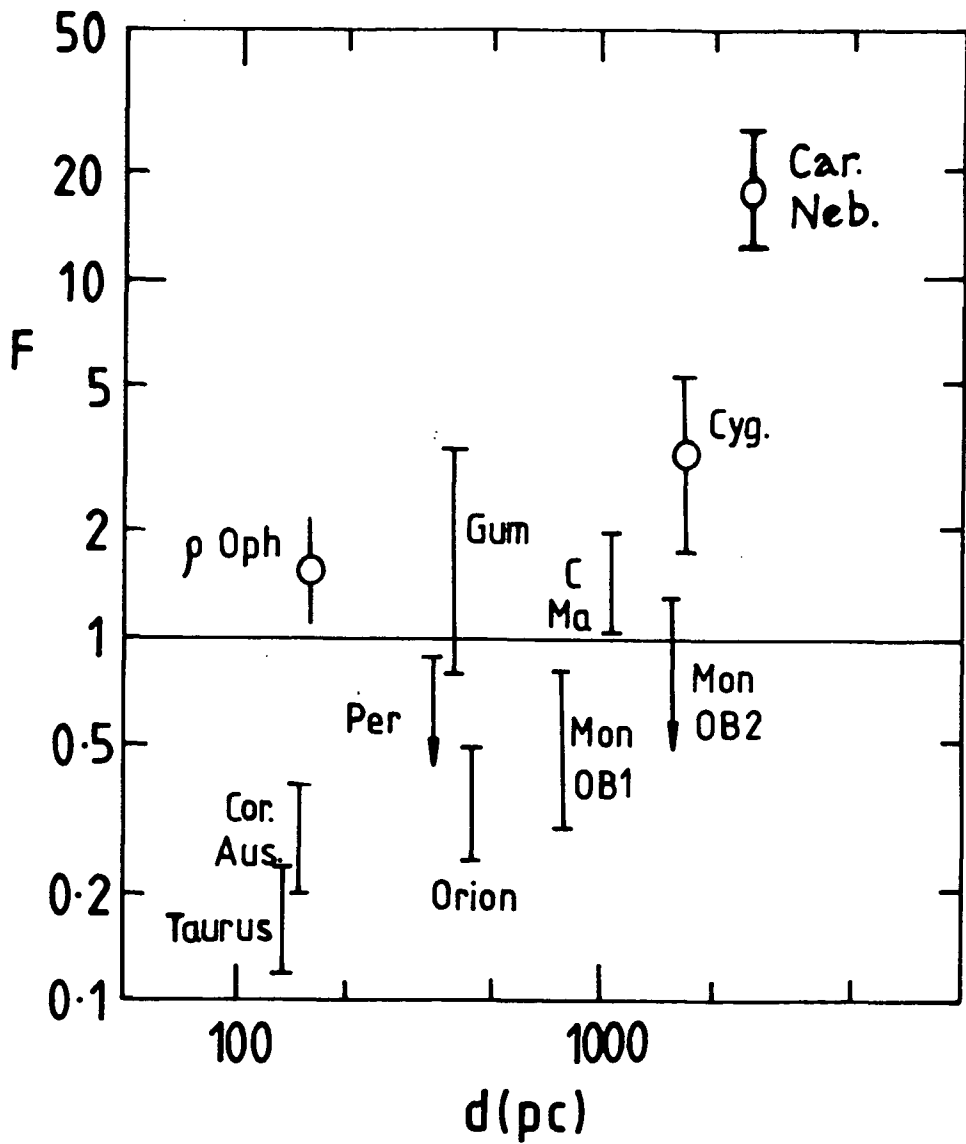


Fig. 2.1 Gamma-ray fluxes above 100 MeV from local giant molecular clouds divided by our predicted fluxes. 'd' is the distance of the cloud from the Sun. Those values with circles were denoted as 'discrete sources' in the 2CG catalogue of COS B (after Issa and Wolfendale 1981).

together with the extended GMC studied by Issa and Wolfendale, and perhaps even some of the ambient flux itself, might be due to an enhanced irradiation of the clouds (ECRI). Whilst sources of cosmic rays inside the clouds, such as supernovae or pulsars, are an interesting possibility, the prospect of a 'quiet' origin by cloud collapse is a useful initial hypothesis.

The plan of the chapter is as follows. In Section 2 a simple model of a collapsing cloud will be developed which can accelerate cosmic rays adequately. In Section 3 the physical characteristics necessary for the acceleration will be discussed more thoroughly. The comparison of the results with the gamma-ray observations and the modelling of the Carina Nebula (γ Carinae), the most enhanced cloud detected to date, ($F \sim 16$), will be deferred to the next Chapter.

Finally, Section 4 is a brief summary of the main results and conclusions.

2.2 Models of a Collapsing Cloud

2.2.1 Cold spherical cloud in free fall. A cold spherical cloud permeated by a magnetic field of negligible energy density collapses in freefall. If the collapse were to be uniform and isotropic, the radius $r(t)$ of a particular mass shell would satisfy (e.g. Mestel 1965, Spitzer 1978):

$$\frac{d^2 r}{dt^2} = - \frac{GM(a)}{r^2} = - \frac{4\pi a^3 n_H(0) m_p}{3 r^2} \quad (1)$$

(a = initial radius of mass shell, $M(a)$ = mass interior to the shell, m_p = proton rest mass, $n_H(0)$ = initial gas density (H-atoms cm^{-3})). If we assume that the shells do not cross each other, the mass inside a shell stays constant during a collapse. Multiplying equation (1) by dr/dt and integrating yields the energy integral

$$\frac{dr}{adt} = - \left[\frac{8\pi G n_H(0) m_p}{3} \left(\frac{a}{r} - 1 \right) \right]^{1/2} \quad (2a)$$

hence

$$\dot{R}(t) = -2.9 \times 10^5 \left(\frac{M_5}{n_H(0)} \right)^{1/3} \left[\left(\frac{n_H(t)}{n_H(0)} \right)^{1/3} - 1 \right]^{1/2} \text{cm s}^{-1} \quad (2b)$$

where R is the cloud radius.

If we substitute $r/a = \cos^2 \alpha$, still following Spitzer (1978), equation (2) yields

$$\alpha + \frac{1}{2} \sin 2\alpha = \frac{\pi t}{2 t_f} \quad (3)$$

where we let t vanish initially when dr/dt is zero.

All shells reach the centre at the same time when

$\alpha = \pi/2$ and after a 'freefall' time¹ given by

$$t_f = 5.1 \times 10^7 n_H(0)^{-1/2} \text{ years} \quad (4)$$

The collapse speed is given by equation (2b) above.

Suppose the cosmic rays to be trapped within the cloud, perhaps by magnetic fields. The relativistic cosmic ray gas constitutes a fluid with specific heat ratio $4/3$. The collapsing cloud does work dW against the cosmic ray pressure P in a small volume change dV

$$dW = -P dV \quad (W = V \int_{P_0}^{P_{\max}} P' N(P') dP') \quad (5)$$

¹ Spitzer's value is $4.3 \times 10^7 n_H(0)^{-1/2}$ years; updated here

$N(p)dp$ is the number density of cosmic rays with a momentum p to $p + dp$, and p_0 and p_{\max} are (respectively) lower and upper limits to the CR momentum; p_0 might be the CR momentum at injection, p_{\max} the maximum CR momentum trapped by the magnetic field). The cosmic ray pressure P is related to the cosmic ray energy density E by

$$P = \frac{1}{3} E \Rightarrow \frac{dW}{W} = \frac{1}{3} \frac{dV}{V} \quad (6)$$

Hence the convergence (divergence) of the bulk flow leads to an adiabatic heating (cooling) of the cosmic ray gas at a rate

$$\left(\frac{dp}{dt}\right)^{ad} = -p \frac{\dot{R}(t)}{R(t)} \Rightarrow t_{ad}^{-1} = \frac{\dot{R}(t)}{R(t)} \quad (7)$$

(e.g. Ginzburg and Syrovatskii 1969, Longair 1981) where t_{ad} is the timescale over which adiabatic compression or rarefaction takes place and $R(t)$ is the radius of the cloud outer boundary. This result also applies to individual particles.

The result, equation (7), is not so obvious when a magnetic field is present and provides the cosmic ray trapping: it follows by considering the (approximate) conservation of the magnetic moment

$$\frac{p^2 \sin^2 \theta}{B} = \text{constant} \quad (\theta = \text{pitch angle}) \quad (8)$$

and compression of the Larmor orbits of the cosmic rays (the component of the particle momentum parallel to the magnetic field is unaffected), provided that the magnetic

flux through the orbit is approximately conserved. In this case, no particle whose gyroradius $r_g(B)$ is greater than the cloud radius $R(t)$ will be compressed, and the spectrum will be 'cutoff' at a momentum p such that

$$\frac{P_{\max} c}{eV} = 300 Z \left(\frac{B_{\max}}{\text{Gauss}} \right) \left(\frac{R(t)}{\text{cm}} \right) = 2.6 \times 10^{17} Z \frac{n_H(t)^{1/3} M_5^{1/3} \left(\frac{B_0}{3\mu G} \right)}{n_H(0)^{2/3}} \quad (9)$$

for a cloud of $M_5 \times 10^5$ Solar masses and in the isotropic-collapse flux-freezing approximation. Hence $P_{\max}(t)$ (if no energy loss) increases steadily with n_H ; Z represents the particle charge number and B the magnetic flux density. Alternatively, consider reflection of the cosmic ray particles at a perfect mirror (including the Doppler effect) at the cloud boundary - for an isotropic distribution of cosmic ray momentum we again arrive at equation (7) for the rate of acceleration of cosmic rays during adiabatic compression or rarefaction¹. The assumption that the magnetic flux through a closed contour enclosing a particle orbit is (approximately) conserved may be justified theoretically for sufficiently high electrical conductivity of the gas: a necessary condition to ensure this is

$$R_m = \frac{4\pi\sigma v\ell}{c^2} \gg 1 \quad (10)$$

(see Appendix A or e.g. Parker 1969) where R_m is the magnetic Reynolds number, σ is the electrical conductivity,

¹ The general result for the rate of adiabatic heating or cooling) of CR particles in an element of the gas is

$$\left(\frac{dp}{dt} \right)_{\rightarrow}^{ad} = -\frac{1}{3} p \vec{\nabla} \cdot \vec{V}$$

where V is the (vectorial) velocity of the scattering centres.

and l the length-scale of the orbit. An approximate formula for the conductivity measured in "cgs" electrostatic units (e.s.u.) at temperature T (Kelvin), for a partially (collisionally) ionised gas (drift speed of electrons determined by collisions with neutral atoms) is

$$\sigma_i \approx 10^9 T^{3/2} \text{ e.s.u.} \quad (11a)$$

and for a fully ionised gas (drift speed determined by electron-electron encounters and shielding (Debye effect)) is

$$\sigma_f \approx 6.5 \times 10^6 T^{3/2} \text{ e.s.u.} \quad (11b)$$

(the 'Cowling Formula'; e.g. Cowling 1945, Lang 1978). For a typical GMC ($T \sim 10$ to 20K , fractional ionisation n_i perhaps 1×10^{-6} , $l \sim 40$ parsec), $R_m = 10^9$ for 1 GeV proton, 10^6 for 1 MeV proton, so that flux-freezing may be a very good approximation indeed! The estimate of R_m above is a lower limit only. The low energy ($\lesssim 1$ MeV/nucleon) cosmic rays ionise the gas by Coulomb collisions with atoms of the gas cloud offset by recombination. Ionisation rates of $\gamma = 10^{-16} n_H \text{cm}^{-3} \text{s}^{-1}$ to $10^{-17} n_H \text{cm}^{-3} \text{s}^{-1}$ averaged over the cloud have been reported in the few cases where measurements are available (e.g. Duley and Williams 1984).

The cosmic rays of kinetic energy above 700 MeV/nucleon lose energy by inelastic nuclear collisions with atoms of the gas cloud (the products are gamma rays, electrons, positrons, antiprotons). The loss time t_l due to strong inelastic collisions is given by

$$\left(\frac{dp}{dt}\right)^{\text{coll}} = -\rho \frac{\beta c m_p n_H(t)}{X} \Rightarrow t_e^{-1}(t) = \frac{\beta c m_p n_H(t)}{X} \quad (12a)$$

(βc = particle speed ($\beta \rightarrow 1$), $n_H(t)$ = cloud density (H-atoms cm^{-3}), X -attenuation grammage for high energy cosmic rays in hydrogen = 66 g cm^{-2} , excluding the spectral shape factor, used by e.g. Nakano and Tademaru 1972). Numerically,

$$t_e = 4.1 \times 10^7 \beta^{-1} n_H(t)^{-1} \text{ years} \quad (12b)$$

If we suppose the cosmic ray pressure to be small compared to the gravitational pressure at all times (in fact they are initially nearly equal) the number of cosmic rays N in the cloud of momentum p at time t after the start of the collapse satisfies a Boltzmann equation

$$\frac{\partial N}{\partial t} = \frac{\partial}{\partial p} \left[N \left\{ \left(\frac{dp}{dt}\right)^{\text{ad}} + \left(\frac{dp}{dt}\right)^{\text{coll}} \right\} \right] \quad (13)$$

If the cosmic ray spectrum remains of power-law form up to a 'cutoff' momentum $p_{\text{max}}(t)$, then $N_1(t)$ satisfies equation (14).

$$\begin{aligned} \frac{\partial N_1}{\partial t} &= (\gamma-1) N [t_{\text{ad}}^{-1}(t) - t_e^{-1}(t)] \\ N &= N_1 (p/p_0)^\gamma : p_0 \leq p \leq p_{\text{max}}(t) \end{aligned} \quad (14)$$

Hence the number of cosmic rays inside the cloud at time t after the start of the collapse is enhanced, or diminished if $F < 1$, by a factor F

$$F = \left(\frac{n_H(t)}{n_H(0)} \right)^{4/3} \cdot \exp \left[-(\gamma-1) \left\{ \frac{\beta c m_p n_H(0)}{X} \cdot \frac{4 t_f}{\pi} \left(t \tan \alpha + \frac{1}{3} t \tan^3 \alpha \right) \right\} \right] \quad (15)$$

and the momentum p at time t of a cosmic ray injected into the collapse with momentum p_0 at time $t_0 < t$ is

given by

$$P(t) = P_0 \left(\frac{n_H(t)}{n_H(0)} \right)^{4/3} \exp \left[- \frac{\beta_{\text{cmp}} n_H(0)}{X} \cdot \frac{4 t_f}{\pi} \left(\tan \alpha + \frac{1}{3} \tan^3 \alpha \right) \right] \quad (16)$$

provided $P \leq P_{\text{max}}(t)$, as defined in equation (9), where α_0 is given by $R(t)/R_0 = \cos^2 \alpha_0$. The spectral shape is unchanged (this is a similarity solution).

Referring to Figure 2.2 we see that the masses of molecular cloud complexes lie in the range $\sim 10^4$ to (at most) $\sim 10^7 M_\odot$ (Gordon and Burton 1980, for an alternative view see Bhat et al. 1984).

The choice for $n_H(0)$ is not completely clear but does not greatly affect the magnitude of the gravitational energy released for $n_H(0) \gtrsim 1 \text{ cm}^{-3}$ (average density in the ISM) for GMC's of density $n_H \sim 600 \text{ cm}^{-3}$, with easily a factor 2 uncertainty in the GMC density or mass, the latter due partly to the uncertain $\text{CO} \rightarrow \text{H}_2$ conversion factor (Scoville et al. 1984, Houston and Wolfendale 1984).

However, the enhancement of cosmic ray intensity is exponentially sensitive to $n_H(0)$ through the loss factor. Figure 2.3 shows some results of this Model 1 for a range of initial cloud densities. The model is completely specified by one parameter $n_H(0)$ if the ambient interstellar spectral (ISS) shape, $\gamma = 2.5$ is adopted, (it should, however, be noted that the result is sensitive to the choice of γ).

Figure 2.4 shows the run of the cosmic ray enhancement with time for $n_H(0) = 1 \text{ cm}^{-3}$.

Figure 2.5 shows the run of the cloud density with time for this initial density.

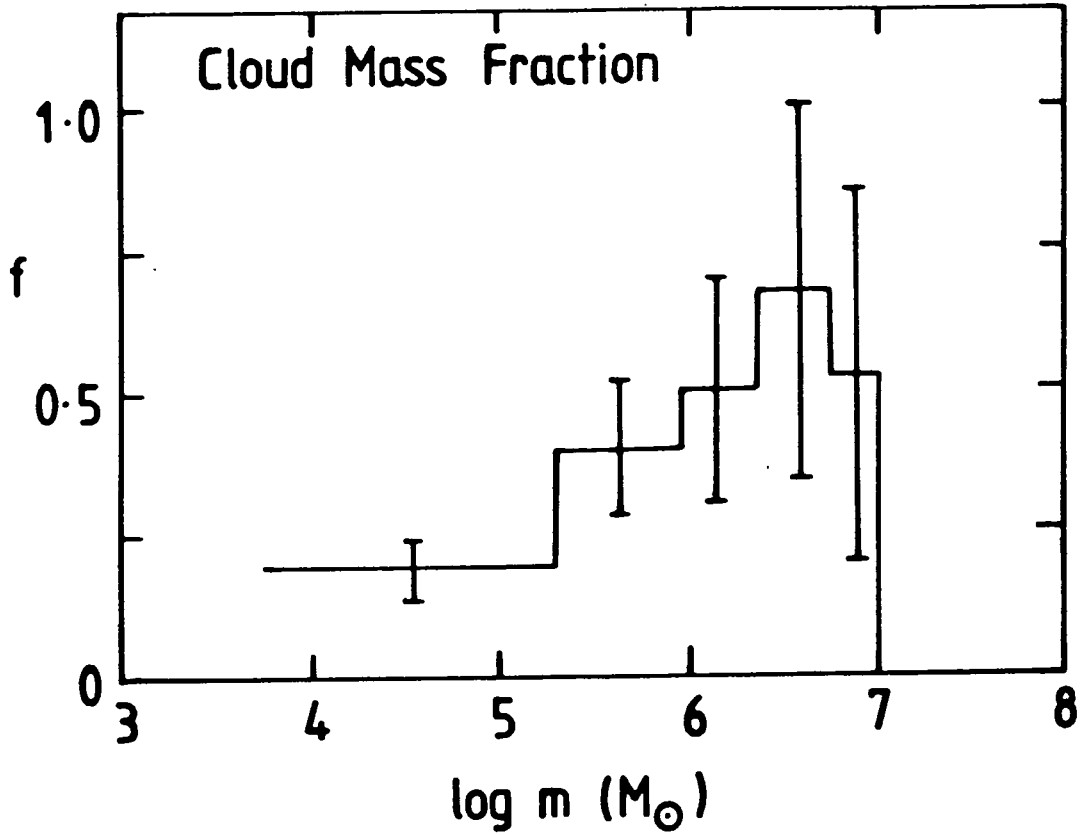


Fig. 2.2 The fraction of total mass contained in Giant Molecular Cloud complexes of mass m per logarithmic interval.

The error bars are determined by the sample size. The greatest uncertainty in m stems from the uncertainty in $^{13}\text{CO}/\text{H}_2$.

(taken from Gordon and Burton 1980)

Cosmic ray enhancement v Cloud density

(Freefall, losses)

Initial gas density

a: 10^{-2} b: 10^{-1} c: 10^0 d: 10^1 cm^{-3}

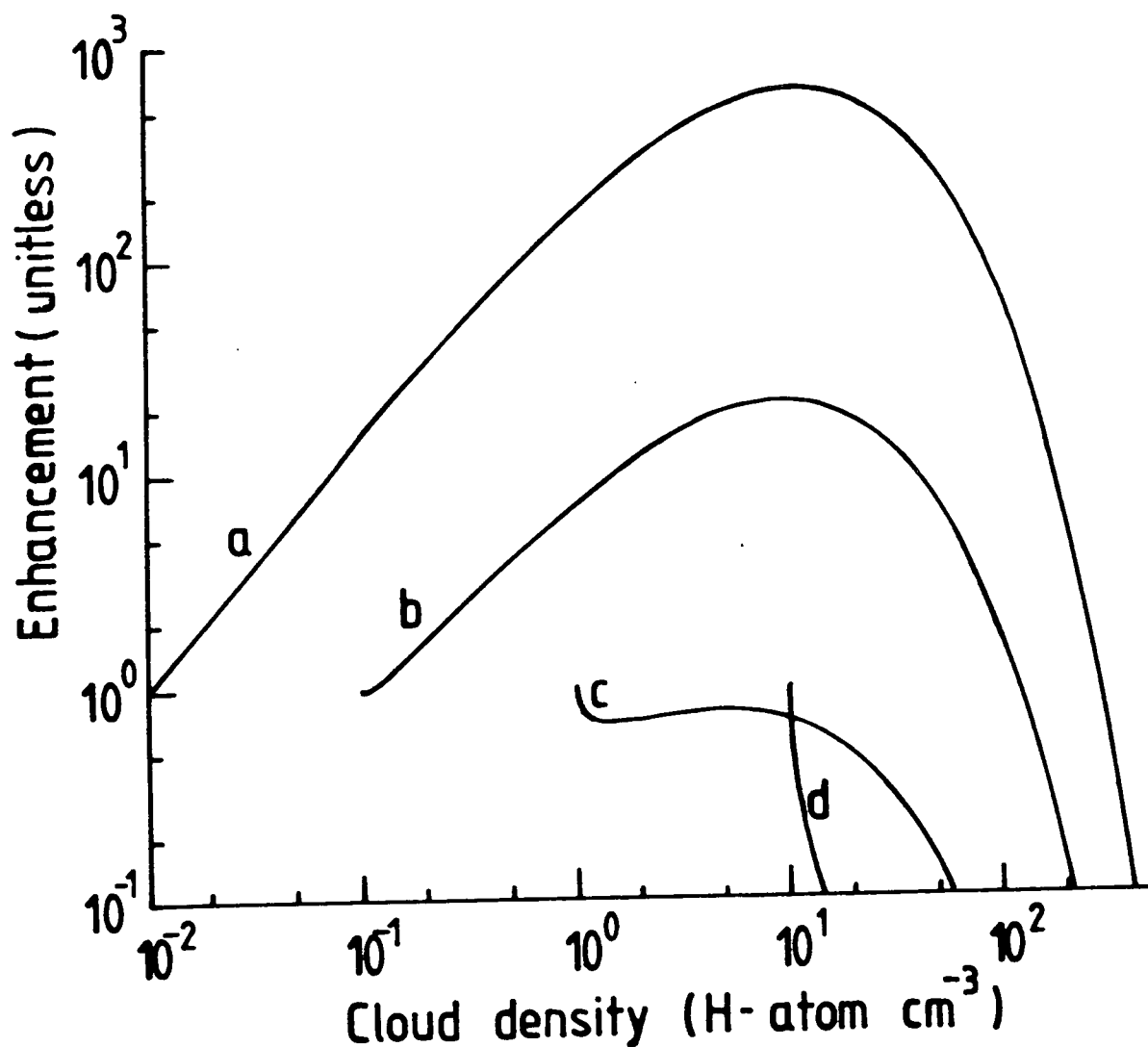


Fig. 2.3 Cosmic ray enhancement v Cloud density for the freefall collapse of a gas cloud, permeated by test particle cosmic rays, considering four values of the initial gas density.

Cosmic ray enhancement v Cloud density

Model 1: No losses 2: Freefall, losses 3: Kiraly flow, losses

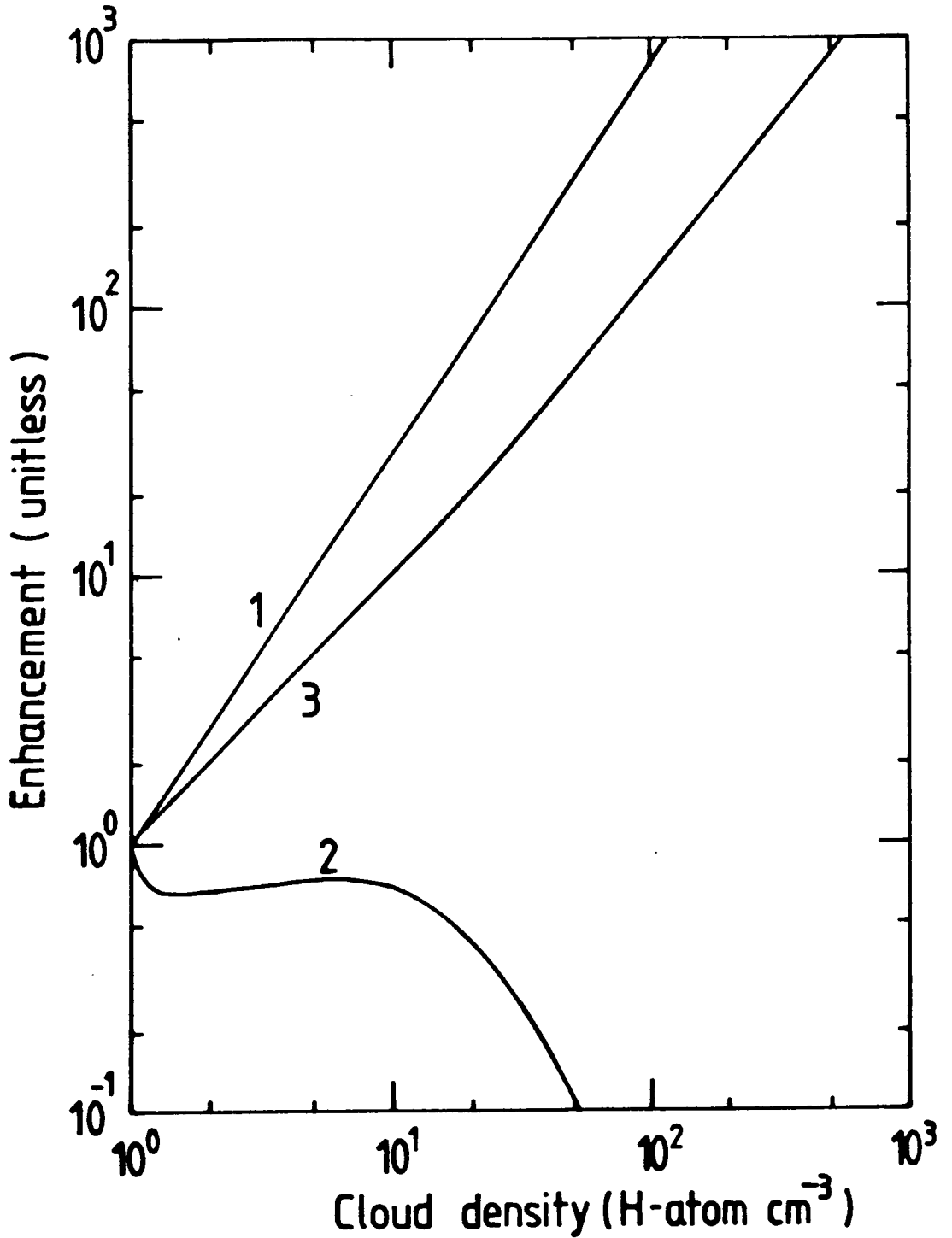


Fig. 2.5 Cosmic ray enhancement v Cloud density for three models of the collapse of a gas cloud (initial density 1 H-atom cm⁻³) permeated by test particle cosmic rays.

2.2.2 Cold spherical imploding cloud. The enhancement of cosmic ray intensity F would be increased if an implosion caused by an external shock wave starts the contraction (Dogiel et al. 1983, this thesis). In this case we might have a 'negative escape velocity' of the cloud boundary initially, i.e. the sum of the kinetic and potential energies is zero. The motion of the cloud boundary is given by

$$R(t) = R_0 \left(1 - \frac{t}{t_c}\right)^{2/3} \quad (\text{'Kiraly' flow}) \quad (17)$$

where

$$t_c = 2.2 \times 10^7 n_H(0)^{-1/2} \text{ years} \quad (18)$$

and the collapse speed is given by

$$\dot{R}(t) = -4.3 \times 10^5 M_5^{1/3} n_H(t)^{1/6} \text{ cm s}^{-1} \quad (19)$$

for cloud mass $M_5 \times 10^5$ solar masses. Figure 2.5 includes the enhancement of cosmic ray intensity on this model for the same initial density as for Model 1, viz. 1 H-atom cm^{-3} .

Figure 2.6 shows the run of cloud density with time for freefall and Kiraly flow.

$$F = \left(\frac{n_H(t)}{n_H(0)}\right)^{4/3} \cdot \exp\left[-(\gamma-1) \frac{\beta c m_p n_H(0)}{\chi} \cdot 3t_c \left(1 - \left(\frac{n_H(t)}{n_H(0)}\right)^{-1/6}\right)\right] \quad (19)$$

The momentum $p(t)$ at time t of a particle injected into the collapse with momentum p_0 at time $t_0 < t$ is given

$$P(t) = p_0 \left(\frac{n_H(t)}{n_H(0)}\right)^{4/3} \cdot \exp\left[-\frac{\beta c m_p n_H(0)}{\chi} \cdot 3t_c \left(1 - \left(\frac{n_H(t)}{n_H(0)}\right)^{-1/6}\right)\right] \quad (20)$$

for $P \leq p_{\max}(t)$.

Cloud density v Time

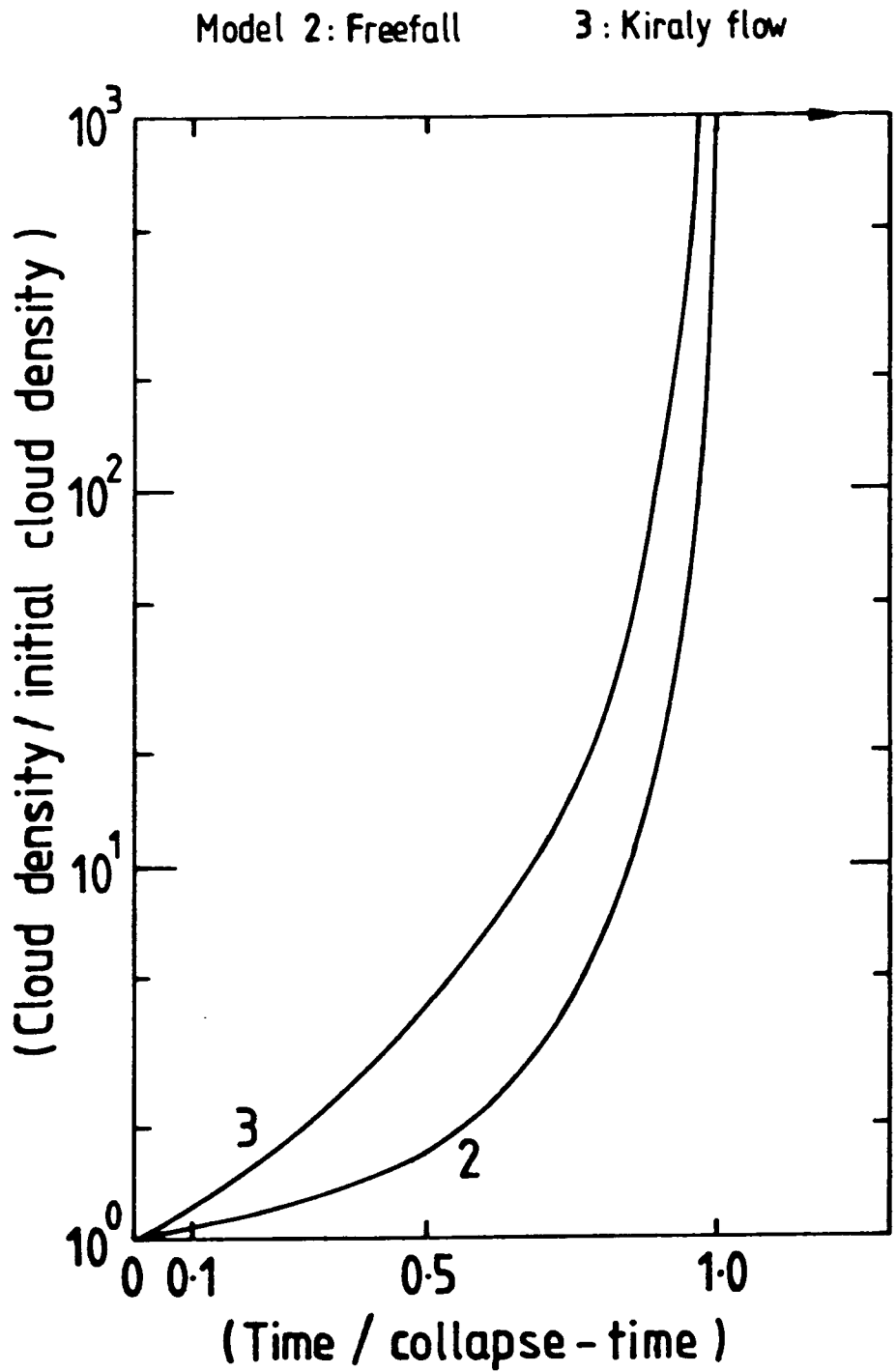


Fig. 2.6 Cloud density v Time for two models of the collapse of a gas cloud (initial density 1 H-atom cm^{-3}).

Maximum CR energy v Cloud density
(inertial confinement)

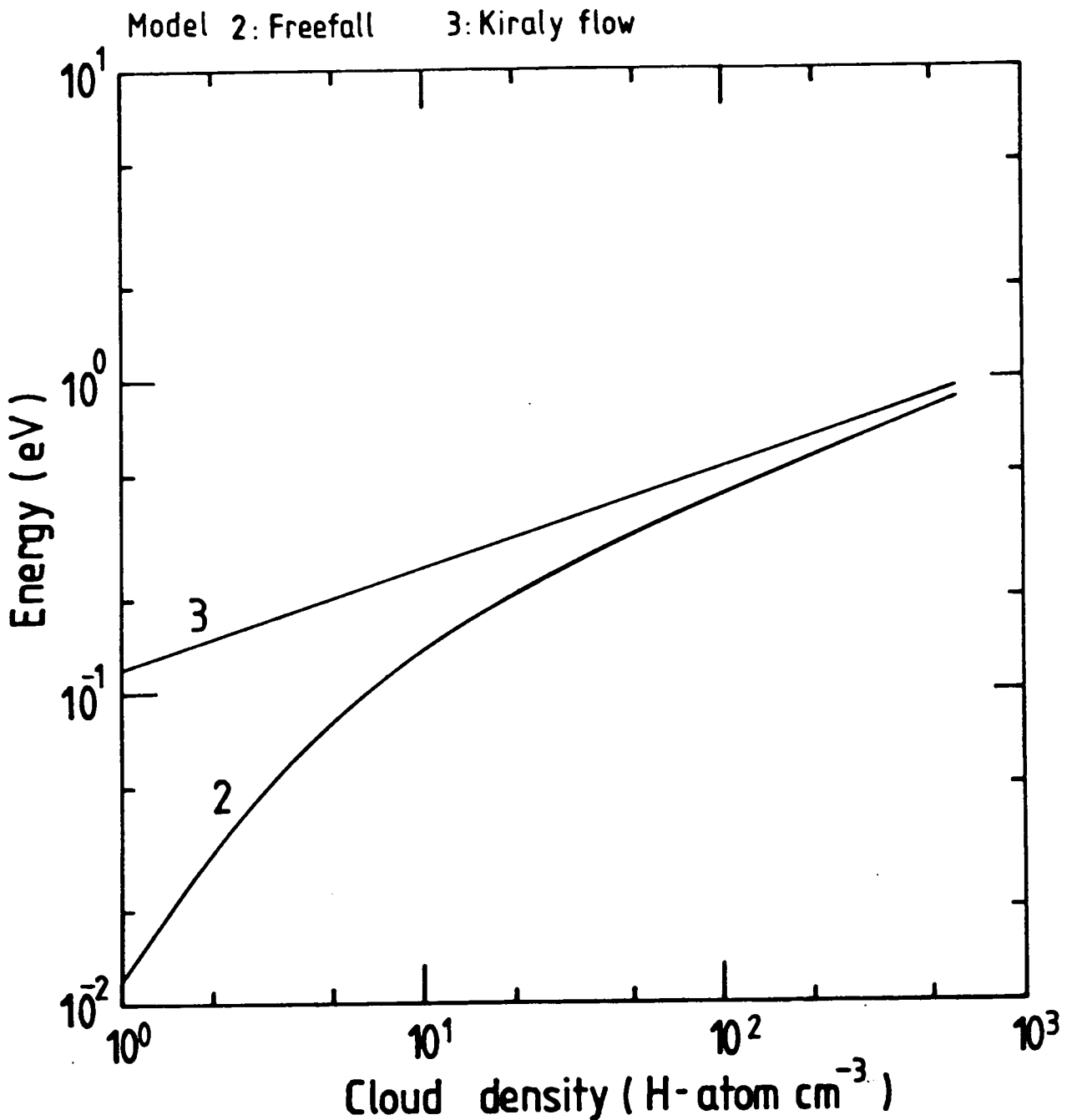


Fig. 2.7 The run of energy at which CR protons become inertially confined, with cloud density, for a typical GMC (Mass = $5 \times 10^5 M_{\odot}$, initial density = 1 H-atom cm⁻³) considering two models of cloud collapse.

The initial collapse speed for a typical GMC would be 5 km s^{-1} , perhaps not too high for the observations (see the review by Lequeux 1977, also Blitz and Shu 1980).

The effects of escape of the cosmic rays from the cloud will be considered next.

2.3 Escape of Cosmic Rays from the Cloud

2.3.1 Confinement by straight-line transit time. This is effective only when the straight-line transit time t_r is much greater than the acceleration timescale. In the case of adiabatic compression (Model 1 or 2)

$$t_r = \frac{R(t)}{\beta c} \gg \frac{R(t)}{\dot{R}(t)} \Rightarrow \beta c \ll \dot{R}(t) \quad (22)$$

If confined initially, this model predicts the cosmic ray protons to be confined; for kinetic energy $\lesssim 1 \text{ eV}$ for model 2 and a typical GMC; grains may also be confined and accelerated by the betatron effect, see Shull 1978, Duley and Williams 1984).

Figure 2.7 shows the run of energy at which cosmic rays become trapped, with cloud density, for Model 2 and Model 3, for a typical GMC and initial density $n_H(0) = 1 \text{ H-atom cm}^{-3}$.

2.3.2 Confinement by magnetic scattering on resonant Alfvén waves. Cosmic rays would be effectively trapped if they were to diffuse against the inflow of scatterers moving with the matter, provided the modulation (fractional energy-gain) parameter $q(p,t) \equiv \int_0^{R(t)} \frac{V(r,t)}{K_{||}(p,t)} dr$

$$q(p, t) = \frac{V(t) R(t)}{2 K_{rr}(p, t)} \lesssim -1 \quad (23)$$

The argument for this is that the probability of escape from the cloud, in the case that V and K_{rr} (the isotropic part of the CR diffusion coefficient) are constant, $1-r$ is very small if $VR/K_{rr} \lesssim -1$, see e.g. Freedman et al. 1979, 1980, or Cowsik and Lee 1983 (for a more complicated case). The parameter q determines the modulated spectrum in the Solar Wind (e.g. Jokipii 1971, review) or Galactic Wind (e.g. Freedman 1979, 1980 or Schlickeiser 1979, 1980; references therein).

An approximate escape timescale in the case of combined diffusion and inwards convection (including adiabatic acceleration), in spherical geometry, is t_{esc} , given by

$$t_{esc} \approx \frac{R^2(t)}{3 \langle K_{rr}(p, t) \rangle} \left[\frac{1}{2} + \frac{1}{\mathcal{E}} \right] \quad (24)$$

where \mathcal{E} is related to the anisotropy δ by the relations

$$\mathcal{E} = \frac{2R}{3 \lambda_{||}(p)} \left(\frac{1-r}{1+r} \right) : \delta = \frac{3 \langle K_{rr} \rangle}{\beta c} \frac{1}{n_{CR}} \left(\frac{\partial n_{CR}}{\partial R} \right) = \left(\frac{1-r}{1+r} \right) \quad (25)$$

where $\lambda_{||}(p)$ is the scattering mean free path along magnetic field lines at CR momentum p . The 'angle-brackets' in equation (24) denote an isotropic average over CR pitch-angles. The return probability r is here defined as the probability that a CR particle, starting from the cloud centre, ever returns there (R here is the radial distance). An approximate expression for \mathcal{E} , valid for spherical geometry and converging bulk flow is

$$\mathcal{E} = q \left[(1 - \exp(-q))^{-1} + \gamma - 1 \right] \quad (26)$$

These expressions are obtained by considering the case of infall of scattering centres in a plane parallel geometry (see Freedman et al. 1980, this thesis). In that case, the factor $(\gamma - 1)/3$ replaces $(\gamma - 1)$ above. This timescale t_{esc} diverges for strong convergent ($V \propto$ radial distance) inwards convection and scattering when

$$q < q_c = -\ln\left(\frac{\gamma}{\gamma-1}\right) = -0.5 \text{ for } \gamma = 2.5 \quad (27)$$

This means that any collision between the CR particle and scattering centres results in deflection towards the cloud centre. (This corresponds to the Cowsik and Lee (1983) model case $\alpha + \beta = 0$, where the diffusion coefficient scales as radial distance to the power β (at fixed cloud radius), and convection speed scales as radial distance to the power $(-\alpha)$). In the case of weak scattering ($q_c < q < 0$), t_{esc} as detailed above (equation (24)) will be used in the rest of this chapter. In principle, scattering centres fixed in the cloud could provide a CR diffusion coefficient proportional to the cloud density. The diffusion part of the escape time-scale would then be given by

$$t_{diff} = 4.6 \times 10^4 \left[\left(\frac{M_5}{n_H(0)} \right)^{2/3} \frac{1}{k_{28}} \right] \left(\frac{n_H(t)}{n_H(0)} \right)^{1/3} \text{ years}$$

where k_{28} denotes the diffusion coefficient in units of $10^{28} \text{ cm}^2 \text{ s}^{-1}$. If the escape time-scale exceeds the remaining time to complete collapse the CR's will become effectively trapped.

Figure 2.8 shows this escape time-scale, remaining

Diffusion escape timescale and remaining time to complete collapse v. Cloud density.

Curve a, 1MeV; b, 1GeV; c, 10GeV

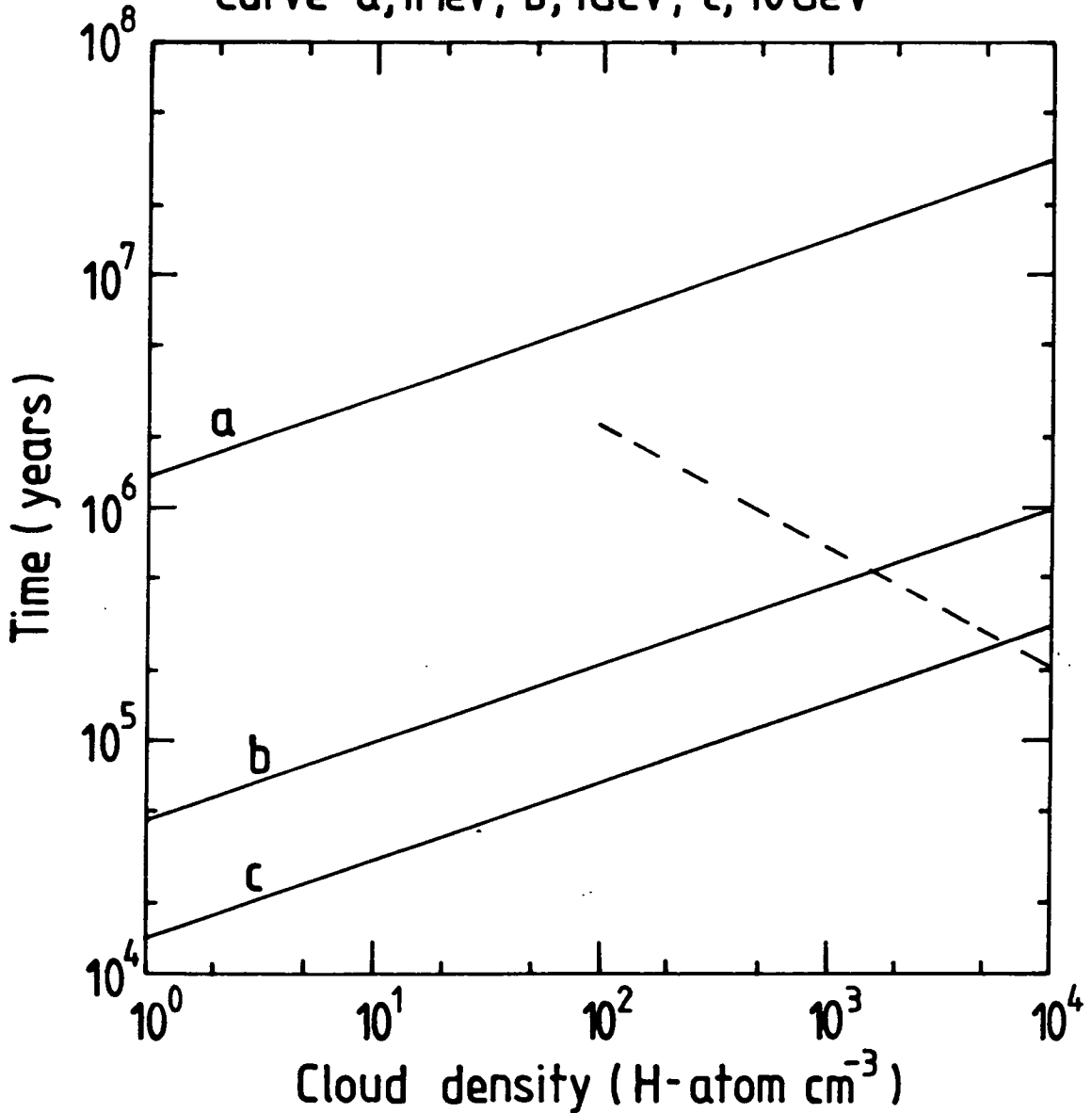


Fig. 2.8 Diffusion escape timescale and remaining time to complete collapse v. Cloud density, for a typical GMC in which the cosmic ray diffusion coefficient $k \propto n_H^{-1} \cdot (p/\text{GV})^{\frac{1}{2}}$.

Convective CR trapping is negligible.

The dotted line represents the remaining time to complete collapse.

collapse-time ratio for proton energies 1 MeV, 1 GeV and 10 GeV respectively and Kiraly flow (assuming $K_{rr} = 10^{28} \left(\frac{P}{GV}\right)^{\frac{1}{2}} \text{ cm}^{2-1} \text{ s}^{-1}$). The 1 MeV protons are very effective ionizers of the cloud; the attenuation grammage is 3 g cm^{-2} (see Penston 1969b, also Césarsky and Volk 1978). If trapped, the ~ 1 MeV CR's may, in principle, contribute significantly to the pressure inside the cloud.

Static molecular clouds with negligible infall of matter have been discussed by Skilling and Strong (1976), Césarsky and Volk (1978) and Morfill (1982), and a model for the Carina Nebula, based on the confinement of stellar-wind accelerated protons by resonant Alfvén waves excited in an associated HII region, has been proposed by Montmerle (1981).

The last two models (and that for cosmic ray exclusion from dense clouds by Skilling and Strong just mentioned) rely on the well-known result that cosmic rays, streaming relative to a cold ionised plasma, excite Alfvén waves, on the length scale of their gyroradius, which travel in the direction of the cosmic ray streaming and reduce it to slightly more than the Alfvén speed relative to the background plasma (Wentzel 1974, Skilling 1975a,b,c; see review by Césarsky 1980 for the current status of this hypothesis).

In the case of both freefall and 'Kiraly flow', the collapse speed is much less than the typical Alfvén

speed in the ionised¹ part of the plasma, throughout the motion from $n_H = 1$ to 600 cm^{-3} :

$$V_A^* = \frac{B}{\sqrt{4\pi n_i n_H m_p}} = 6.5 \times 10^8 \left(\frac{n_H}{1 \text{ cm}^{-3}} \right)^{\frac{1}{6}} \left(\frac{n_i}{10^{-6}} \right)^{-\frac{1}{2}} \left(\frac{B_0}{3 \mu G} \right) \text{ cm s}^{-1}$$

but not the non-ionised part

$$V_A = \frac{B}{\sqrt{4\pi n_i n_H m_p}} = 6.5 \times 10^5 \left(\frac{n_H}{1 \text{ cm}^{-3}} \right)^{\frac{1}{6}} \left(\frac{B_0}{3 \mu G} \right) \text{ cm s}^{-1}$$

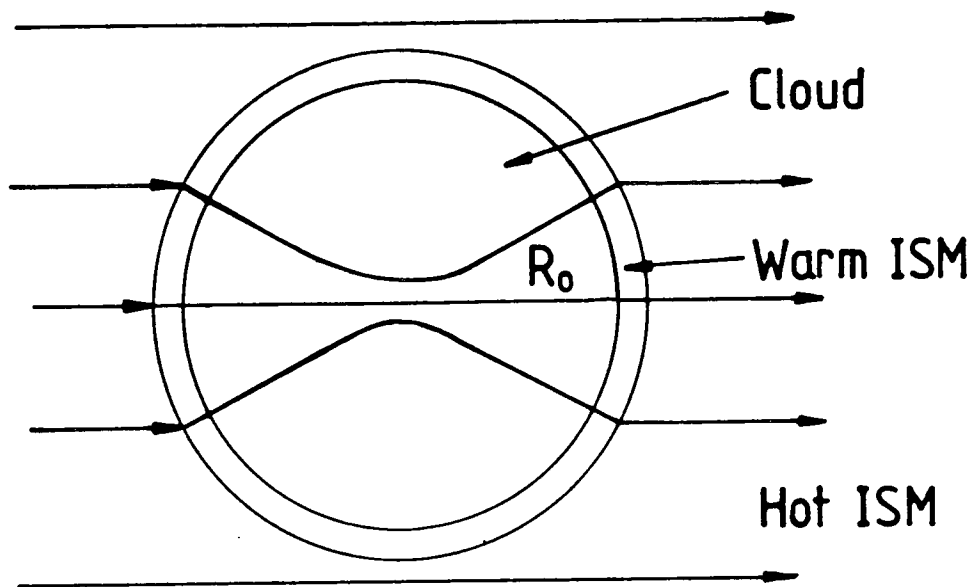
according to $k \gtrless k_D$ (see footnote). (B = magnetic field (Gauss), n_i = fractional ionisation of plasma, n_H = number density in plasma, m_p = proton rest mass) so that little confinement could be expected on that hypothesis (for CR's above 540 MeV/nucleon), even if the energy to maintain the waves against ion-neutral damping were to be available. (We could imagine a hot ($\sim 10^4 \text{ K}$), thin ($\sim 10^{10} \text{ cm}$), 100% ionised, low-density ($\sim 10^{-2} \text{ cm}^{-3}$) 'rarefaction' zone behind the cloud travelling at roughly three times (actually $2/(\gamma_g - 1)$ where γ_g is the specific heat ratio for the background gas; probably 5/3) the isothermal sound speed to contain such self-excited or gravitationally-driven waves (see Figure 2.9): if MHD instabilities of (say) the Kelvin-Helmholtz or flux-interchange type were

¹ The cosmic rays are decoupled from the motion of the neutrals or not according to

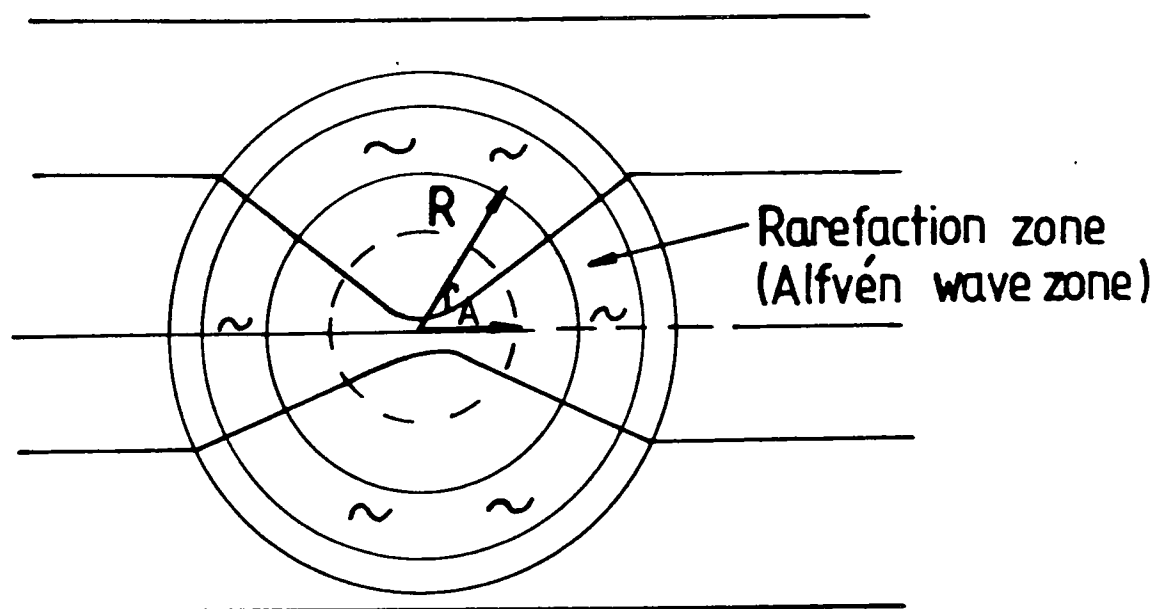
$$k \gtrless k_D = v_i / 2 V_A^* = 1.8 \times 10^{-18} \left(\frac{n_H}{1 \text{ cm}^{-3}} \right)^{5/6} \left(\frac{n_i}{10^{-6}} \right)^{-1/2} \left(\frac{B_0}{3 \mu G} \right) \text{ cm}$$

(where $k(p)$ is the wave-number of Alfvén waves whose wavelength is the gyro-radius of CR's at momentum p , and v_i the ion-neutral collision frequency for protons with H_2 molecules. The critically-damped case (Kulsrud and Pearce 1969) $k_D^* <$

$k < k_D$ will not be considered here. The above condition is satisfied for CR's above 540 MeV/nucleon throughout the motion.



a) Initial conditions



b) Formation of rarefaction (Alfvén wave) zone and shock possibly at "accretion radius."

Fig. 2.9 Collapse of a magnetized cloud.

R_0	initial cloud radius	during collapse
R	cloud radius	
r_A	"accretion radius"	

to operate in this zone then minimal energy ($\sim 10^{25} \text{ erg s}^{-1}$) would be expended in maintaining against ion-neutral damping an isotropic wave-field which confines the cosmic rays.)¹ Probably the Kelvin-Helmholtz instability creates MHD waves streaming out of the cloud.

Magnetic pinching of the cloud (e.g. Alfvén 1982) offers a solution to both the problem of cosmic ray confinement in the cloud and the fact that the cloud in freefall does not collapse fast enough to produce an enhancement of cosmic ray intensity (Figure 2.2). A current (closed at large distance) flows through the cloud, the current being more axial than the magnetic field linking the cloud. The maximum rate of collapse is that for the 'classical' Bennett pinch (Bennett 1934) in which the current is purely axial and the magnetic field purely toroidal throughout the motion (see also Alfvén and Carlqvist 1978). The motion of the cloud outer boundary is given

$$\text{by } \frac{\partial \vec{B}}{\partial t} = \text{curl}(\vec{V}_D \times \vec{B}) \Rightarrow B R(t)^2 = B_0 R_0^2 \quad (28a)$$

$$\begin{aligned} n_H(t) m_p \frac{\partial \vec{V}_D}{\partial t} &= \frac{\text{curl}(\vec{B}) \times \vec{B}}{4\pi} = \vec{\nabla} \left(\frac{B^2}{8\pi} \right) - \frac{1}{4\pi} (\vec{B} \cdot \vec{\nabla} \vec{B}) \\ &= - \frac{B^2}{4\pi R(t)} \end{aligned} \quad (28b)$$

in the limit of rapid transfer of momentum from ions to neutrals by collisions, and with the assumption of flux-freezing (V_D = ion drift speed, B = magnetic field (Gauss)). Hence

¹ For an initial magnetic field of $3 \mu\text{G}$, a 1 GeV proton at cloud density 600 cm^{-3} has gyroradius 10^9 cm , less than the width of this zone. The total rate of gravitational energy released is ten orders of magnitude greater than that expended in confinement of CR.

$$\frac{d^2 R(t)}{dt^2} = - \left[\frac{B_0^2 R_0^3}{m_p n_H(0)} \right] \cdot \frac{1}{R(t)^2} \quad (28c)$$

A timescale t_{mag} for this process is given by

$$t_{\text{mag}} \lesssim 10^{-15} t_f \quad \text{for a typical GMC and } n_H(0) = 1 \text{ cm}^{-3}; \quad (29)$$

$B_0 = 3 \mu\text{G} ; \text{ mass} = 5 \times 10^5 \text{ solar masses.}$

Mestel (1965) notes that a spherical magnetized cloud may be subject to contractive magnetic pinch forces.

In practice, the collapse timescale for scattering centres is limited by ambipolar diffusion to $t_{\text{mag}} \lesssim \frac{R(t)}{v_A}$ or $\frac{R(t)}{v_A^*}$ as appropriate. Hence some CR may be left behind by the cloud (good for star formation). Note, in passing, that the currents flowing in the cloud may, in principle, take the form of small self-pinch loops. Their size may be dictated by the condition that the pinch magnetic pressure is initially nearly balanced by the gas thermal pressure, just as the Jeans' mass (e.g. Spitzer 1978) is dictated by the initial near balance of self-gravitational and thermal pressures. We do not discuss fragmentation here.

The cosmic rays will mirror from the pinched magnetic field by scattering in which the magnetic moment is conserved. The proportion r of an initially isotropic distribution of cosmic rays returning to the cloud is given by

$$r = 1 - \frac{\int_{-\theta_0}^{\theta_0} \sin^2 \theta d\theta}{\int_{-\pi/2}^{\pi/2} \sin^2 \theta d\theta}, \text{ with } \sin^2 \theta_0 = \frac{B_{\text{min}}}{B_{\text{max}}} \quad (30a)$$

For

$$\theta_0 \ll 1, \quad r \approx \frac{2}{3\pi} \left(\frac{B_{\text{min}}}{B_{\text{max}}} \right)^{3/2} \quad (30b)$$

where B_{\min} is the minimum field along the line of force and B_{\max} the maximum. The magnetic field configuration reported by Mestel (1966) yields a peak value B_{\max} (at fractional density increase 10^3), given by

$$B_{\max} \approx B_0 \left(\frac{n_H(t)}{n_H(0)} \right)^{2/3} \quad (31a)$$

and minimum value B_{\min} (a = isothermal sound speed outside cloud; 10^4 K). For $0 \leq \cos \theta \leq \eta$, B_{\min} is given by:

$$B_{\min} \sim B_0 \eta; \quad \eta \simeq \frac{4}{A} \quad \text{where } A \sim 1.7 \times 10^2 B_0^2 / (8\pi m_p n_H(0) \times a^2) \quad (31b)$$

corresponding to cloud density $n_H(t) = 1000 \text{ cm}^{-3}$. Hence the mean time to escape for CR's trapped by the pinch

effect is given by t_{pinch} for a typical GMC and initial density 1 cm^{-3} .

$$t_{\text{pinch}} = 4.6 \times 10^4 (P/GV)^{-1/2} \left[\left(\frac{n_H}{1 \text{ cm}^{-3}} \right)^{1/3} + 0.24 \left(\frac{n_H}{1 \text{ cm}^{-3}} \right)^{2/3} \right] \text{ years} \quad (32)$$

Figures 2.10 and 2.11 show the results of a typical GMC collapse, following this discussion.

A relevant point to note here is that the magnetic field does not always slow the collapse, even though the tension in the field lines and turbulence (if present) would slow collapse by a factor $\sqrt{3}$ if their energy densities $B^2/8\pi$ and $(\delta B)^2/8\pi$ were to be in equipartition with the kinetic energy density. The factor ~ 3 quoted by Lequeux (1977) might be due to either the gas pressure (Larson 1969a,b) or magnetic fields. A further magnetic phenomenon which may assist collapse is the Parker Instability (Parker 1969, see also Blitz and Shu 1980).

2.3.3. Cold spherical magnetized rotating cloud.

Cloud rotation might create a ridge of enhanced spirals magnetic field at the surface of the cloud (or collapsing

Pinch effect escape timescale and remaining
time to complete collapse V Cloud density

Curve a, 1GeV; b, 10GeV

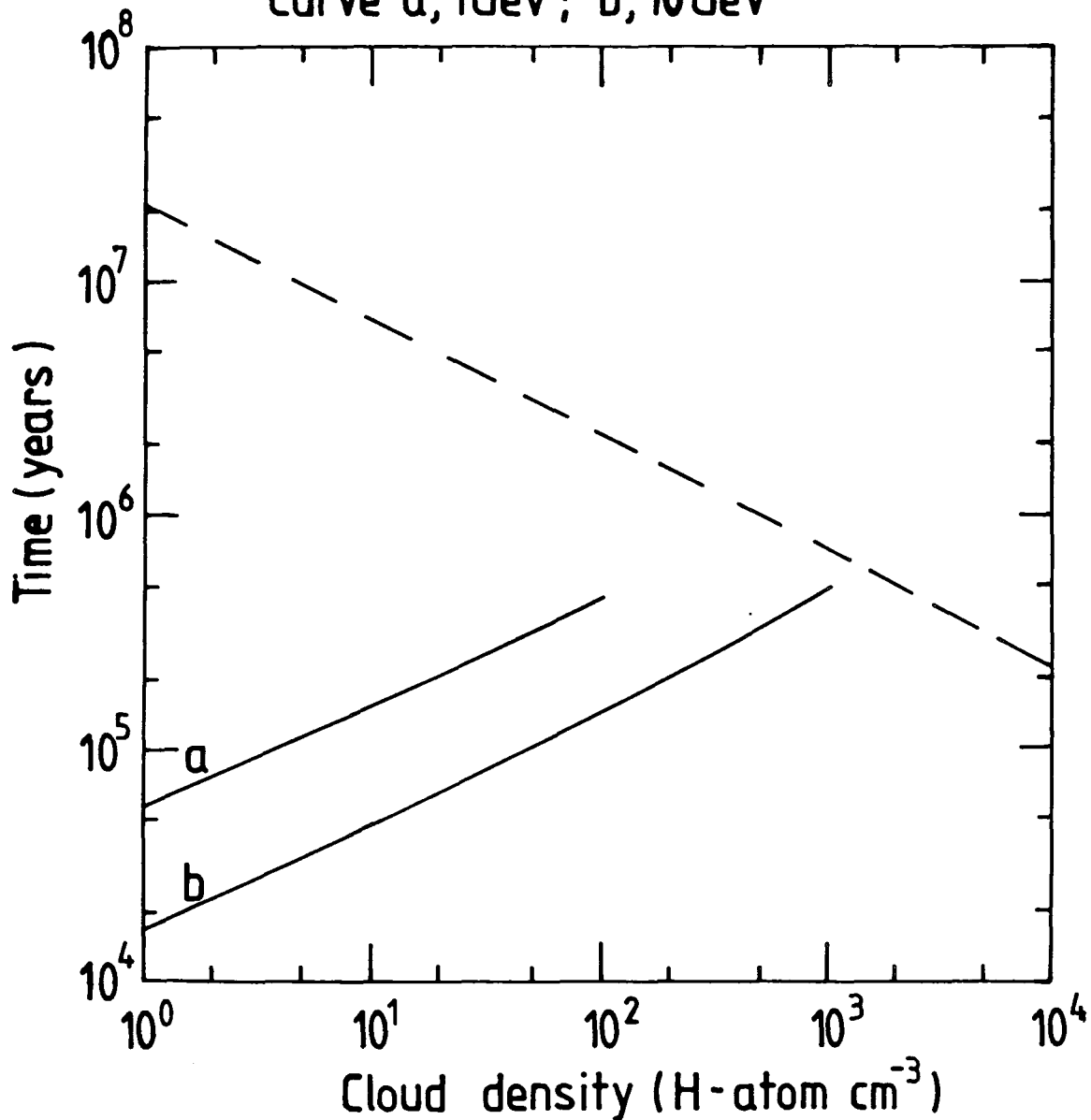


Fig. 2.10 Pinch-effect escape timescale and remaining time to complete collapse V Cloud density, for a typical GMC in Kiraly flow. The magnetic field is taken to be enhanced locally by a factor 100, in a narrow equatorial zone ($0 < \cos(\theta) < 0.04$), at 3 x Cloud radius (cf. Mestel 1966). The Cosmic Ray diffusion coefficient in the cloud is taken to be

$$^{(1/3)}\beta \text{ c (1 pc) } n_H^{-2/3} \cdot (p/GV)^{+0.5}$$

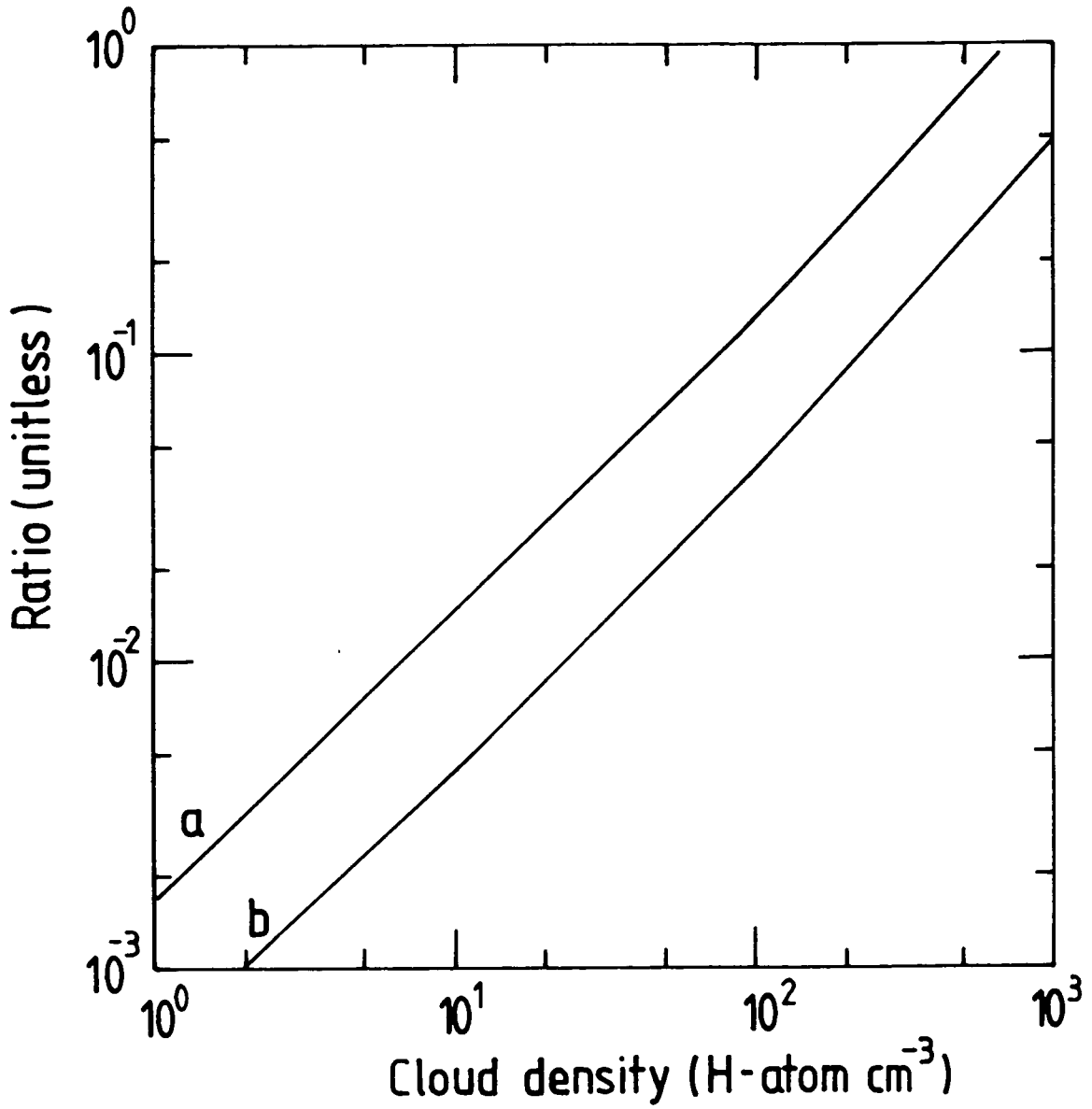


Fig. 2.11 Ratio of acceleration to loss or (pinch-effect) escape rate, for test-particle cosmic rays compressed in a typical GMC in Kiraly flow.
Curve a, 1 GeV; b, 10 GeV.

fragment) the flux being expelled on a timescale long compared with the rotation period but at most comparable with the freefall timescale (Parker 1969) when the rotation axis is perpendicular to the initial magnetic field. The component of magnetic field along the rotation axis is unaffected. In the reference frame of the cloud, the rotating magnetic field appears as a time-varying electric field: this phenomenon is the familiar 'skin effect' associated with the transmission of high-frequency currents along a conductor (Parker 1969) and the depth of the skin is the same. If the magnetic Reynolds number is R_m and the collapse speed is V , the magnetic field is wound up and amplified to a maximum of equipartition with the kinetic energy density ($\frac{1}{2}\rho v^2$), where the time-asymptotic peak field B_{max} is nB_0 , where n is the number of rotations since the onset of collapse. This field strength decreases exponentially into the cloud as

$$B(r) = B_{max} \cdot \exp(-r/\delta) ; \delta \approx \frac{6.5 \times 10^5}{W^{1/2}} \text{ cm} \quad (33)$$

(gas temperature $\sim 10K$, partly ionised) where δ is the skin-depth, w the rotation angular speed, and B_0 the initial magnetic field. The proportion of cosmic rays, r , returning to the cloud is asymptotically

$$r = 1 - (2/3) R_m^{-1/2} \sim 1 - 7 \times 10^{-6} \text{ at } 1 \text{ GeV/nucleon} \quad (34)$$

by equation (30b). An upper limit of $R_m^{1/3} B_0$ is set by the diffusion (reconnection) of oppositely directed field strands into each other. Observational evidence (M. Scarrott, personal communication), obtained by optical polarimetry (which probes the alignment of dust grains

in magnetic fields), indicates that the clouds observed to rotate do so with their rotation axis parallel to the magnetic field, and moreover appear to have rotated only a few times. The component perpendicular to the initial magnetic field has probably been damped very rapidly by magnetic braking. This phenomenon (Mestel 1965, Parker 1969, Piddington 1977), essentially the loss of cloud angular momentum by the transport of long wavelength ($\gtrsim 1$ parsec) magnetosonic waves out of the cloud, has often been considered in an attempt to resolve the well-known problem that a cloud initially rotating with the Galactic rotation angular speed ($\omega = 10^{-15} \text{ s}^{-1}$) (the equipartition speed is roughly five times higher for a typical GMC), cannot collapse to stellar densities due to the centripetal force acting on the matter, if the angular momentum is conserved. Three-dimensional simulations of the collapse of a rotating magnetised interstellar cloud (Dorfi 1982) show that the transport of angular momentum by the torque transmitted by magnetic fields is very effective. Furthermore, long linear plasma waves are preferentially damped by accelerating cosmic rays (and gas) whose mean free path for scattering is much less than the wavelength (Ptuskin 1981). If we assume the waves to be ejected with the Alfvén speed V_A relative to the rotating fragment, and the gas to be the principal load on the system, the wave growth rate Γ_R^+ (and angular momentum loss rate) is given by

$$\Gamma_R^+ = \frac{1}{\omega} \left| \frac{d\omega}{dt} \right| = \frac{5 (\pi n_H m_p)^{\frac{1}{2}} B R^2}{4 M} = 3.8 \times 10^{-15} \left(\frac{B_0}{3 \mu G} \right) \left(\frac{n_H(0)}{1 \text{ cm}^{-3}} \right)^{-1/6} \times M_5^{-\frac{1}{2}} \text{ s}^{-1}$$

(35)

for the case when the rotation axis is parallel to the initial magnetic field. When the rotation axis is perpendicular to the initial magnetic field, we will adopt a value for Γ_R^+ a factor of ten larger, (e.g. Spitzer 1978, Dorfi 1982). The damping rate Γ_R^- is a maximum for these (fast) magnetosonic waves travelling at an angle θ to the magnetic field lines and is given by

$$\Gamma_R^- = \eta \left(\frac{\epsilon_0 + P_0}{P_0 \cdot K_{||}} \right) \cdot \frac{\tan^2 \theta}{(1 + \sin^2 \theta) [1 + (K_{\perp}/K_{||}) \tan^2 \theta]} \quad (36)$$

$$\sim 3 \times 10^{-16} \left(\frac{10^{28} \text{ cm}^{-2} \text{ s}^{-1}}{K_{||}} \right) \left(\frac{0.1 \text{ cm}^{-3}}{n_H} \right)$$

(Ptuskin 1981). Hence an initially isotropic distribution of cosmic rays (if re-isotropised by some scattering, perhaps caused by mirror or firehose instabilities) (for the usual case $K_{\perp}/K_{||} \ll 1$) is accelerated in momentum at a rate t_R^{-1}

$$t_R^{-1} = \frac{1}{p} \frac{dp}{dt} = \frac{2}{3} M R(t) R_0 \omega_0^2 \Gamma_R^- \Gamma_R^+ \exp(-\Gamma_R^+ t) \quad (37)$$

for a uniform gas cloud. Non-uniformity increases the numerical value ($\frac{2}{3}$). Rotation slows the collapse due to the centripetal force acting on the gas, so the motion of the cloud boundary is adequately given by the expressions without considering rotation, if the accretion is considered to take place essentially within a funnel of semi-angle ψ given by

$$\psi = \sin^{-1} \left(\frac{GM}{R^3 \omega^2} \right) = \sin^{-1} \left(0.47 \left(\frac{n_H(0)}{1 \text{ cm}^{-3}} \right) \cdot \frac{1}{\omega_{-15}^2} \right) \quad (38)$$

The cloud will not collapse steadily unless the ratio of the rotational to gravitational energy is initially less than ~ 0.42 (Larson 1972) (even so, the gas may

undergo a 'centripetal bounce'). Energy is transferred from the waves (coupled to the gas) to the high energy CR (which resonate with shorter wavelength waves decoupled from the motion of the neutrals) via cascading down to the wavelengths just mentioned, followed by ion-neutral collisions which stir up Alfvén mode waves and then scatter CR¹. Hence the high energy CR are accelerated in momentum at a rate t_R^{*-1}

$$t_R^{*-1} = \frac{1}{p} \frac{dp}{dt} = \Gamma_{i-n}^- \Gamma_R^+ t_R^{-1} \quad (39)$$

where Γ_{i-n}^- is the ion-neutral damping rate in hydrogen:

$$\Gamma_{i-n}^- = 10^{-9} \left(\frac{T}{10^3 K} \right)^{-0.4} s^{-1} \text{ (e.g. Kulsrud and Pearce$$

1969). We see at once that the wave-zone close to the cloud outer boundary is that most favourable to this mechanism.

It is important to note that, in an isotropic uniform collapse, the gravitational and magnetic energy densities are proportional to $R(t)^{-4}$. If angular momentum were to be conserved, and collapse still physically possible, the rotational kinetic energy density would be proportional to $R(t)^{-5}$. The cloud would not collapse to a density beyond that which the rotational and infall kinetic energies were in balance (except, perhaps for a 'bounce'). Observations (e.g. Lequeux 1977, review) appear to indicate that, if anything, the angular velocity is conserved during

¹ Kinetic Alfvén waves (which occur in a warm plasma) may scatter CR and are compressible to first order in kinematic viscosity.

collapse. If the rotational kinetic energy has been transferred to cosmic rays, (magnetic braking ...) and all this energy were to remain in the cloud (a likely occurrence if a magnetic bottle were to be formed), CR's would be accelerated at a rate t_R^{-1} given by

$$t_R^{-1} = \frac{1}{p} \frac{dp}{dt} = \frac{5 \dot{R}(t)}{R(t)} \quad (40)$$

This is faster than the pure compression acceleration (see Figure 2.12).

This calculation may be applied to both the cloud and collapsing fragments. For a typical GMC 'core' (mass 20-30 M_\odot , radius ~ 1 parsec, density $\sim 10^{10} \text{ cm}^{-3}$) this acceleration rate amounts to $10^{26} \text{ erg s}^{-1}$, perhaps more effective than adiabatic acceleration, but also a means of transferring cloud angular momentum to cosmic rays which then possibly leave the cloud rapidly removed at the Alfvén speed V_A on timescale t_A (or V_A^* of t_A^*)

$$t_A = \frac{R(t)}{V_A} = 1.4 \times 10^7 \left(\frac{M_5}{n_H(t)} \right)^{1/3} \cdot \left(\frac{n_H(t)}{1 \text{ cm}^{-3}} \right)^{-1/6} \cdot \frac{1}{(B_0 / 3 \mu G)} \text{ years} \quad (41a)$$

$$t_A^* = R(t)/V_A^* = t_A \cdot n_i^{-1/2} \sim t_A / 1000 \quad (41b)$$

The ratio of the rotational to collapse kinetic energies in the cloud is roughly given by

$$E_{\text{Rot}}/E_{\text{Kin}} = \frac{(3/10) M R^2 \omega_0^2 \sin^2 \phi}{(3/10) M \dot{R}^2} = \left(\frac{R \omega \sin \phi}{V} \right)^2 \quad (42)$$

The angle ψ between the normal to the magnetic field lines and the infall velocity of the scattering centres \vec{V} is given by

$$\tan \psi = \frac{R \omega \sin \phi}{V} = 3 \left(\frac{M_5}{n_H(0)} \right)^{1/3} \cdot \frac{\omega_{-15} \sin \phi}{V (\text{km s}^{-1})} \quad (43)$$

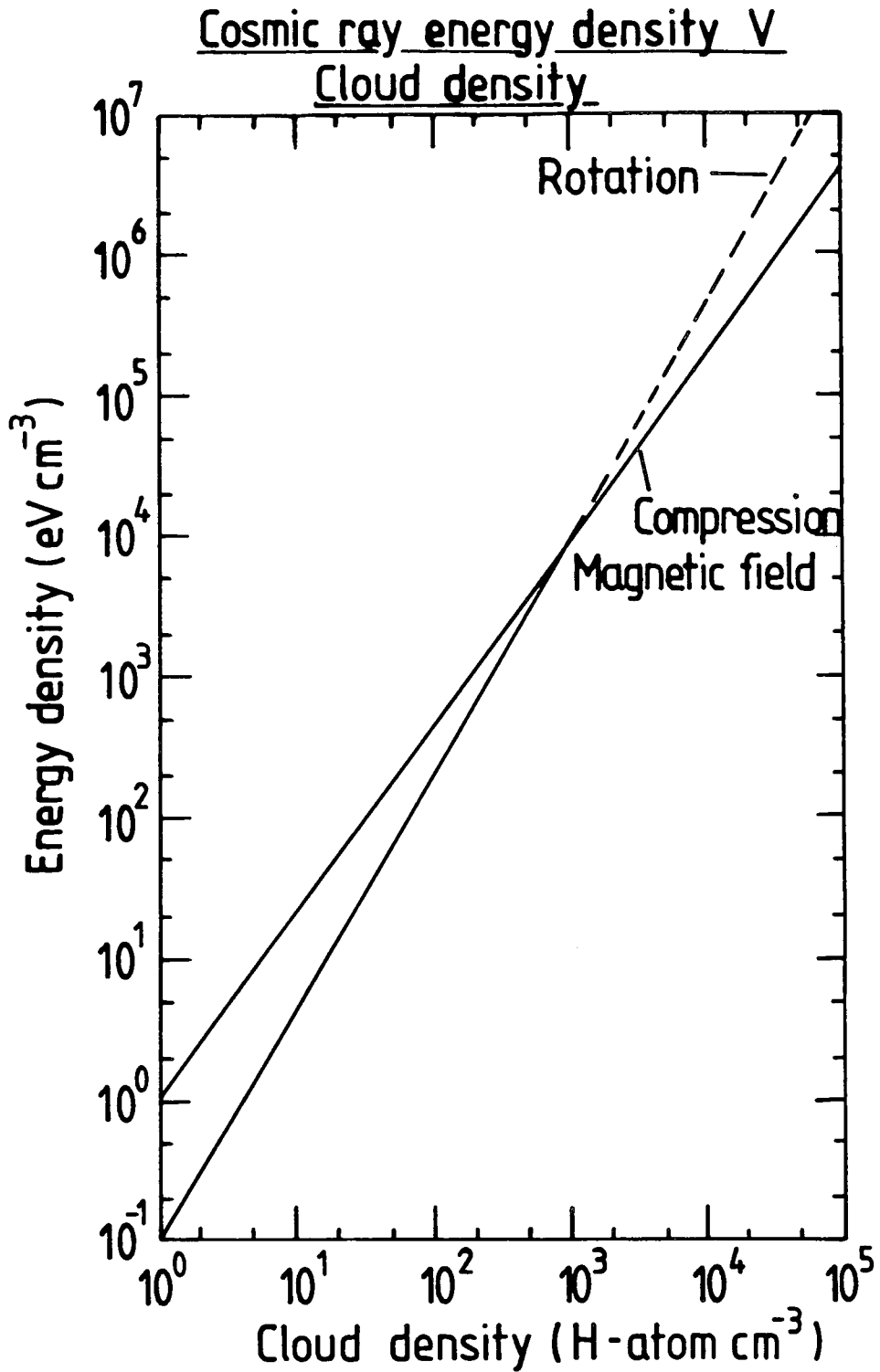


Fig. 2.12. Upper limit to Cosmic Ray energy density ν Cloud density for the adiabatic compression of test particle cosmic rays in a rotating typical GMC during isotropic collapse.

(Mass = $5 \times 10^5 M_{\odot}$, initial uniform density = 1 H-atom cm^{-3} , initial angular speed = 10^{-15} s^{-1}).

in strict analogy with the case for the solar wind (see review by Jokipii 1971), where ϕ is the latitude ($\pi/2$ on equator), and solid body rotation out to the cloud boundary is assumed.

It has been recently noticed that the effect is sufficient to prevent acceleration of cosmic rays and ions at the stellar terminal shock of an OB star (typically, $2\pi/\omega = 10^6 \text{ s}^{-1}$, shock radius = 2 parsec, wind speed $V = 2000 \text{ km s}^{-1}$; Jokipii 1968, Cassé and Paul 1980, Fisk 1969, Volk and Forman 1981, Axford 1981a,b,c, Webb et al. 1982) unless the wind is gusty, as the cosmic ray diffusion coefficient for isotropic magnetic scattering is reduced so that the particles cannot move upstream from the shock to repeat the acceleration cycle.

Cloud rotation reduces the isotropic component K_{rr} of the CR diffusion coefficient according to

$$K_{rr} = K_{\parallel} \cos^2 \psi + K_{\perp} \sin^2 \psi \quad (44)$$

where K_{\parallel} and K_{\perp} refer to the diffusion coefficients parallel to, and perpendicular to the magnetic field respectively, and ψ is the angle between the normal to the magnetic field lines and the infall velocity of the scattering centres given by equation (2b). However, K_{\parallel} and K_{\perp} satisfy

$$K_{\parallel} \cdot K_{\perp} = K_B^2 : K_B = \frac{1}{3} \beta c r_g(B) = 10^{14} \beta \cdot \frac{(\text{pc/eV})}{(B_0/\mu\text{G})} \cdot \left(\frac{n_H(0)}{n_H(t)} \right)^{2/3} \text{ cm}^2 \text{ s}^{-1} \quad (45)$$

assuming flux-freezing where K_B is the 'Bohm' diffusion coefficient, i.e. when the mean free path for magnetic scattering is the gyroradius (its smallest possible value).

Unfortunately, to confine the cosmic rays, the rotation must also reduce the gas accretion rate (here of course we assume that CR particles are well bound to their magnetic line of force). The Archimedean spiral form of magnetic field (e.g. Parker (1969)):

$$B(R) = B_0 (R_0/R)^2 [1 + (R\omega/\dot{R})^2 \sin^2 \phi]^{1/2}$$

$$= \left(\frac{B_0}{\mu G} \right) \left(\frac{n_H(t)}{n_H(0)} \right)^{2/3} \left[1 + \left(3 \left(\frac{M_5}{n_H(0)} \right)^{1/3} \frac{\omega_{-15} \sin \phi}{\dot{R} (km s^{-1})} \right)^2 \right]^{1/2} \mu G \quad (46)$$

shows a magnetic field decreasing (for strong uniform rotation) with radius to the power -1. Betatron CR oscillations in such a magnetic field are not stable. The guiding centres of CR's, whose momentum p is less than the critical momentum $p^*(t)$, given by

$$\frac{p^*(t)c}{eV} = p_{max}(t) \left[1 + \left(3 \left(\frac{M_5}{n_H(0)} \right)^{1/3} \frac{\omega_{-15} \sin \phi}{\dot{R} (km s^{-1})} \right)^2 \right] \quad (47)$$

(with $P_{max}(t)$ defined by equation (9) above) are likely to spiral inwards, whilst those whose momentum is greater than p^* are likely to slowly spiral outwards. In this sense, the magnetic field traps particles.

Figure 2.12 shows the results of a typical GMC collapse, following this discussion.

2.3.4 Is there any evidence for enhanced magnetic fields in clouds?. The best evidence for the existence of enhanced magnetic fields in clouds is the 21cm Zeeman effect measurements on clouds of interstellar density ($\sim 1cm^{-3}$) to OH-maser densities ($\sim 10^8 cm^{-3}$) by the Manchester Group (Davies 1982) although some measurements have since been made for a smaller range by Heiles, Troland

Magnetic field v HI density

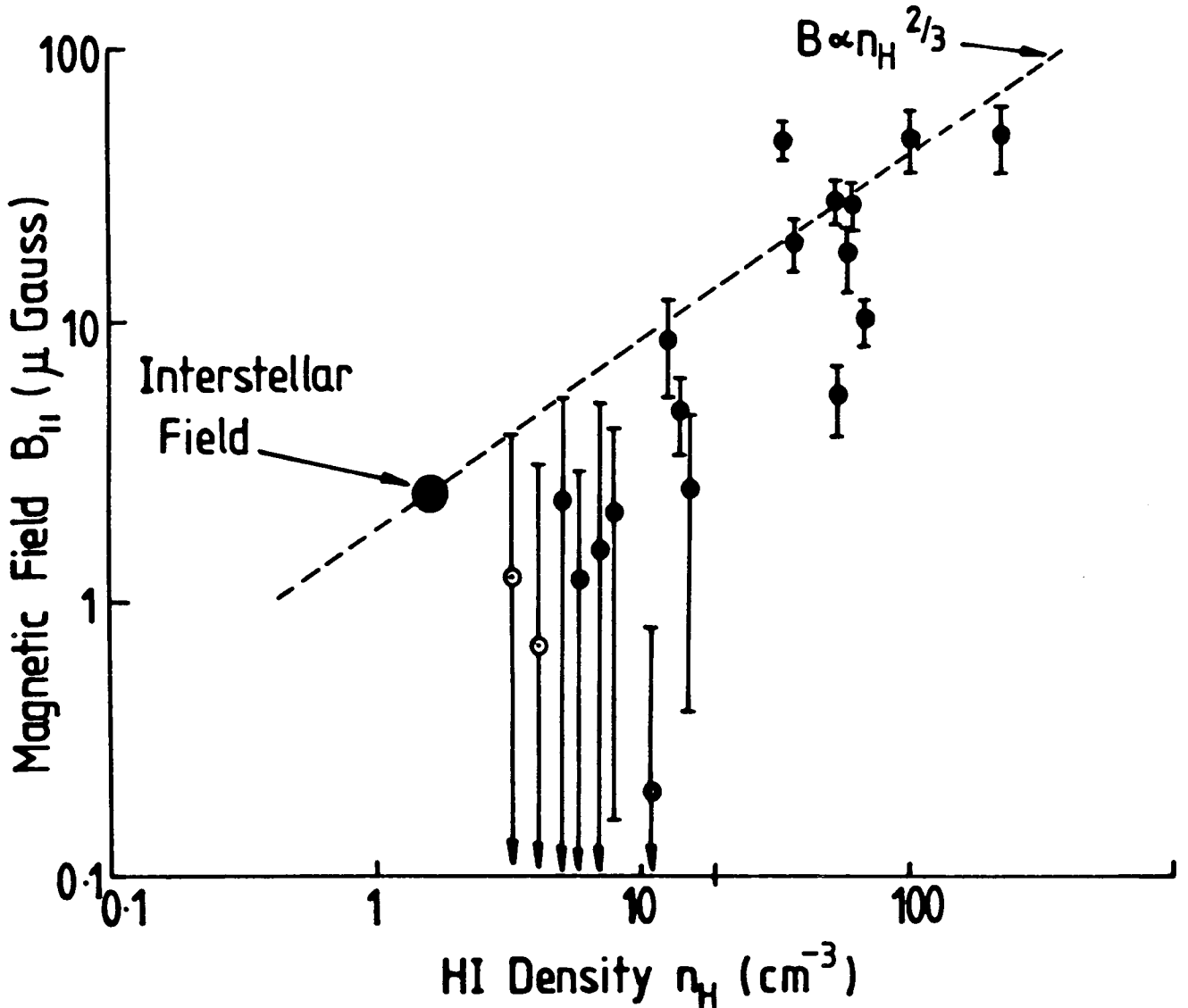


Fig. 2.13 The line-of-sight component of magnetic field ($B_{||}$) measured by the 21cm Zeeman splitting effect, plotted against the estimated HI density (n_H). The filled circle represents the interstellar magnetic field measured from pulsar Faraday rotation; the assigned gas density is the mean density in spiral arms. The two lowest points with heavy error bars represent the mean magnetic fields found in the Orion and Perseus spiral arms. The dashed line is the relation $B \propto n_H^{2/3}$ expected for the isotropic collapse of a self-gravitating gas cloud with frozen-in magnetic field.

(after Davies 1982)

and Stevens (1982a,b). The results (Figure 2.13, taken from Davies' paper) show a remarkable power-law increase in magnetic field with density. The law

$$B = (1 \text{ to } 3 \mu G) \left(\frac{n_H}{1 \text{ cm}^{-3}} \right)^\alpha; \alpha = 0.47 \pm 0.05 \quad (48)$$

(preserving the direction of the mean field) may well have some theoretical interpretation such as the conservation of magnetic flux during the anisotropic collapse of a magnetized cloud of very high electrical conductivity (Mouschovias, 1976a,b, Mouschovias, and Paleologou, 1979, Elmegreen 1980, Scott and Black 1980). There is some debate about the magnitude of the magnetic field in the emission clouds ($\sim 1 \text{ cm}^{-3}$) in which the seed magnetic field may reside, in addition to that concerning the clouds which lie within the hot bubble of gas close to our Solar System (Loop I).

We next consider the cooling of external ambient cosmic rays by the retreating magnetic mirror and rarefaction region behind the cloud.

2.3.5 Cooling of external ambient cosmic rays.

The rarefaction region behind the cloud decelerates ambient cosmic rays by adiabatic cooling. A larger number of ambient cosmic rays would be cooled than heated by the retreating magnetic mirror. The reduction in cosmic ray intensity behind the cloud is given by the general expression

$$F = \left(\frac{n_H(t)}{n_H(0)} \right)^{4/3} \cdot \exp \left[-(\gamma-1) \left\{ \int_0^t \left(\frac{\beta c m_p n_H(t')}{X} + \frac{1}{t_{esc}(t')} \right) dt' \right\} \right] \quad (49)$$

(if CR's escape) where $n_H(t)$ is the gas density

at time t in the rarefaction zone, and rotation is not considered behind the cloud (see Hunter 1960, Bodenheimer and Sweigart 1969, Hunter 1977, Shu 1977, Gerola and Glassgold 1980). Penston (1969b) gives a similarity solution valid for hydrodynamic isothermal cloud collapse if the sound crossing time t_s is less than the remaining time to total collapse $t_f - t$.

A plateau develops in the cloud density profile (see Figure 2.14), a power law relation between cloud density and radius then holding beyond the plateau out to the maximum radius where accretion occurs (roughly $R - 3tc_s$, where R is the initial cloud radius and c_s the isothermal sound speed; CR pressure could increase c_s somewhat). The exponent in this power law is $-12/7$ for non-zero temperature, a realistic case (exponent is -2 for absolute zero temperature). In the opposite case, $t_s \gg t_f - t$, the exponent is -5 or -6 ; Gerola and Glassgold 1980.

There are two points to notice:

- (1) A cloud unresolved by the gamma ray detectors (angular width 2 to 4 degrees) may show no enhancement, even if the central region were to be enhanced, as the envelope will show a reduction in CR intensity.
- (2) The contrast in gamma rays across a GMC may be increased by this effect. In particular, the exponent in any power law relation between gamma-ray flux and gas density would be altered from roughly

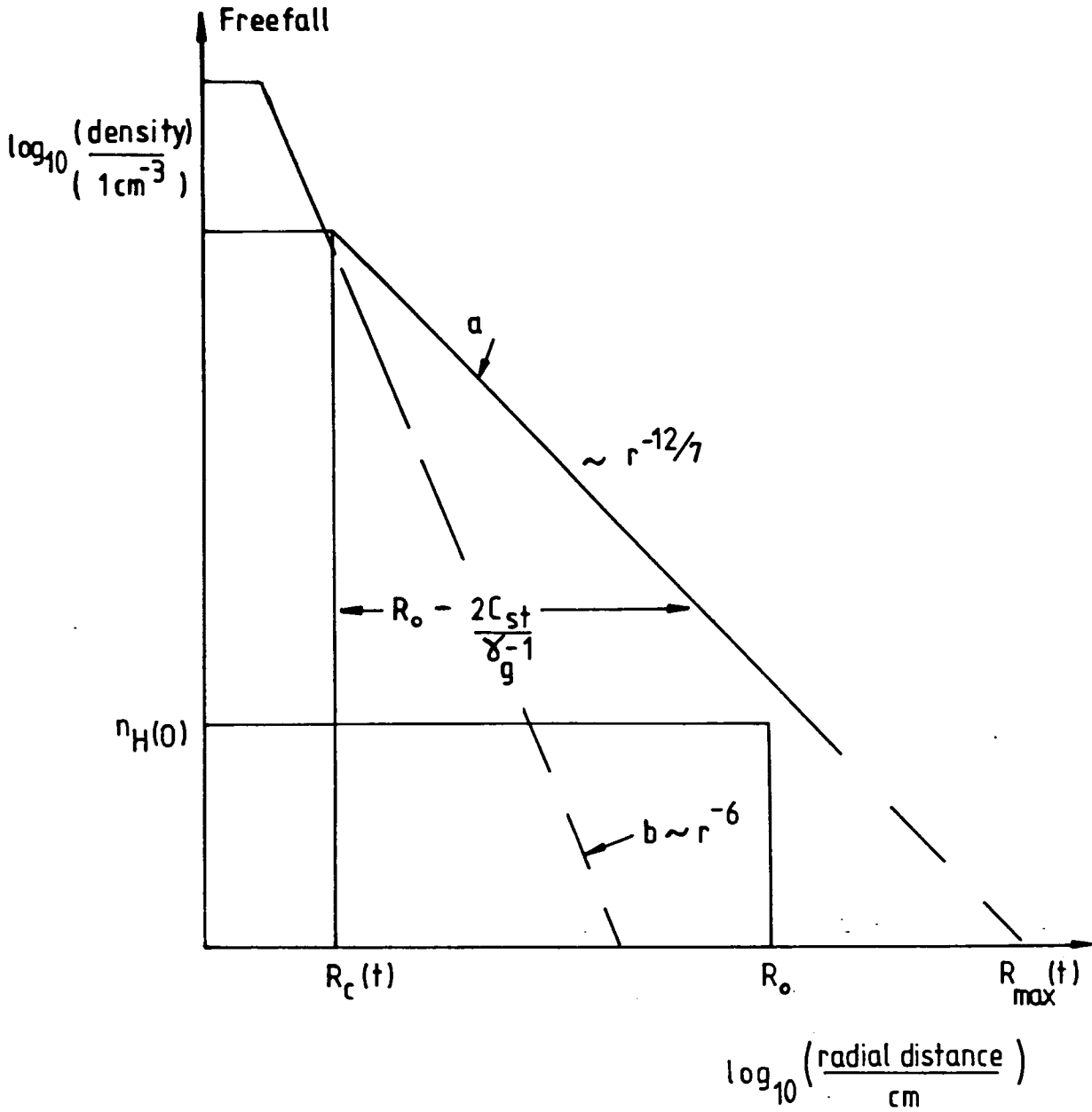


Fig. 2.14. Schematic gas density distribution for collapsing gas cloud.

Curve a, freefall time \gtrsim sound crossing time;

b, freefall time \ll sound crossing time.

γ_g isothermal gas specific heat ratio.

C_s isothermal sound speed

t time elapsed since onset of collapse

$R_{\text{max}}(t)$ radius within which the cloud initial mass resides.

$$1 \text{ (for } B \propto n_H^{\frac{1}{2}} \text{) or} \quad (50a)$$

$$4/3 \text{ (for isotropic collapse, } B \propto n_H^{\frac{2}{3}} \text{)} \quad (50b)$$

$$\text{to } \left(\frac{n_H}{F} \right) \left(\frac{\partial F}{\partial n_H} \right) \quad (50c)$$

(see Houston and Wolfendale 1984), in the presence of energy loss.

It should be noted that the result obtained by Houston and Wolfendale (1984), for the Orion molecular cloud complex, (a minimum χ^2 'best exponent' of 0.8, with 0.5 and 3 equally likely values, at a one standard deviation confidence level) holds only between gamma-ray intensities and cloud densities convolved down to the resolution of the COS B gamma-ray detector (about 3 degrees). In reality, the relation between cosmic ray intensity and gas density might be considerably sharper.

2.4 Summary and Conclusions

The main results and conclusions of this chapter are:

- * The cloud must collapse faster than freefall to produce an enhancement of cosmic ray intensity by adiabatic acceleration.
- * The necessary increase in speed may be achieved by self-pinching of the cloud magnetic field, or external compression of the cloud.
- * Cloud rotation may improve trapping of the cosmic rays, and also transfer energy to them.
- * The run of cosmic ray enhancement with gas density may (in principle) be modelled, including the effects of energy loss.

CHAPTER 3

3. Can Cosmic Rays be Accelerated in Collapsing Molecular Clouds? (Part II)

3.1 Introduction

In this chapter, we move on now to consider the important topic of acceleration of cosmic rays inside the cloud by shock waves.

The plan of this chapter is as follows:

In Section 2, the shock acceleration of cosmic rays trapped inside the cloud will be discussed.

In Section 3, the model predictions will be compared with the gamma-ray observations, and the Carina Nebula (η Carinae), the most enhanced cloud detected to date ($F \sim 16$) will be modelled.

Section 4 is a discussion of wider implications for Galactic and Protogalactic p Origin hypotheses, including the hierarchical collapse of protogalaxies.

Finally, Section 5 is a brief summary of the main results and conclusions.

3.2 Shock Acceleration of Cosmic Rays trapped inside the cloud

Cosmic rays may be further accelerated by shock waves within the cloud. The shock waves may be caused by:

- (a) an external shock wave compressing the cloud, creating a sound wave which increases in amplitude as it approaches the centre of the cloud on which it is focused (e.g. Landau and Lifshitz 1959).

- (b) an incipient shock wave which forms due to the supersonic collapse, most probably at the 'sonic point', where the flow decelerates from super- to subsonic at the 'accretion radius' $r_A \sim R(t)/10$ (say) (Larson 1969a),
- (c) a shock wave which forms at a later stage of cloud collapse when the central density in a very non-uniform collapse has reached $\sim 10^{10} \text{ cm}^{-3}$, so that the core is opaque to Infrared radiation and cannot cool rapidly, presenting a nearly incompressible object to the supersonic inflow of matter (Larson 1969a,b; Penston 1969a, Larson 1973 (review)),
- (d) a shock wave which forms in a rotating cloud when the innermost parts undergo a 'centripetal bounce' and meet the infalling envelope. Other types of discontinuity are possible in this case - see the simulation studies undertaken by Larson 1972, Larson 1973 (review), Tscharnuter 1975, Black and Bodenheimer 1976, Rozyczka et al. 1980, Dorfi 1982 (including the effects of a flux-frozen magnetic field on the collapse),
- (e) the shock waves caused by rotation in a cloud (or indeed galaxy) - possibly 'spiral arms',
- (f) shock waves caused by collisions between turbulent units (e.g. collapsing fragments of the cloud),
- (g) shock waves connected with sources of cosmic rays within the cloud, viz: stellar winds, buried supernovae (which use thermonuclear energy), compact objects (neutron stars whose spin has decayed, black holes...) etc.

Consider a shock wave located at distance $r(t)$ from the centre of the cloud and converging on it at speed $V(r, t)$

$$V(r, t) = r(t) \frac{\dot{R}(t)}{R(t)} + C_s(t) \quad (R = \text{cloud radius}) \quad (1)$$

where $C_s(t)$ is the isothermal sound speed which, in the test-particle and weak magnetic field approximation will not be much increased by cosmic ray or magnetic pressure.

Let $k_{rr}(r, p, t)$ represent the isotropic part of the diffusion coefficient for cosmic ray (CR) particles, and $f(r, p, t)$ represent the concentration of CR's in phase space; the number density in 'ordinary' space $n(r, p, t)$ per unit $|p|$ is related to f by

$$n(r, p, t) = 4\pi p^2 f(r, p, t) \quad (2)$$

The CR transport equation, valid to $O(V/\beta c)^2$ is

$$\frac{\partial f}{\partial t} - \vec{\nabla} \cdot \underline{K} \vec{\nabla} f + \vec{V} \cdot \vec{\nabla} f - \left(\frac{dp}{dt} \right)^{\text{total}} \frac{\partial f}{\partial p} = 0 \quad (3)$$

where \underline{K} is the CR diffusion tensor (e.g. Jokipii 1971).

If the CR scattering on both sides of the shock is sufficiently strong

$$K_{rr(1,2)} \lesssim 4 R_s V_{(1,2)} \quad \begin{array}{l} V_1 \text{ upstream} \\ V_2 \text{ downstream} \end{array} \quad (4)$$

where R_s is the shock radius, then the shock appears locally plane to the cosmic rays. If the shock width L is greater than the CR gyroradius, $r_g(B)$, the crossing and recrossing of the shock by CR's leads to a momentum acceleration on the timescale (if there are no boundaries for escape or return within the zone of width $2a$ where $Va/K \lesssim 1$)

where

$$t_{acc} = \frac{1}{P} \left(\frac{dp}{dt} \right)^{acc} \approx \frac{3}{V_1 - V_2} \left(\frac{K_1}{V_1} + \frac{K_2}{V_2} \right) \quad (5)$$

for the case where K_1 and K_2 are not functions of momentum (a more general formula is available (Drury 1983, review)), and V_1 , K_1 and V_2 , K_2 refer to each side of the shock respectively (Bell 1978a,b, Michel 1980, Césarsky and Lagage 1981, Axford 1981a,b,c (reviews); Freedman et al. 1979 independently considered the effective reflection coefficient for CR's). The shock will be supersonic, but may be either sub- or super-Alfvénic; the gas may or may not be ionised by the dissipation of energy in the shock front, according as $V_1 \gtrless 10^7 \text{ cm s}^{-1}$, if all that energy were to go into heating the plasma. Case (a) above has been considered by Blandford and Cowie (1982) in an effort to:

1. modify the van der Laan theory of supernova remnant (SNR) evolution to take account of the lumpy ISM and thereby,
2. explain the anomalously high radio and perhaps gamma-ray luminosity of supernova remnants of size $\gtrsim 20$ parsec.

For their purposes, they include the cloud adiabatic compression and CR acceleration by a locally plane strong shock, but neglect the effect of losses or subsequent cloud collapse. The CR pressure sets one upper limit to the acceleration by compression: however CR pressure can mediate a shock (e.g. Eichler 1980, Volk and McKenzie 1982, Achterberg et al. 1984) increasing the width L

so that an ever-decreasing number of ever more energetic particles (with gyroradii $L < r_g(B) < R(t)$) maintain a constant pressure downstream (Drury 1983, review).

To return to our calculation, if the shock is strong (large Mach number) and linear, the compression ratio approaches 4 and

$$t_{acc} \sim \frac{4k}{\dot{R}(t)^2}$$

Incorporating this timescale t_{acc} into the Boltzmann equation, we arrive at the enhancement of cosmic ray intensity F for Model 4 (freefall):

$$F = \left(\frac{n_H(t)}{n_H(0)} \right)^{4/3} \cdot \exp \left[-(\gamma-1) \left\{ \frac{\beta c m_p n_H(0)}{X} \cdot \frac{4 t_f}{\pi} \cdot \left(\tan \alpha + \frac{1}{3} \tan^3 \alpha \right) - \frac{\pi R_0^2}{3 K_0 t_f} \tan^3 \alpha \right\} \right], \quad (5)$$

and for Model 5 ('Kiraly' flow)

$$F = \left(\frac{n_H(t)}{n_H(0)} \right)^{4/3} \cdot \exp \left[-(\gamma-1) \left\{ \frac{\beta c m_p n_H(0)}{X} \cdot 3 t_c \cdot \left(1 - \left(\frac{n_H(t)}{n_H(0)} \right)^{-1/6} - \frac{R_0^2}{9 K_0 t_c} \left[\left(\frac{n_H(t)}{n_H(0)} \right)^{1/2} - 1 \right] \right) \right\} \right] \quad (6)$$

with the momentum p at time t of a particle injected at time $t_0 < t$ with momentum p_0 for Model 4 :

$$p(t) = p_0 \left(\frac{n_H(t)}{n_H(0)} \right)^{4/3} \cdot \exp \left[- \left\{ \frac{\beta c m_p n_H(0)}{X} \cdot \frac{4 t_f}{\pi} \cdot \left(\tan \alpha + \frac{1}{3} \tan^3 \alpha \right) - \frac{\pi R_0^3}{3 K_0 t_f} \tan^3 \alpha \right\} \right], \quad (7)$$

and for Model 5

$$p(t) = p_0 \left(\frac{n_H(t)}{n_H(0)} \right)^{4/3} \cdot \exp \left[- \left\{ \frac{\beta c m_p n_H(0)}{X} \cdot 3 t_c \cdot \left(1 - \left(\frac{n_H(t)}{n_H(0)} \right)^{-1/6} - \frac{R_0^2}{9 K_0 t_c} \left[\left(\frac{n_H(t)}{n_H(0)} \right)^{1/2} - 1 \right] \right) \right\} \right] \quad (8)$$

The diffusion coefficient has been assumed to scale with time according to

$$K(t) = K_0 \left(\frac{B(t)}{B_0} \right) = K_0 \left(\frac{R(t)}{R_0} \right)^2 = K_0 \left(\frac{n_H(t)}{n_H(0)} \right)^{-2/3} \quad (9)$$

and flux-freezing is assumed (the usual restrictions on p hold). This scaling is only required over a very short distance, $2a$ such that $Va/k \lesssim -1$ (in later stages of collapse and with nonionised gas the ion-neutral damping would be a prohibitive energy drain if we were to assume a small diffusion coefficient throughout the cloud, see Césarsky and Volk 1978). Figure 3.1 shows some results of Model 5 for three instructive cases; case (1) where the enhancement F achieves 16 at cloud density 300 molecules of $H \text{ cm}^{-3}$, this being the minimum requirement to model η Carinae by this process, case (2) where the diffusion coefficient is scaled from the typical value in the Hot Interstellar Medium (HISM)

$$K_{\text{HISM}}(p) \sim 10^{28} \left(\frac{p}{\text{GeV}} \right)^\alpha \left(\frac{n_H(t)}{n_H(0)} \right)^{-2/3} \text{ cm}^2 \text{ s}^{-1} \quad (10)$$

and case (3), a smaller value of k than discussed in case (1). The effect of choosing the minimum possible diffusion coefficient for magnetic scattering of CR particles, the 'Bohm' coefficient $K_B(t)$ (given p)

$$K_B(t) = \frac{1}{3} \beta c r_g(t) B(t) = 10^{14} \beta \left(\frac{p}{\text{eV}} \right) \left(\frac{n_H(t)}{n_H(0)} \right)^{-2/3} \left(\frac{B_0}{\mu G} \right) \text{ cm}^2 \text{ s}^{-1} \quad (11)$$

In case (2) $\alpha = 0.35$ to 0.5 for $p < 18 \text{ GeV/c}$ and perhaps $\alpha = 0.7$ for $p > 18 \text{ GeV/c}$ as suggested by an analysis of the very

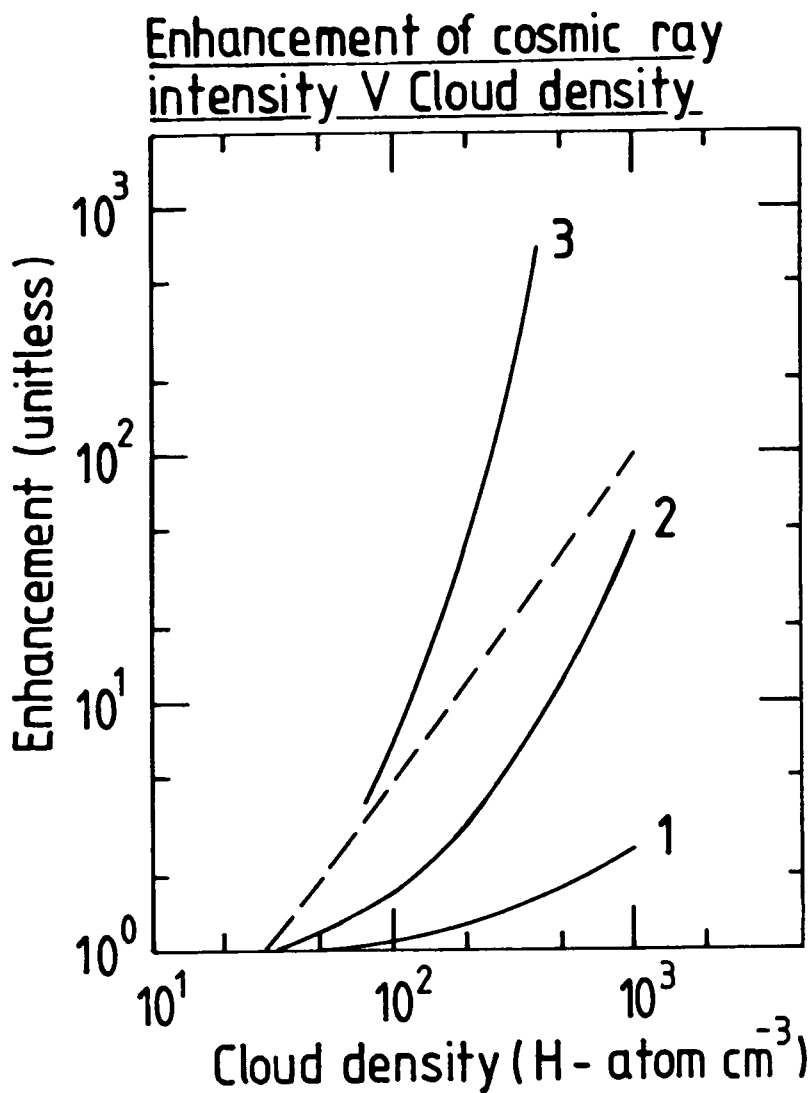


Fig. 3.1 Enhancement of cosmic ray intensity v. Cloud density for a shocked compressed GMC in Kiraly flow.

(Initial density = 30 cm^{-3} , mass = $5 \times 10^5 M_{\odot}$)

Curve 1, $k = 10^{27}$; 2, 3.6×10^{25} ; 3, $10^{25} \text{ cm}^2 \text{ s}^{-1}$.

The dashed line refers to the adiabatic compression of test-particle cosmic rays without energy loss.

precise HEAO-3 satellite cosmic ray abundance measurements (Ormes and Protheroe 1983; references therein). In each case, the initial density was chosen as that of the small clouds, $\sim 30\text{cm}^{-3}$.

This scaling is insufficient to yield appreciable cosmic ray acceleration. The CR's are supposed to be trapped within the cloud, perhaps by magnetic fields.

The energy requirement W for effective acceleration in case (1) is given by

$$W(t) = \Gamma_{i-n}^{-} (n_H(t), T) \cdot 4\pi R^2(t) \cdot \frac{B^2(t)}{8\pi} \cdot \frac{2K_0(B_0/B)}{\dot{R}(t)} \quad (12)$$

where it is assumed that the turbulence is due to cosmic ray streaming instabilities for which the wave growth rate is

$$\Gamma_{CR}^{+} \simeq \frac{\pi}{8} \Omega_0 \frac{n(>1/k)}{n_H(t)} \cdot \left[1 - \left| \frac{V_R}{V_A^*(t)} \right| \right] \quad (13)$$

(Ω_0 = gyroradius of cosmic ray proton, $n(>1/k)$ is the number density of CR's of gyroradius $2\pi/k$, n_H is the number density of neutral atoms, V_R the streaming speed relative to the thermal plasma, and V_A^* the Alfvén speed in the ionised part of the plasma assuming the waves to be coupled to the ions). See Wentzel (1974) for a review, also Césarsky and Volk (1978). The ion-neutral damping rate in a medium of number density n_H at a temperature T (Kelvin) is given by

$$\Gamma_{i-n}^{-} \simeq 10^{-9} \left(\frac{n_H}{1\text{cm}^{-3}} \right) \left(\frac{T}{10^3\text{K}} \right)^{-0.4} \text{ s}^{-1} \quad (14)$$

(Kulsrud and Pearce 1969, McIvor 1981). If the waves are located in a thin zone both upstream and downstream

of the shock of width a , and $Va/K \lesssim -1$, the energy requirement for model 5 (case 1) and temperature 20K obtained by

inserting (14) into (12) is

$$W = 1.9 \times 10^{36} n_H^{5/6} \cdot K_{0.25}^{-1} \cdot M_5^{1/3} \cdot n_H(0) \cdot T_3^{-2/3} \left(\frac{B_0}{3\mu G} \right)^{-0.4} \quad (15)$$

$$\sim 4.6 \times 10^{33} \text{ erg s}^{-1}$$

in the wave-zone where $n_H = 300 \text{ cm}^{-3}$, $n_H(0) = 30 \text{ cm}^{-3}$, $K_0 \sim 10^{25} \text{ cm}^2 \text{ s}^{-1}$

$a \propto K$, and $B \propto 1/K$ from quasilinear theory. Comparing this to the total gravitational energy release rate

$$\dot{E}_g \sim E_g/t_f \sim 3.9 \times 10^{35} \text{ erg s}^{-1} \text{ (typical GMC)}, \quad (16)$$

we see that this energy is easily available. The (sound) cascade rate, from length scales of $R(t)$ to the mean free path of cosmic rays of momentum p is given by using

$$\Gamma_{\text{casc}}^+(p) = \frac{1}{B_K} \frac{\partial B_K}{\partial t} = -16\pi(m-1) \frac{K^2 B_K}{p_i V_A^*} \quad (m > 1) \quad (17)$$

($K = 2\pi/\lambda$, $m \approx 3/2$, wave spectrum $B_K \propto K^{-m}$, cf. Chin & Wentzel 1972), so that the cascade is sufficiently rapid. The waves decay exponentially with distance away from the initiating cosmic rays so that the diffusion coefficient increases away from the shock approximately as

$$K(r) \approx K_0 \exp\left(\Gamma_{i-n}^- r/V_A^*\right) \quad (18)$$

$$\sim K_0 \exp\left(r/0.3 \text{ parsec}\right)$$

in that wave-zone.

In the case of a super-Alfvénic shock wave, the cosmic ray streaming ahead of the shock is limited to little more than the Alfvén speed so no CR or other production of turbulence is needed to ensure that the shock catches up with the particles. For a sub-Alfvénic shock to accelerate CR particles, some other scattering is essential.

The downstream wave growth behind the shock is given

$$\text{by } \left(\frac{\delta B}{B}\right)^2 \sim M_A \quad (M_A \text{ is Alfvén Mach number}) \quad (19)$$

(Volk and McKenzie 1982, Morfill and Scholer 1977).

For effective additional acceleration by the shock, the acceleration timescale should be much faster than the adiabatic timescale. This, in turn, implies that the shock appears to be quasistationary. If the acceleration is so rapid that losses can be neglected, the appropriate solution of the transport equation (3) is that given by e.g. Cowsik and Lee (1983). Attempts to modify their solution in the case of losses, along the lines of the perturbation methods advocated by Drury (1983, review), show that much of the physics remains when the spectral index found by Cowsik and Lee in the appropriate case is used in our solution, equations (5 and 6) above. This is mainly because the advection-time dependence equation is also the zero order (in q) approximation to the transport equation (see Appendix A). Cowsik and Lee (1983) consider velocity distributions of the form $V = V_0 (r/R)^\alpha$ and diffusion coefficient zero downstream and of the form $K = K_0 (r/R)^\beta (p/p_0)^\gamma$ upstream, together with some supposed injection of CR particles by the shock itself. The $\alpha + \beta = 2$ solution ($\gamma = 0$) shows a spectral index which depends on q at high energy for strong compression as

$$-\sigma \left[1 - 2\beta q^{-1} \left(\frac{1}{3}\sigma - 1 \right) \right] \quad \text{where } \sigma = \frac{3V_1}{V_1 - V_2} \quad (20)$$

and streaming of CR's out of the cloud. The number density of CR's depends exponentially on q , just as it does in the Solar Wind or Galactic Wind (Dynamical Halo) models.

In the interesting case $\alpha + \beta = 1$ (agreeing with the result, equation (26) in the previous chapter), no particles escape the shock and indeed there is a net

streaming S into the shock at a rate given by

$$(4\pi r^2) S = -4\pi v_s r_s^2 g \left(\frac{1}{3} \sigma - 1 \right) e^{-\sigma \delta t} \times (\eta > \eta_c) \\ \exp \left[-x \left(\eta - \frac{1}{3} \sigma (1 + \beta) \right) \right] \quad (21)$$

with $\eta_c \equiv (1 + \beta) \left(\frac{2\sigma}{3} - 1 \right)$

so that the ambient CR population drawn on to provide seed particles comes from an ever-increasing volume, typically up to a radius R_{\max}

$$R_{\max} \sim -vt + (\kappa t)^{\frac{1}{2}} \quad (|v| < v_A^*(t), \quad t < t_c) \quad (22)$$

unless further CR's are injected from somewhere (the shock itself, stars, stellar winds ...). In this case the number spectrum is very hard, up to $'\gamma' = -1$. This demonstrates that the acceleration could be more effective in the case of accretion than in the case of a plane or divergent bulk flow, as the shock acceleration is not partly undone by adiabatic cooling as in that case, for which the hardest spectral index (on the power law section) is $'\gamma' = -2$. However, the transition to zero velocity at the cloud boundary partly undoes this acceleration, especially in the rarefaction zone considered earlier.

Let us move on now to consider Case (c), as Cases (a) and (b) are not very different mathematically to

the case above. Here, a stationary shock wave has formed above an opaque proto-stellar core of density $\sim 10^{10}$ atom cm^{-3} . Depending on the stage of collapse, the radiation from the shock front is likely to heat at least a few solar masses in the neighbourhood of the collapsing fragment to temperatures in the range 300 K (non-ionised gas) to 8000 K (ionised gas at recombination temperature). At these temperatures and with the possibility of ionisation (though the low-energy Cosmic Rays might have already sufficiently ionised the gas) the Alfvén waves may easily be excited and the gas is almost in free fall, see Larson (1969a). If the shock width is $\sim 10^{15}$ cm, as suggested by Figure 3.2 (taken from Larson's paper)¹ and the shock radius is $\sim 10^{16}$ cm, only weakly dependent on time, the maximum momentum the Cosmic Rays can reach on their power-law section of the spectrum may be

$$p^* \sim 10^{15} \text{ to } 10^{18} \text{ eV/c} \quad (23)$$

However, the shock transition(s) in Larson's paper (and similar papers) are usually smoothed over several integration-zones by the artificial viscosity method, so that although the jump conditions for the flow variables on either side of the shock were used, the transition appears smooth on the graph.

¹ The shock width will not be less than the gyroradius of a thermal proton, typically 10^9 cm ($T \sim 10$ to 20 K, $B \sim 3 \mu\text{G}$). The Debye length is an approximate upper limit for the linear case considered here, but, in the non-linear case, the shock could be broadened by Cosmic Ray diffusion to the length scale of the gyroradius of a typical Cosmic Ray proton, $r_g \sim 10^{10}$ cm at momentum $\sim 3 \times 10^9$ eV/c.

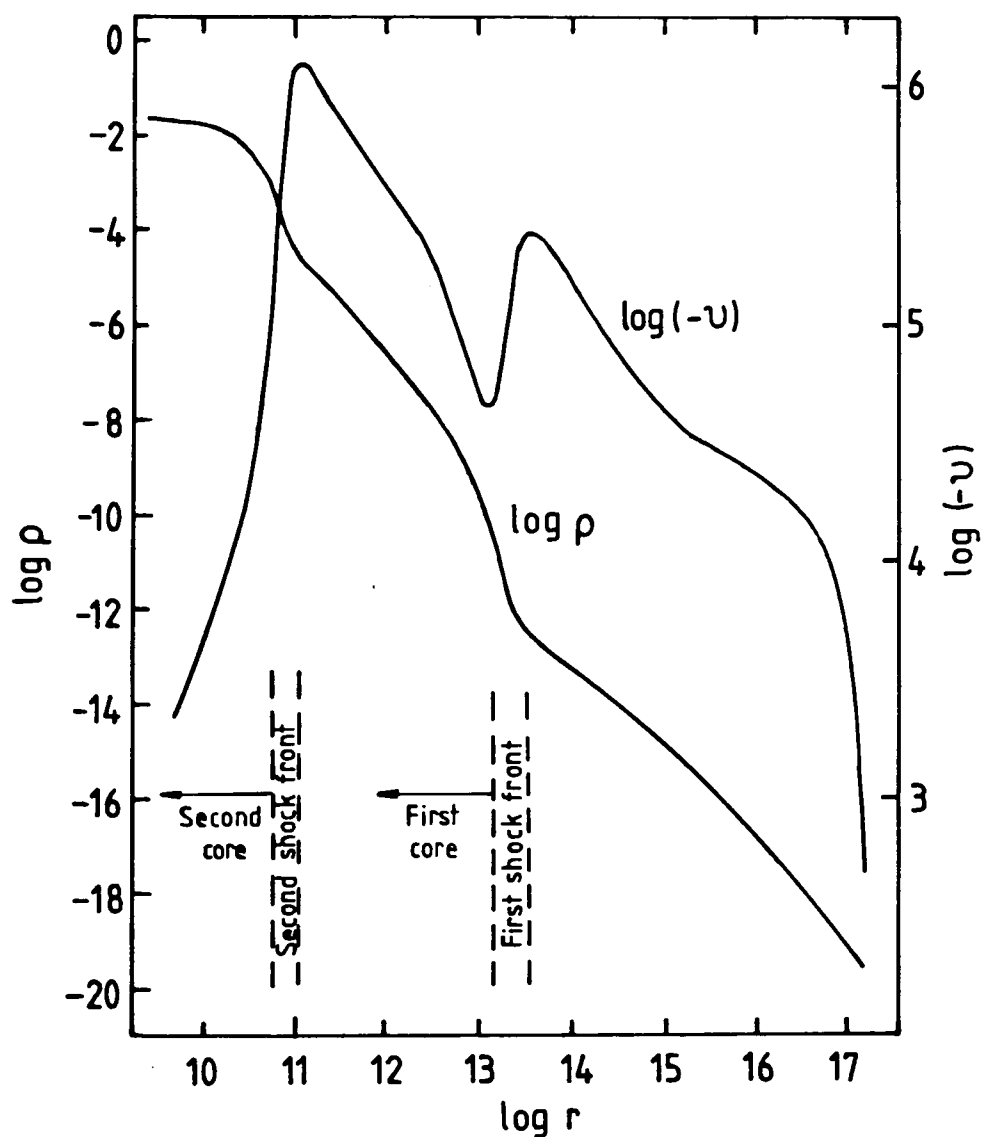
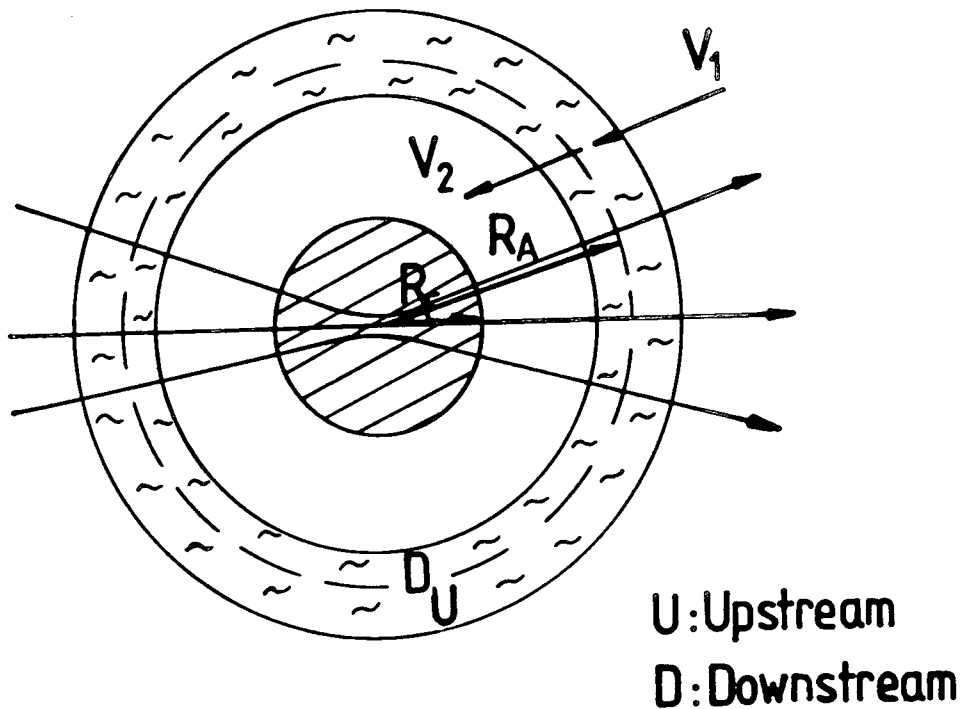


Fig. 3.2 Curves showing the density and velocity distributions at a time shortly after the formation of the second (stellar) core (CGS units). The shock fronts are represented by the regions of steep positive slope in the velocity curve.

(taken from Larson 1969a)



Expanded view of central region when the core becomes opaque to Infrared radiation. A shock front is formed during the main accretion phase [Larson 1969a]. A strongly turbulent zone is formed downstream of the shock whilst particles accelerated at the shock generate waves upstream.

Fig. 3.3 Collapse of a magnetised cloud core.

R_A	" accretion radius "
R_C	core radius
V_1	in front of shock
V_2	behind
	infall speed of scattering centres

Consider the maximum enhancement of CR intensity F for this Model 6, where the maximum scattering and a magnetic field of initially $B_0 = 3$ microGauss was assumed. The ratio of acceleration to loss timescales is

$$t_{\text{acc}}/t_{\ell} = 20 \beta \left(\frac{\text{PC}}{\text{GeV}} \right) \quad (24)$$

so acceleration is marginal at best and only for low-energy CR.

The remarks about cloud rotation, its effect on the CR diffusion coefficient, magnetic confinement, cloud collapse and CR acceleration rate, made in Chapter 2 hold here as well.

The main difference here is that rotation may itself produce a spiral 'shock' or discontinuity - the main output may not be in the form of Infrared photons, but accelerated CR which then escape.

Figure 3.4 shows the CR enhancement v. gas density relation for a typical shocked rotating GMC. The CR are assumed to be trapped inside the cloud.

3.2.1 The effect of proton pressure on the collapse.

If the enhancement of cosmic ray intensity is F (implying an energy density $\sim F \text{ eV cm}^{-3}$, therefore pressure $0.6 \times 10^{-12} F \text{ dyne cm}^{-2}$) inside the cloud and $F = 1$ outside the cloud, the motion of the cloud boundary is given by equation (25)

$$\frac{dV}{dt} = - \frac{GM(1+\alpha)^{-1}}{R^2} + \frac{4\pi}{3} \frac{(F(t)-1)P_{\text{CR}}(0)R^2}{M} \quad (25)$$

(α = magnetic/gravitational energy)

together with the Boltzmann equation solution (cf. equation 2.49) with boundary conditions

$$\begin{aligned} \dot{R}(0) &= -2R_0/3t_c, \quad n_H(0) = 30 \text{ cm}^{-3}, \quad t_c = 2.2 \times 10^7 n_H(0)^{-\frac{1}{2}} \text{ years} \\ F(0) &= 1, \quad P_{\text{CR}}(0) = 0.6 \times 10^{-12} \text{ dyne cm}^{-2} \end{aligned} \quad (26)$$

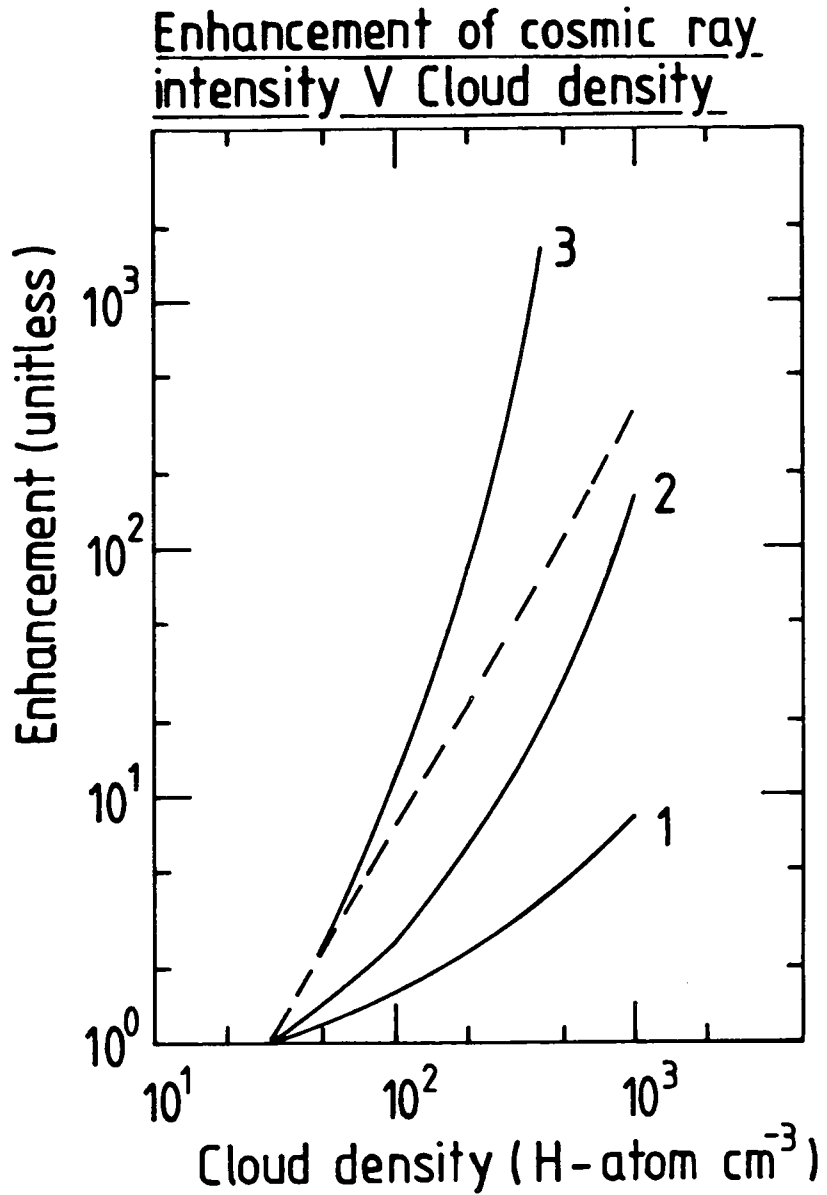


Fig. 3.4 Upper limit to the enhancement of cosmic ray intensity v Cloud density for a shocked compressed rotating GMC in Kiraly flow.

(Initial density = 30 cm^{-3} , mass = $5 \times 10^5 M_{\odot}$).

Curve 1, $k = 10^{27}$; 2, 3.6×10^{25} ; 3, $10^{25} \text{ cm}^2 \text{ s}^{-1}$.

The dashed line refers to the compression of test-particle cosmic rays in a rotating cloud, without energy loss.

These equations may be solved with the aid of a computer¹. In the case where the enhancement is less than, or equal to the adiabatic value (adiabatic compression, energy loss, escape ...) the cosmic ray pressure, if initially unable to prevent collapse, continues to do so (just like the magnetic field which obeys the same law of adiabatic compression) but slows the collapse, which in turn leads to a reduction in cosmic ray intensity which speeds the collapse etc. In the case of shock acceleration, the enhancement may be greater than the adiabatic value unless the CR stream away so the cosmic rays may prevent collapse. Figure 3.5 illustrates this solution for a typical GMC and various conditions.

3.3 Comparison of Model Predictions with Gamma-Ray Observations

3.3.1 Comparison with observations of local molecular clouds. Figure 3.6 shows the enhancement factors for some nearby clouds (those in Figure 2.1) organised by cloud total mass. If at most 50% (say) of cloud gravitational energy was free to be transferred to cosmic rays, as suggested by the Virial Theorem

$$\frac{1}{2} \frac{d^2 I}{dt^2} = 2T + 3\pi + M\mathcal{L} + W + \frac{1}{4\pi} \int_S (\underline{r} \cdot \underline{B})(\underline{B} \cdot d\underline{s}) - \int_S (P^2 + \frac{B^2}{8\pi})(\underline{r} \cdot d\underline{s})$$

$$\text{where } I = \int \rho r^2 dV, T = \frac{1}{2} \int \rho v^2 dV, \pi = \int P dV, \quad (27)$$

$$M = \frac{1}{8\pi} \int B^2 dV, W = - \int \rho \underline{r} \cdot \nabla \phi dV$$

and the cosmic rays exerted negligible pressure (or promptly left the cloud) the enhancement factor F for a cloud of mass M , for fixed initial and final gas densities, scales as

$$F \propto M^{2/3} \quad (28)$$

¹An algorithm to solve coupled first-order differential equations by the Runge-Kutta method, supplied by the Numerical Algorithm Group, was used.

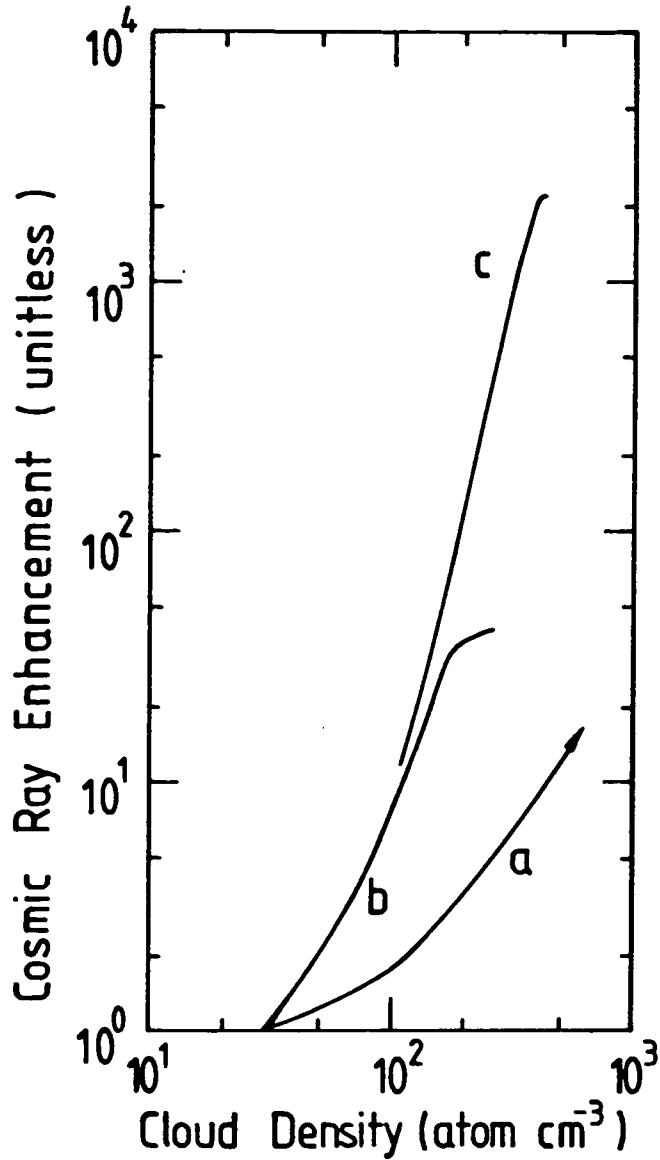


Figure 3.5 Enhancement of cosmic ray intensity v. Cloud density for a shocked cloud with cosmic ray pressure.

Various conditions; Mass = $5 \times 10^5 M_{\odot}$, Initial density = 30 atom cm^{-3}
 Curve a) $K = 3.6 \times 10^{25} \text{ cm}^2 \text{ s}^{-1}$, $P_{\text{CR}}(0) = 0.6 \times 10^{-12} \text{ dyne cm}^{-2}$;

CR pressure is negligible in Eta Carinae solution.

b) $K = 5 \times 10^{24} \text{ cm}^2 \text{ s}^{-1}$, $P_{\text{CR}}(0) = 60.0 \times 10^{-12} \text{ dyne cm}^{-2}$;

Cloud stops contracting at density $\sim 200 \text{ cm}^{-3}$.

c) $K = 5 \times 10^{24} \text{ cm}^2 \text{ s}^{-1}$, $P_{\text{CR}}(0) = 6.0 \times 10^{-12} \text{ dyne cm}^{-2}$;

Cloud stops contracting at density $\sim 400 \text{ cm}^{-3}$.

(Appendix A). There is no sign that a constant proportion of the gravitational energy is transferred to cosmic rays. Another possibility is that the various methods of acceleration discussed above would, in the non-linear case, yield an equipartition between cosmic ray, magnetic field and kinetic energy densities. There is no sign of equipartition. From the mechanisms we have now discussed the enhancement factors, (which depend on mass only insofar as the enhanced or reduced flux of gamma-rays appear to be only in those clouds which, according to the Virial Theorem to be discussed), may collapse. The CR may have been left behind by the cloud in case of reduced flux, or T Tauri stars' mass loss responsible for an outflow of scatterers; F , observed to span the range 0.2 to 16-27, can be accounted for with reasonable physical parameters. The most enhanced cloud might be explained by shock acceleration with adiabatic compression of the cloud for an initial diffusion coefficient of $K_0 = 3.6 \times 10^{25} \text{ cm}^2 \text{ s}^{-1}$ for cosmic ray momentum $\gtrsim 1 \text{ GeV}/c$ when the initial density is 30 cm^{-3} . In this sense, we may not need any contribution to the cosmic ray flux above $1 \text{ GeV}/\text{nucleon}$ from the very luminous star η Carinae. If the cosmic rays are trapped by a magnetic pinch, the maximum gamma-ray luminosity would come from the molecular cloud (unlike Montmerle's 1981 model), with very few particles outside.

The increased enhancement factors for some clouds at distances larger than 1 kiloparsec has been considered to be evidence for the existence of a large-scale cosmic ray gradient in the Galaxy (however, luminosity-distance

selection effects operate) by Issa and Wolfendale (1981a) and Wolfendale (1984) from which the data were taken. Notice however, that only those clouds with mass greater than $\sim 3 \times 10^5 M_{\odot}$ seem to contain enhanced or diminished CR fluxes.

Perhaps fortuitously, the mass of gas just unstable to collapse at temperature $T \sim 10$ to 20 (Kelvin) with gas density 1 H-atom cm^{-3} and initial magnetic field 3 micro-Gauss is given by M_c

$$M_c = 1.9 \times 10^4 \left[\frac{B_0 (\mu G)}{n_H (0)^2} \right] M_{\odot} \approx 3 \times 10^5 M_{\odot} \quad \text{for a typical GMC} \quad (28)$$

(e.g. Spitzer 1978). However, Lequeux (1977, review) quotes only the Orion cloud(s) and $\rho \text{ Oph}$ (at the molecular peak), out of our sample, as showing evidence of collapse (self-absorbed ^{12}CO line-shape ...), none of which have large enhancement factors, so the situation remains uncertain. It is possible that some of the clouds are collapsing, with cosmic rays trapped inside with enhancement factor $F < 1$ (see Figure 3.6). These could be seen as point-like sinks of cosmic rays from a sufficient distance or perhaps as envelopes of reduced cosmic ray intensity at the boundary of the cloud rarefaction zone (see Figure 2.7) for nearby clouds.

3.3.2 Are there point-like regions of reduced cosmic ray intensity? Some of the above clouds have cosmic ray intensity $F < 1$. A search of SAS II satellite data for gamma-ray energies $> 100 \text{ MeV}$ revealed no obvious candidate sinks of cosmic rays. The method was to scan across the sky, searching for regions where the gas density

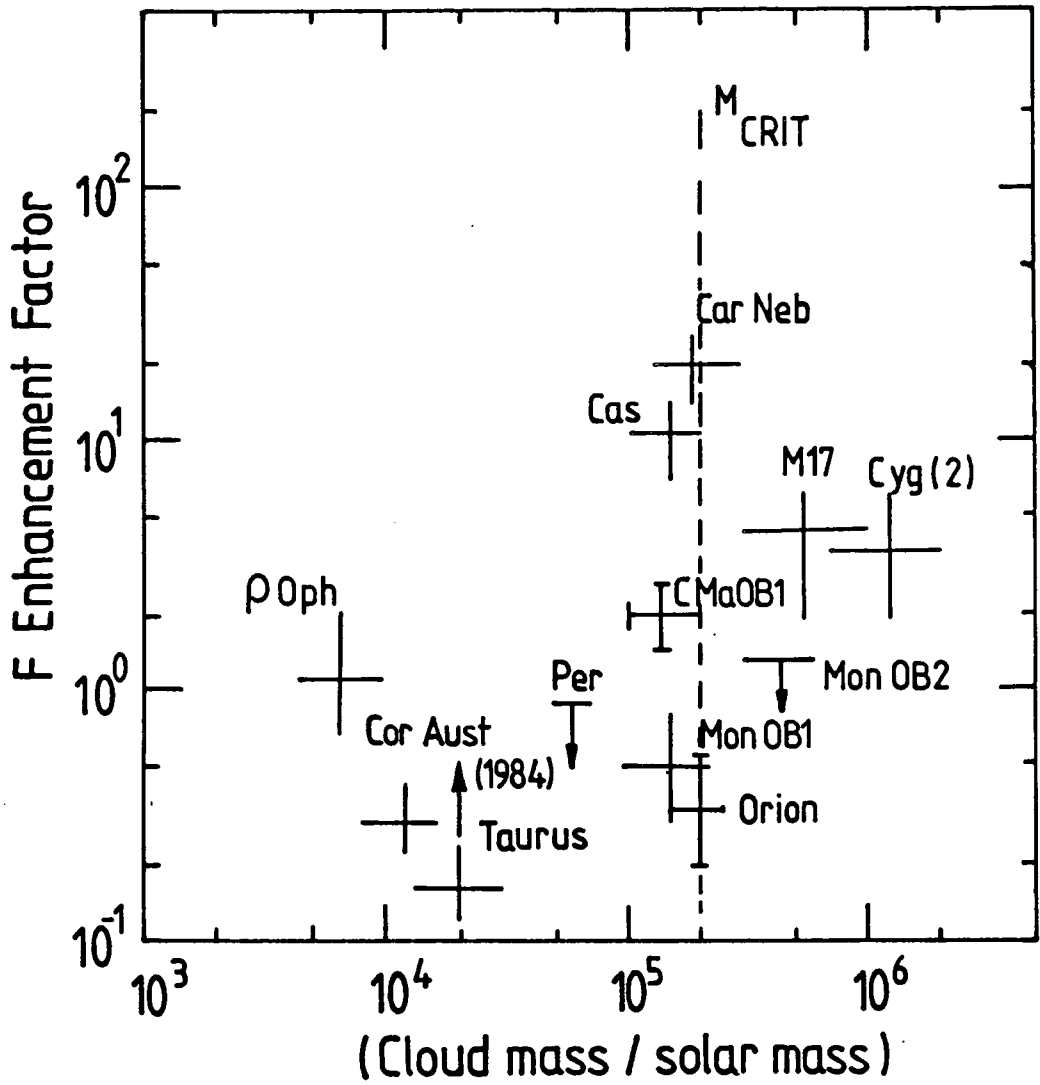


Fig. 3.6 Enhancement factors for some nearby clouds (cf. Fig. 2.1) organised by cloud total mass. The dashed line represents the minimum mass above which a cloud supported by an initial magnetic field of $3 \mu\text{G}$ may collapse.

(after Wolfendale 1984)

was high but the gamma-ray density low, i.e. for large negative correlation between the ratio of gamma-ray count to gas column density and the point spread function of the SAS-II instrument. Very good statistics (long observing time) and high contrast (e.g. on the Galactic plane) together with careful analysis of the significance of the anti-correlation coefficient obtained by simulation would be needed to locate such regions, should they exist.

3.4 Implications for Galactic and Protogalactic Proton Origin

These results may be applied to both Galactic and Protogalactic phenomena. In the Galactic case, the addition of a number of sources of cosmic rays with high grammage (gamma-ray, antiproton and positron fluxes ..) would assist the explanation of these effects (see also Garcia-Munoz et al. 1983 who argue that a thin shell of matter surrounding some cosmic ray sources, together with energy-dependent leakage, is needed for fitting the grammage distribution at each fixed energy). The model of Blandford and Ostriker (1980) would now contain some accretion shocks in the ISM in addition to the supernova-remnant expanding shocks described therein. Their redistribution function $\phi(x)$

$$\phi(x) = \int_4^{q'} (q-3) D(q) F(q)^{q-3} \exp[(4-q)x] dq \quad (29)$$

(also quoted by Axford 1981 a,b,c (reviews)) now includes some values of the shock strength parameter q smaller than 4 (i.e. lower limit to integration may be below

4). Attempts have been made to consider supernova explosions in dense clouds as such sources (Zwiebel and Shull 1982, Stephens and Mauger 1984), in an effort to explain the surprisingly high measured flux of low energy antiprotons (see Chapter 4). There would be a better fit to the mean grammage versus energy relation Blandford and Ostriker deduce if either of these alternatives were true. The same considerations apply to the cloud-crushing model of Blandford and Cowie (1982), discussed earlier; the cloud compression (in their model) takes place in a thin shell. An approximate average grammage for their model gives an upper limit by assuming the CR protons to be well confined:

$$\bar{x}_{\max} = 4 \beta c m_p n_H \left(\frac{d_1}{10 \text{ pc}} \right) \cdot \frac{f}{V_{\text{shock}}} \sim 1 - 10 \text{ g cm}^{-2} \quad (30)$$

for the skin of the dense clouds entering the remnant ($d_1 = 1$, $n_H = 40 \text{ cm}^{-3}$, filling factor $f \sim 0.01-0.1$, $V_{\text{shock}} \sim 220 \text{ km s}^{-1}$). This ties in with paucity of short path-lengths; also the accelerated maximum CR energy is increased.

In the protogalactic case, energy losses by strong inelastic collisions would be negligible. If cosmic rays were trapped during the collapse to galactic densities, any primordial cosmic rays (or those injected by stars which form early in the collapse) will be powerfully accelerated; perhaps to the extent that the cosmic ray energy in excess of that in equipartition with the magnetic field energy density would stream freely into the intergalactic medium. The energy lost by the adiabatic deceleration of the cosmic rays will eventually go into heating the intergalactic medium (IGM). The maximum energy attainable by a cosmic ray proton for reasonable initial gas density ($\sim 2.6 \times 10^{-5} \text{ H-atom cm}^{-3}$, $0.1 \times$

closure density, mass $\sim 5 \times 10^{12} M_{\odot}$, temperature $T \sim 10^4 K$ (unless SN explosions have occurred, when $10^6 K$ is more appropriate), collapse timescale $\sim 10^{10}$ years, and magnetic field $2.3 \times 10^{-12} G$ (scaled back from 3 micro-Gauss at density 1 cm^{-3}) is 10^{15} eV . A very rough estimate of the diffusion coefficient may be obtained by scaling from the usual estimate in the HISM,

$$K_{\text{HISM}} \sim 10^{28} \left(\frac{B}{B_0} \right) \left(\frac{Pc}{G \text{ eV}} \right)^{\frac{1}{2}} \text{ cm}^2 \text{ s}^{-1} \quad (31)$$

Estimating the collapse speed V as $R/t \sim 50 \text{ km s}^{-1}$ we obtain that $|VR/K|_{\text{HISM}} \sim 10^9 (P/GV)^{-0.5}$ hence the cosmic rays up to 10^{15} eV may be trapped inside! (The high energy cosmic rays above $10^{15} \text{ eV/nucleon}$ probably have a different origin, or originate in Supercluster formation). The available gravitational energy for a Galaxy similar to ours (mass 10^{11} to $5 \times 10^{12} M_{\odot}$), considering the possible massive halo, is $3.5 \times 10^{61} \text{ erg}$, not a significant fraction of the rest mass energy $9.0 \times 10^{66} \text{ erg}$ as may be required for the Hillas model (Hillas 1968) to work (Wolfendale 1983) down to 10^8 eV . It may be necessary for thermonuclear CR sources (early supernovae ...), or primordial CR to inject suitable supra-thermal particles for that process to work.

We may envisage the collapse of a cluster or super-cluster of galaxies to take place with fragmentation into individual galaxies. The enhanced cosmic ray intensity would be present at the start of the collapse of each fragment, unless the cosmic ray travel time were to be rendered so long by turbulent magnetic fields that com-

munication between members of a cluster were to be too slow (a situation relevant to the anti-proton origin problem, see Chapter 4). Although the adiabatic compression is reversible, the acceleration is not if scattering (betatron mechanism) or shock acceleration were to operate. Particles might travel from cloud to cloud, or even galaxy to galaxy obtaining energy as they go.

Finally we may mention the possibility that the acceleration of cosmic rays during Galaxy Formation may dissipate energy, reducing the formation timescale.

3.5 Summary and Conclusions

The main results and conclusions of this chapter are:

- * If a plane incipient cloud shock accelerates cosmic rays, the enhancement factors for some nearby clouds can be modelled.
- * The Carina Nebula may be modelled without the source of cosmic rays being η Carinae. This is important since OB stars may not accelerate cosmic rays.
- * Protogalaxies may have been powerful amplifiers of cosmic rays up to 10^{15} eV/nucleon.

CHAPTER 4

4. Antiproton Origin Models

4.1 Introduction

The plan of this Chapter is as follows. After a brief summary of the experimental situation, some previous antiproton origin models are reviewed, discussed and brought up to date. The effects of a Galactic Wind on Extragalactic and Galactic antiprotons are derived in the Dynamical Halo Model. The possibility of acceleration of Cosmic-rays to very high energy at the Galactic Wind terminal shock is considered; the implications for Extragalactic \bar{p} origin are discussed. Finally, a brief summary of the main results and conclusions of this Chapter is presented.

Attention may be directed to the reviews of Kiraly (1982), Eichler (1982) and the rapporteur paper by R. Schlickeiser at the 1983 International Cosmic Ray Conference (Bangalore). Some of the effects of a Galactic Wind on extragalactic anti-matter have been independently discussed by Ahlen et al. (1982); the present discussion goes much further.

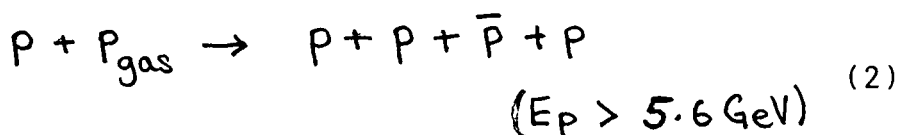
4.2 Brief Summary of Experimental Situation

The most compelling evidence so far for the existence of antiprotons (\bar{p}) in the Cosmic Radiation is provided by three recent experiments. Some older experiments which set only upper limits to the flux of antiprotons and antinuclei (\bar{Z}) are listed by Steigman (1976).

In balloon-borne experiments with magnetic spectrometers Golden et al. (1979) report a \bar{p}/p ratio of $(5.2 \pm 1.5) \times 10^{-4}$ in the rigidity interval 5.6 to 12.5 GeV/c. Bogomolov et al. (1979) report $(6 \pm 4) \times 10^{-4}$ in the interval 2 to 5 GeV/c and Buffington et al. (1981a,b) report $(2.2 \pm 0.6) \times 10^{-4}$ in the low-energy interval 130 to 320 MeV/c. We adopt the view that the experiments are correct: the flux of atmospherically produced \bar{p} is correctly allowed for (see Bowen et al. 1983 for a different view) as is the sign of the charge determined for each \bar{p} candidate.

It is of interest to note that Buffington et al. (1981a,b) report an upper limit of 2.2×10^{-5} for the \bar{He}/He ratio (at the 95% confidence level) although no antinuclei were detected¹.

The most common \bar{p} production mechanism is



The spectral shape shows a pronounced turnover at ~ 3 GeV due to kinematic factors and each \bar{p} of kinetic energy ($E_{\bar{p}}$) is produced from a collision where the median initiation Cosmic-ray proton energy is $\sim 10 E_{\bar{p}}$.

The maximum yield of \bar{p} in this model occurs when the Galaxy is closed to escape (Peters and Westergaard 1977). Curve (a) in Figure 4.1 shows the result.

¹ The reported anti-triton (Apparao et al. 1983) has still to be confirmed. If true, the low flux of He is surprising.

Bogmolov's and especially Buffington's points lie well above this prediction. Furthermore, the 'Closed Galaxy Model' is well-known to predict a gamma-ray flux and flux of secondary electrons and positrons much higher than that observed.

Curve (b) represents the more reasonable prediction of the 'Leaky-Box Model' where CR protons traverse $\sim 5 \text{ g cm}^{-2}$ of matter before escaping the Galaxy.

The discrepancy between observations and the prediction is at least a factor of 100 at $\sim 730 \text{ MeV}$.

Figure 4.1 shows the demodulated flux for Buffington's point using various values of the modulation function ϕ . The lower flux limits were obtained by ignoring the partial exclusion of particles by energy-conserving convection-diffusion effects, while the dashed lines represent plausible deviations from Liouville's Theorem.

The point for $\phi = 600 \text{ MeV}$ should be considered to be the best value. Note that the \bar{p}/p ratio will hardly be affected by this type of modulation.

There is some evidence from observations of the e^-/p ratio (Evenson et al. 1981) that charge - dependent drifts (Jokipii and Kopriva 1979) operate in the heliosphere. If so, the demodulated \bar{p} flux and \bar{p}/p ratio at Solar maximum could be even higher, perhaps by a factor of two.

4.3 Solar Modulation

Solar modulation (see e.g. Jokipii 1971 for a review) affects all particles entering the Solar System especially

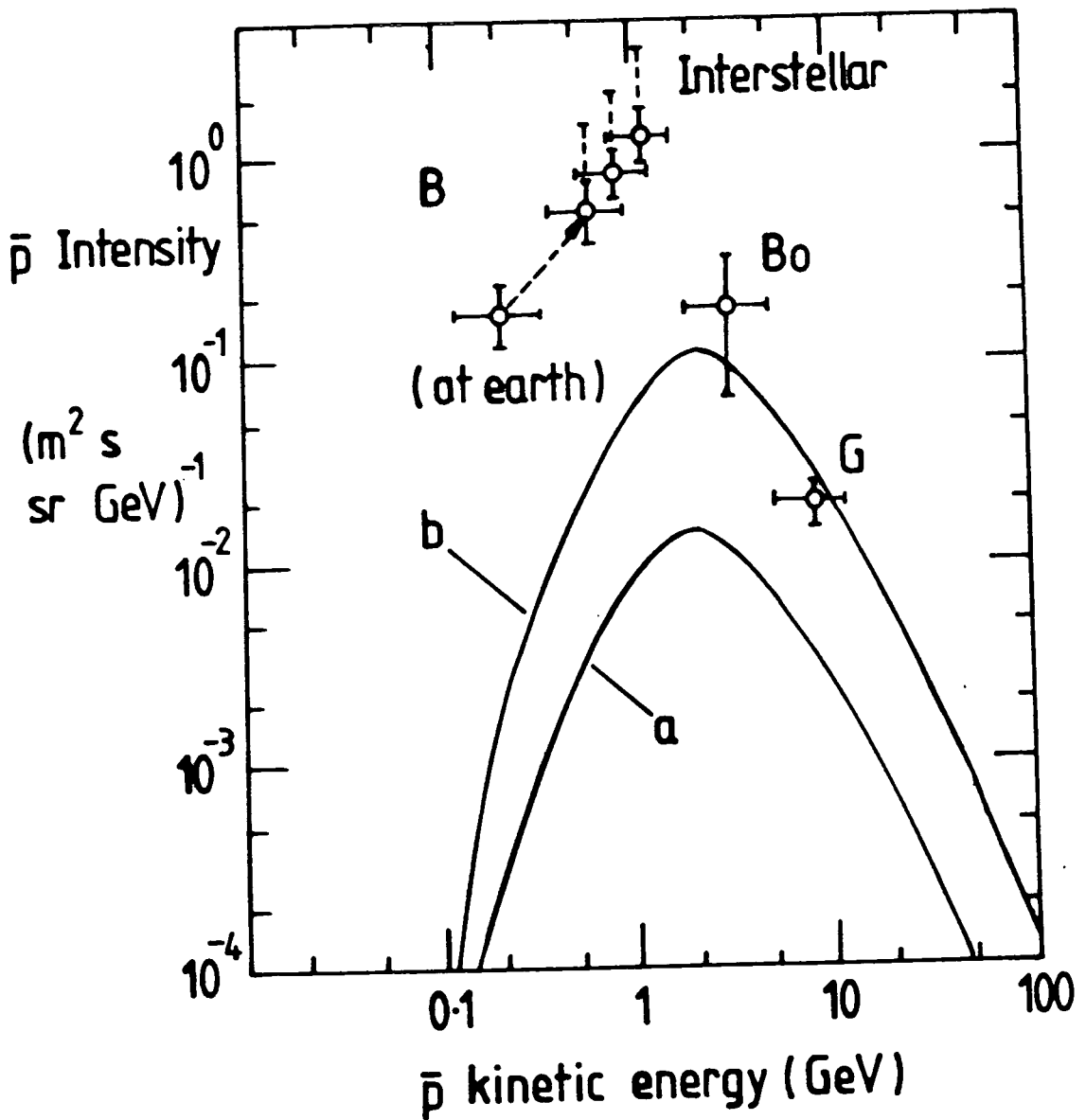


Fig. 4.1 Secondary antiproton flux predictions. a, Leaky box model with $\lambda = 5 \text{ g cm}^{-2}$; b, closed Galaxy model. The displacement of the Buffington et. al. point (marked B) is to allow for Solar modulation. The points correspond to mean adiabatic energy losses of 400, 600 and 900 MeV. The horizontal error bars represent the energy intervals from which $\sim 70\%$ of the measured flux at Earth is expected. The most likely value is ~ 600 MeV. The highest value (900 MeV) is unreasonably high for protons or primary \bar{p} 's with a power-law spectral shape, but is quite possible for the peaked spectra of secondary \bar{p} 's. The dashed lines represent plausible deviations from Liouville's theorem. Bo denotes Bogomolov et. al.; G denotes Golden et. al.

(after Kiraly et. al. 1981)

at a time of Solar maximum, which applies to Buffington's point. Each fixed \bar{p} energy observed at earth corresponds statistically to a range of (higher) energies in interstellar space. These effects are most important for momenta $\lesssim 1$ GeV/c, and are negligible above several GeV/c. Gleeson and Axford (1968) showed that the average flux $j(r, W)$ observed at heliocentric radius r and kinetic energy W is approximately related to the flux j_∞ in inter-stellar space by an analogue of Liouville's Theorem

$$\frac{j(r, W)}{W^2 - T_0^2} = \frac{j_\infty (W + \phi)}{(W + \phi)^2 - T_0^2} \quad (1)$$

where ϕ represents the mean energy loss per particle and T_0 the rest energy. This is valid for the small proportion of incident particles which penetrate more deeply than one scattering mean free path into the Solar System. For Solar minimum conditions $\phi = 400$ MeV applies, for Solar maximum $\phi = 600$ MeV applies and only in the case of Solar maximum conditions and a 'peaked' spectrum of incident particles $\phi = 900$ MeV could apply. Urch and Gleeson (1973) have calculated the distribution of interstellar particle energies using these parameter values.

4.4 Previous Origin Models

In a conventional origin model, Cosmic-ray protons traverse the Galaxy, colliding with gas protons, producing secondary (p, \bar{p}) pairs as well as (n, \bar{n}) , e^+ and secondary e^- via the $\pi^- - \mu^- - e^-$ chain, as well as gamma-rays.

4.4.1 What is the secondary \bar{p} production cross-section? This cross-section has been the subject of much debate; (even a deliberate attempt to make anti-protons directly at low energy near the threshold by accelerator physicists has been foiled by the kinematic factors - C. Rubbia comment in Wolfendale and Stecker 1984). Early attempts to estimate the cross-section from experimental data (Gaisser and Maurer 1973, Badhwar et al. 1975, Szabelski et al. 1980) seemed to indicate near agreement with the observed antiproton/proton ratio measured by Golden et al. (1979) and even possibly Bogomolov et al. (1979). But the Buffington et al. point is completely outside this prediction (as explained above) even when the detailed (important) initiating proton spectrum is allowed for; some of the controversy is due to lack of knowledge of the appropriate scaling or empirical parametrization of the cross-section outside the realm of accelerator data. Recent work (e.g. Tan and Ng 1981) shows good agreement with the earlier Gaisser and Maurer prediction, but not the Badhwar and Golden value (even though both groups used the same data).

Figure 4.2 shows the run of the predicted \bar{p} flux with energy.

4.4.2 Shrouded CR source models

The observed low-energy antiprotons are assumed to be made at higher energies, then decelerated by adiabatic expansion, or strong inelastic collisions. Advocates of this rather conventional model include Zweibel and Shull (1982), Axford (1981a review), Eichler (1982) and

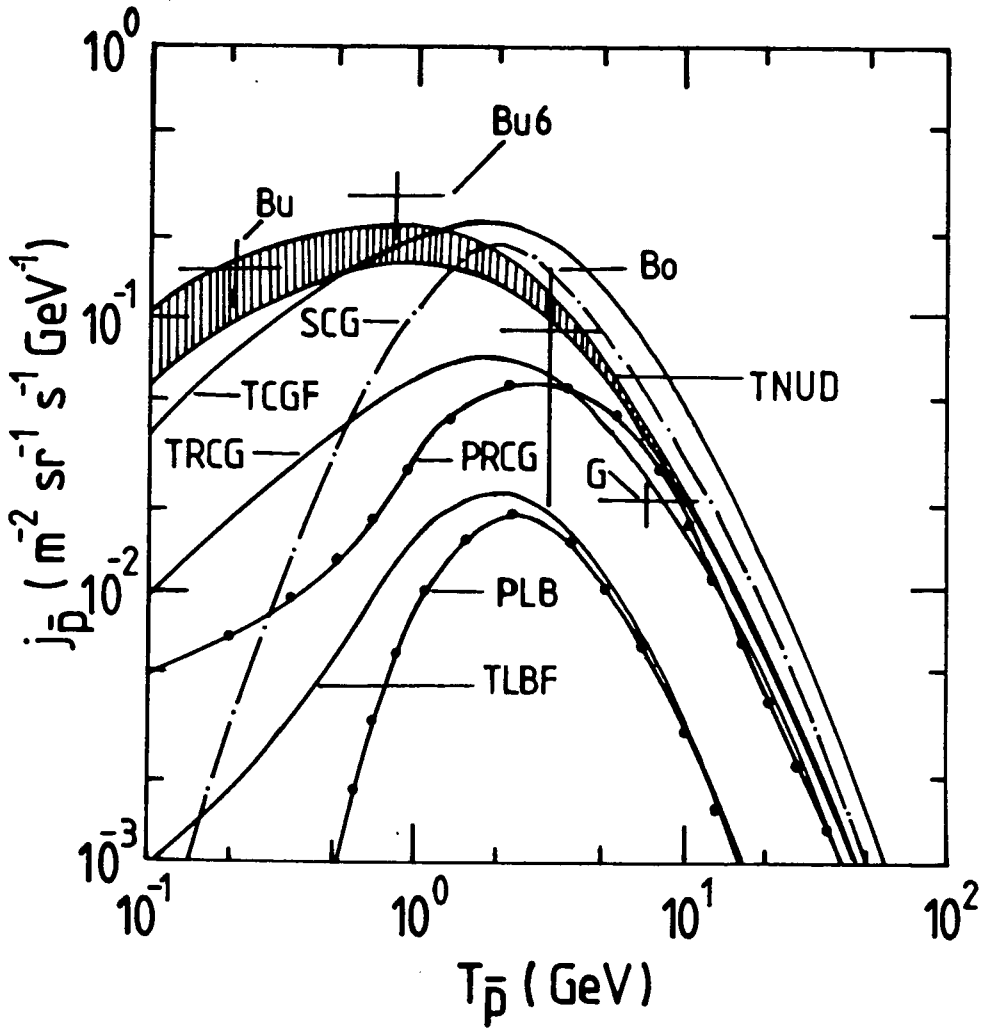


Fig. 4.2 Comparison of various predicted \bar{p} fluxes with experimental data. Bu, datum of Buffington et al. (1981), undemodulated. Bu6, demodulated with $\phi = 600$ MV. Bo, datum of Bogomolov et al. (1979). G, datum of Golden et al. (1979). Predictions for the leaky-box model: PLB, Protheroe (1981); and TLBF, TN I. Predictions for the closed galaxy model: SCG, Stephens (1981c); and TCGF, TN 1. Predictions for the revised closed galaxy model; PRCG, Protheroe (1981); TCRG, TN I. Prediction for the nonuniform galactic disk model; TNUD (Shaded strip), this work. (From Tan and Ng 1983, references therein; TN I refers to their Paper I).

Stephens and Mauger (1984). In all cases, a supernova is supposed to take place inside a dense gas cloud. A rough estimate of the number of such events occurring is made by Morfill et al. (1984, review on gamma-ray source mechanisms).

Cosmic ray (CR) protons then create secondary particles by collision with atoms of the gas cloud, the secondary antiprotons being subsequently adiabatically decelerated. It is difficult to make sufficient low-energy antiprotons in such a cloud without violating known constraints on the low energy (35-100 MeV) Bremsstrahlung gamma-ray flux, high energy (> 100 MeV) pionisation gamma-ray flux and secondary electrons and positrons. However, there is an excess (determined by radio synchrotron observations) of electrons and positrons over the Galaxy above that determined by collecting electrons on earth (the Solar Wind excludes these low energy electrons). Where available, the low energy positron/(electron + positron) ratio appears to flatten, even approach 0.5 at low energies. Such clouds might appear to be gamma-ray sources (Morfill et al. 1984, review). About 20% of all supernovae would have to take place in a dense cloud for this model to be viable.

4.4.3 Stochastic acceleration models. Eichler (1982) has considered the possibility that the low energy antiprotons have been accelerated from even lower energy antiprotons in the interstellar medium (ISM) or hot inter-galactic medium (Halo). He states that the differential

number spectrum of antiprotons at momentum p would approach the form p^2 by diffusion in momentum space, as a result of repeated scattering by magnetic turbulence (random large-scale motions). Such a spectrum is completely different from that observed.

Yet such a process must produce a peak in the spectrum where losses due to momentum-dependent spatial diffusion balance gains due to momentum diffusion (see e.g. Axford 1981a, review), perhaps at energies even lower than observed to date. This idea does not seem to have been pursued.

4.4.4 Non-annihilation inelasticity deceleration models. The non-annihilation inelastic scattering of CR \bar{p} on gas protons may, in principle, decelerate high energy \bar{p} . Tan and Ng (1981) and other workers have considered this effect to fill in much of the kinematic dip at ~ 1 GeV.

Figure 4.2 includes progress in this area to date.

4.4.5 Secondary \bar{p} origin, cosmological deceleration models. Eichler (1982) has briefly considered the question of the antiprotons being secondaries formed early in the Universe. The present \bar{p} cosmic ray energy density $\mathcal{E}_{\bar{p}} \sim 10^{-4} \text{ eV cm}^{-3}$. The \bar{p}/ν ratio in high-energy collisions is $< 10^{-2}$, which implies $\mathcal{E}_{\nu} \gtrsim 10^{-2} \text{ eV cm}^{-3}$. But the Reines experiment (e.g. Crouch et al. 1978) limits the cosmic ν background at $E > 0.5$ GeV to $< 3 \times 10^{-3} \text{ eV cm}^{-3}$, ruling out the cosmological deceleration scenario. Nearly all antiprotons formed in the Big-Bang will have annihilated by now (baryon/photon $< 10^{-9}$).

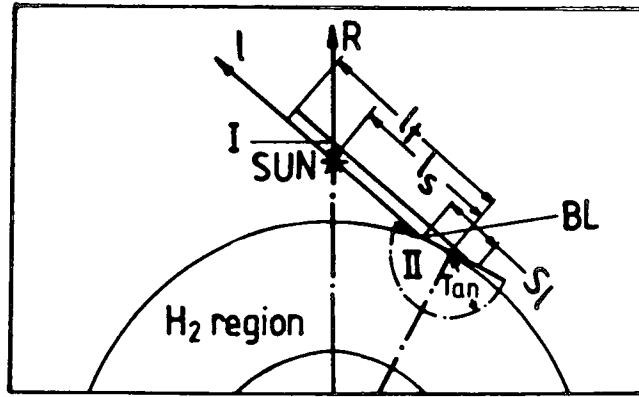


Fig. 4.3(a) The nonuniform galactic disc model according to Tan and Ng (1983).

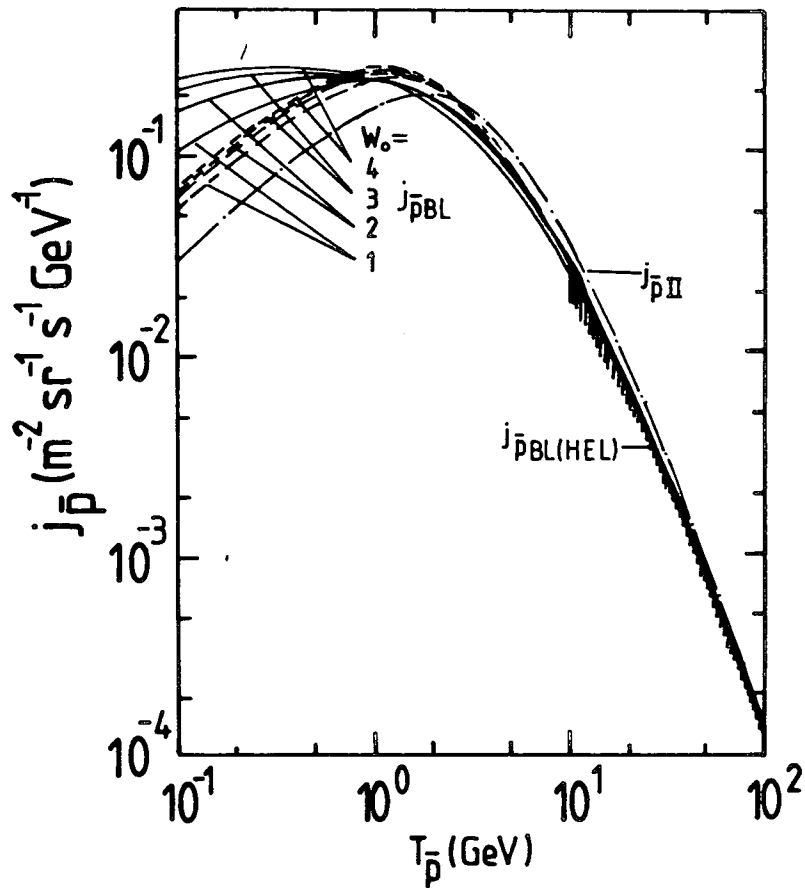


Fig. 4.3(b) The predicted \bar{p} fluxes for that model; $j_{\bar{p} \text{ II}}$, in region II; $j_{\bar{p} \text{ BL}}$, in boundary layer BL after the \bar{p} adiabatic deceleration (see their text); $j_{\bar{p} \text{ BL (HEL)}}$ representing the high-energy limit of $j_{\bar{p} \text{ BL}}$ derived from the cosmic ray proton gradient (assumed) and $j_{\bar{p} \text{ II}}$. (after Tan and Ng 1983).

4.4.6 Galactic Centre (GC) explosion models.

This old idea (Khazan and Ptuskin 1977, Giler et al. 1981) for the formation of p has been extended to \bar{p} , much as in the supernova-explosion adiabatic deceleration model discussed above. The \bar{p} could be formed in the initial event, or subsequently by secondary production. Even if the initial electron/proton ratio were unity, the present value ($\sim 1/30$) could be accounted for as a result of the deceleration.

The reported excess of 511 keV non-redshifted 'annihilation radiation' towards the GC seems to support this hypothesis by suggesting an excess of electrons and positrons there (e.g. Leventhal et al. 1978).

4.4.7 Non-uniform Galactic disc models. The ISM is known to be lumpy; in these lumps the \bar{p} production is increased relative to the surrounding gas: Tan and Ng (1983) have shown that this can account for the observed \bar{p} flux, if some other assumptions are also made.

Figure 4.3 shows the fit to the observed antiproton data.

4.4.8 Exotic models.

(a) $N-\bar{N}$ oscillation models.

Sivaram and Krishnan (1982) propose a model where neutrons, surely present in the Hot Interstellar Medium resulting from Supernova explosions, oscillate into anti-neutrons on a timescale that is estimated to be $10^5 - 10^7$ s (as predicted by one particular Grand Unified Theory, Mohapatra and Marshak 1980). The anti-neutrons would then decay with dilated lifetime ($10^3 \gamma$ second)

$$\bar{n} \rightarrow \bar{p} + e^+ + \nu$$

the transformation being inhibited by the magnetic energy associated with the neutron magnetic moment in the HISM-Galactic magnetic field ($\sim 10^{-7}$ to 10^{-6} Gauss), and nearly completely inhibited in a mean Galactic magnetic field (3 micro-Gauss). The Grenoble n - \bar{n} oscillation experiment (Baldo-Ceolin et al. 1981) indicates a lower limit to the oscillation time-scale of $\sim 10^{15}$ seconds, with no actual decay detected. This experiment (the only one to date) relies on the annihilation gamma-ray signature as a result of positrons created by the decay of anti-neutrons interacting with matter. The indicated time-scale means that an apparently unreasonable flux of neutrons would be required (if $B = 10^{-7}$ G and each SN produces $\sim 10^{57}$ free neutrons we need $\sim 10^{55}$ antiprotons in Galaxy for energy density $\sim 10^{-4}$ eV cm $^{-3}$, oscillation time of 10^{15} s (rather than 10^5 s) means that at least the product of 10^{20} SN would have to be stored in the Galaxy. As the oscillation time is now of the order of the residence time, the scenario is unreasonable).

We may speculate that this process occurs in Extragalactic space; a low (10^{-12} - 10^{-8} Gauss) magnetic field, together with a p energy density $\sim 10^{-4}$ eV cm $^{-3}$ indicate a sufficient flux of neutrons. Even in Meta-Galactic space, one would expect $B \gtrsim 10^{-12}$ G. If $\tau_{\text{osc}} \sim 10^{15}$ s (and decay negligible) we might restore the credibility of this scenario. But if the energy density in MG-space is 10^{-4} eV cm $^{-3}$ (a likely value), the energy

density would fall short by a factor 10^{-4} .

(b) Extragalactic low-energy antiprotons (\bar{p} scenario).

Stecker (1981) has shown that if present constraints on the gamma-ray "isotropic" background are not to be violated, matter and anti-matter must be separated on at least the Supercluster scale (e.g. Omnes 1969, Klein 1966). If antiprotons are to arrive here, they must propagate virtually rectilinearly: even a small disordered magnetic field ($\sim 10^{-12}$ Gauss) in the intergalactic medium would cause the travel time to be at least the Hubble timescale. The putative Galactic Wind (see below) would exclude them, altering the spectral shape. However, low-energy electrons and positrons may arrive at the Galaxy, unaffected by interactions with the 3K relic radiation, as the cross-section is proportional to γ^2 (although the same remarks about journey time hold).

(c) Extragalactic high energy \bar{p} (\bar{p} scenario).

We still do not know the CR composition at high ($> 10^{11}$ eV) energies. The particles could be p, Fe or even a 50-50 beam of p and \bar{p} (Stecker and Wolfendale 1984) especially as the annihilation cross-section declines at high energies (black sphere absorber model). Figure 4.4 shows how such a scenario (in the absence of a significant Galactic Wind - perhaps only a "breeze", Chevalier et al. 1979) leads to a "bump" in the observed spectrum at $\sim 3 \times 10^{14}$ eV, as observed, although such an explanation is not unique.

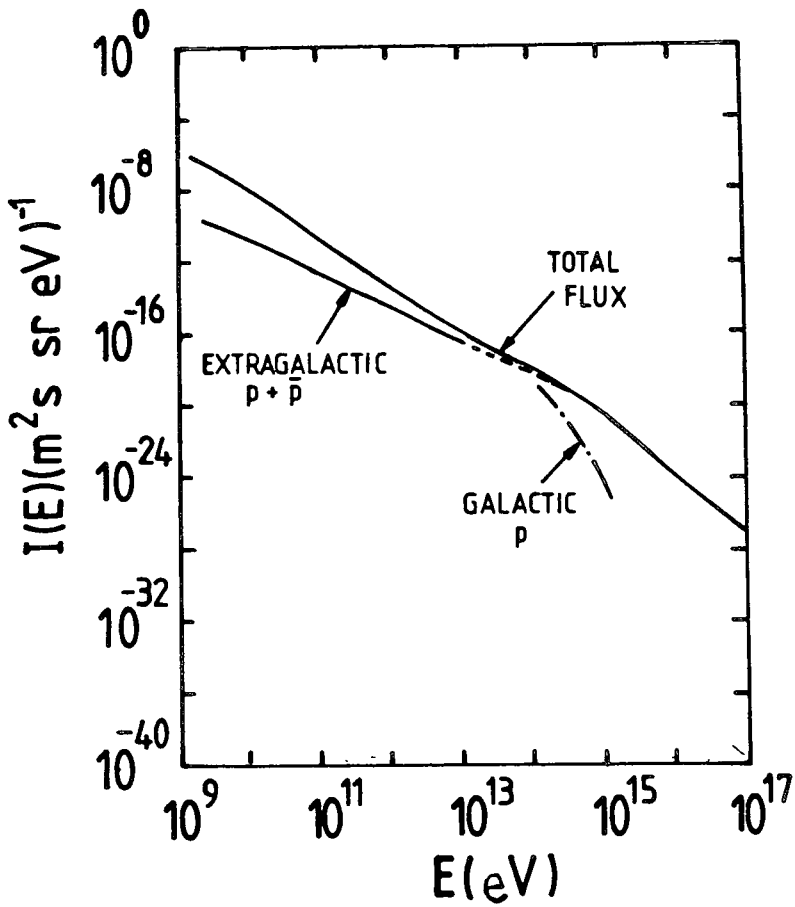


Fig. 4.4 The effect of extragalactic primary protons and antiprotons on the total cosmic ray spectrum according to the model discussed in the text. It can be seen that this model may account for the putative flattening in the observed cosmic ray spectrum near 10^{14} eV. $I(E)$ is the particle intensity, in the units shown.



(d) Primordial Black Hole evaporation models

An efficient process for creating a small ($\sim 1 \times 10^{-4}$) excess of $p \bar{p}$ pairs seems to be the quantum mechanical tunnelling and escape of quarks and anti-quarks from black holes created in the Big-Bang. Hawking (1974) and e.g. Carr (1976) have worked out the fraction of energy going into various types of particle. (Tipler (1980) suggested that the back-reaction of the Hawking radiation on the event horizon causes the event horizon to become unstable - this was contested by e.g. Bardeen (1981)). There are two extreme models: the Elementary Particle model (quarks and antiquarks produced) and Composite Particle model (e.g. $p \bar{p}$ pairs directly produced). The yield of ($p \bar{p}$) pairs is maximised by choosing the Elementary Particle (EP) model. Recent accelerator data (PETRA) show a meson to baryon ratio increasing as successively lower energies are chosen (a meson needs only a quark and antiquark and is of lower mass than a baryon which needs three quarks). This may mean that the low energy antiproton production spectrum from PBH shows some 'cutoff' effect. Black holes with mass $< 10^{15} \text{g}$ will have now exploded; adopting an $M^{-(2 \text{ to } 3)}$ mass spectrum, Kiraly et al. (1981) find a good fit to the antiproton spectrum, which also yields some electron-positron pairs only where they are needed (below $\sim 100 \text{MeV}$). To avoid violating gamma-ray (Bremsstrahlung origin) constraints, the authors placed the Primordial Black Holes (PBH) in an extended Halo (radius $\sim 40 \text{kpc}$) surrounding the Galaxy.

Note that 10^{21} PBH of mass $< 10^{15}$ g make no dynamical effect on the Halo. PBH explosions do not violate any known radio constraint (R.D.Davies, personal communication).

Due to the higher mass, no $\bar{\text{He}}$ would be expected from PBH, even less, any $\bar{\text{T}}$! This is a good hypothesis, economically resolving two problems at once.

We now move on to consider how the spectrum of antiprotons would be modified by a Galactic Wind.

4.5 Modulation of Extragalactic Spectra by Galactic Wind

A simple one-dimensional model of a Galaxy (the Dynamical Halo model: Ipavich 1975, Owens and Jokipii 1977a,b, Jones 1979, Freedman et al. 1980, Schlickeiser 1980, Lerche and Schlickeiser 1980, 1982, see also Webb et al. 1984) could be used to modulate extragalactic spectra in an effort to assess the validity of the $\bar{\text{B}}\bar{\text{B}}$ scenario in the interpretation of the low energy $\bar{\text{p}}$ flux observed at earth. Figure 4.5 shows this model (taken from Freedman et al. 1980). The Galactic disc is taken to be uniform, and all quantities vary only with distance z from the midplane of the Galaxy. The interstellar gas density ρ (in units of a.m.u. per unit volume) is taken to be constant in the disc, which extends to $|z| = a$, and to be zero in the halo. The convection speed is V_0 , directed outwards. The cosmic ray (CR) intensity at $|z| = D$ is held constant to a first approximation. This is because cooling of the extragalactic CR by adiabatic deceleration is balanced by heating of the CR at the

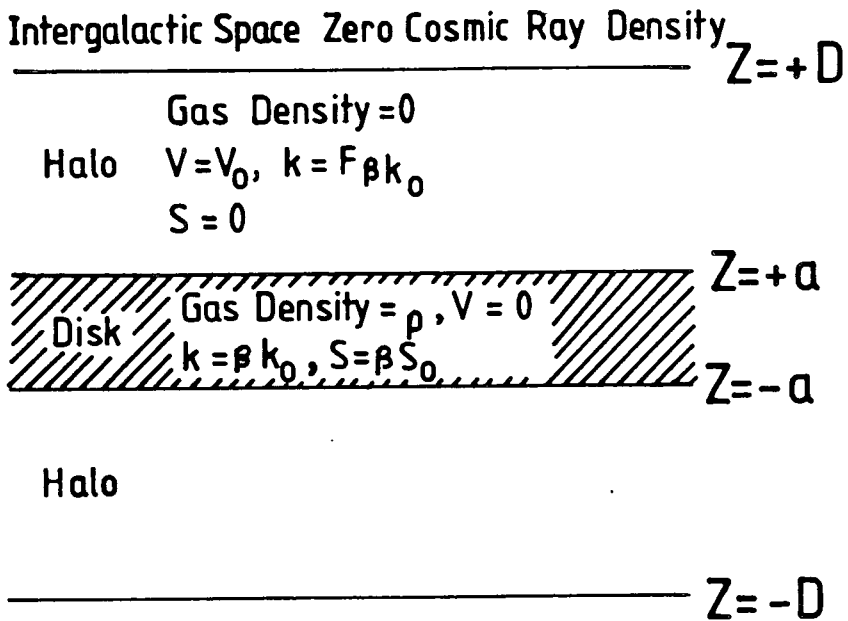


Fig. 4.5 The simple model of the Galaxy.

When galactic modulation of extragalactic spectra is considered, the cosmic ray density in intergalactic space is held fixed at a non-zero value and no source is considered in the Disc.

(after Freedman et al. 1980).

Galactic Wind terminal shock (Jokipii 1968, 1971 (review); see later). Particles are assumed to diffuse in the Halo, and be convected outwards by scattering centres. Following Jones (1979) we may account for the turnover of the secondary to primary ratio below (1-3) GeV/nucleon (see later) by convection at speed V_0 where the diffusion coefficient in the Halo

$$K = \beta K_0 (P/GV)^{\frac{1}{2}} \quad p = \text{rigidity} .$$

Above (1-3) GeV/nucleon, the variation of pathlength with energy (or secondary to primary ratio) is explained by energy-dependent escape or diffusion. The \bar{p} are assumed to stream from anti-Superclusters (Stecker 1981, Wolfendale and Stecker 1984) and propagate virtually rectilinearly (Kiraly et al. 1981) to arrive as a nearly-isotropic flux at the outer boundary of the Halo of our Galaxy.

The convection velocity is taken to be outward directed or inward directed. The evidence for the first case stems from;

- (1) $^{10}\text{Be}/^{7+9}\text{Be}$ ratio (Garcia-Munoz et al. 1977)
also $^{10}\text{Be}/^{7+9}\text{Be}$, $^{26}\text{Mg}/^{24}\text{Mg}$, ^{27}Al (^{26}Al not seen).
- (2) Observations which suggest an outwards directed wind in external galaxies: studies of synchrotron radiation from relativistic electrons (NGC 891 Strong 1981, neglecting (important) adiabatic deceleration; 15 Spiral galaxies seen edge-on (Lerche and Schlickeiser 1982)) in the hope that the diffusion

coefficient and convection speed for nucleons can be scaled to that for electrons at the same rigidity.

3. A growing theory of the Galactic Wind (see above).

In each case gas is convected out of the Galaxy at a rate of several $M_{\odot} \text{yr}^{-1}$ although some falls back when radiative cooling sets in. Perhaps the magnetic field escapes so that CR are not scattered by infalling gas?

4. Accretion of 'primordial' gas (left over from galaxy-formation); Magellanic stream and High Velocity Clouds (HVC: $\sim 10^4 M_{\odot}$, $V \sim 200 - 500 \text{ km s}^{-1}$, distances up to a few 10's of kpc, $0.8 M_{\odot} \text{yr}^{-1}$).

4.5.1 Solution of the transport equation. The expected density $n(z, p, t)$ of particles between z and $z + dz$, rigidities p to $p + dp$ and time t satisfies

$$\frac{\partial n}{\partial t} + \frac{\partial}{\partial z} (nV(z)) - \frac{1}{3} \frac{\partial V(z)}{\partial z} \frac{\partial}{\partial p} (pn) - \frac{\partial}{\partial z} (k \frac{\partial n}{\partial z}) = S(z, p, t) \quad (2)$$

representing explicit time-dependence, convection, adiabatic deceleration, diffusion of field lines and particle sources. A formal derivation of this equation from the Boltzmann equation may be found in Skilling (1975a,b,c); Jokipii (1971) demonstrates that this equation holds in a frame fixed with respect to the Galaxy, provided the scattering is hard enough to drive the flux isotropic. We assume $K(p) = \beta K_0(z)k(p)$ where p is the rigidity; the particle density is static. From (2), where k_H , k_D are diffusion coefficients in the Halo and Disc respectively, we derive:

$$K_h(p) \frac{\partial^2 n}{\partial z^2} - V_0 \frac{\partial n}{\partial z} = 0 \quad a \leq |z| < D \quad (3a)$$

$$K_d(p) \frac{\partial^2 n}{\partial z^2} + S(z,p) = 0 \quad |z| \leq a \quad (3b)$$

The streaming of particles across the Disc is in general defined by

$$\gamma = -K(z,p) \frac{\partial n}{\partial z} + nV(z) - \frac{V(z)}{3} \frac{\partial}{\partial p}(pn) \quad (4a)$$

so that

$$\frac{\partial n}{\partial t} - \frac{\partial}{\partial z} \gamma(z,p) = S(z,p) \quad (4b)$$

(Gleeson 1968, Jokipii 1971) and leads to the boundary condition

$$-K_d \frac{\partial n}{\partial z} \Big|_{z=a-D} = -K_h \frac{\partial n}{\partial z} \Big|_{z=a+D} + n(a)V_0 - n(a) \frac{V_0}{3} \frac{\partial}{\partial p}(pn) \Big|_{z=a+D} \quad (5)$$

Several interesting cases arise.

4.5.2 Escape of \bar{p} from anti-galaxies. Let

us suppose the \bar{p} are produced with a source spectrum $S(p)$ as required for our Galaxy (and suggested on the basis of shock acceleration to be close to $S_0 p^{-2.2}$).

If the density of extra-galactic particles is small enough and there is no reacceleration in the Halo, or at the terminal wind shock, the flux of particles crossing a perfectly absorbing boundary of the Halo per unit time satisfies

$$j(p) = \frac{\beta}{2\pi} \left[-K_h(p) \frac{\partial n}{\partial z} \Big|_{|z|=D} + n(p)V(z) \right] \quad (6)$$

where j is the flux in the forward hemisphere of pitch-angle, and $n(p) = 0$. Solution of equation (3) subject to $n(D,p) = n(-D,p) = 0$ leads to

$$n(z, p) = Y(p) F(z, p) \quad |z| \leq D \quad (7a)$$

where

$$F(z, p) = \frac{e^q - \exp(q|z|/D)}{e^q - 1} \quad (7b)$$

and $q = v_0 D/k(p)$ is a parameter expressing the mean fractional energy loss (or gain) experienced by a particle in escaping the galaxy. Following a method similar to that of Kota' and Owens (1980), who followed Freedman et al. (1979), $Y(p)$ satisfies (in the 'thin disc' limit : $a \ll D$)

$$K_h(p) \frac{q V_0 Y(p)}{(e^q - 1) D} - Y(p) V_0 + \frac{V_0}{3} \frac{\partial}{\partial p} (p Y(p)) = S_0(p) \quad (8a)$$

i.e.

$$\frac{\partial}{\partial p} (p Y) - 3 Y \left(1 - \frac{1}{e^q - 1} \right) = \frac{3 S_0(p)}{V_0} \quad (8b)$$

The source spectrum surely falls eventually as $p \rightarrow \infty$, so with

$$Y \rightarrow 0 \text{ as } p \rightarrow \infty \quad (8c)$$

equation (8b) has the general solution (9a,b) below for $q \gtrless 0$ where for $q_0 > 0, V_0 > 0, A = 0$ exactly. Then $j = \frac{\beta}{2\pi} \frac{V_0 Y(p)}{e^{q(p)} - 1}$

with

$$Y(p) = \frac{1}{p} e^{-h(p)} \left[\left\{ \int_0^p e^{h(p')} \cdot \frac{3 S(p')}{V_0} dp' \right\} + A \right] \quad (9a)$$

where

$$h(p) = \int_0^p \frac{1}{p'} \left[\frac{1}{e^{q(p')} - 1} - 1 \right] dp' \quad (9b)$$

To check the accuracy of $Y(p)$, which represents the intensity observed in the disc of the anti-galaxy, look first at the asymptotic limits for small and large p , in the case $S_0(p) \propto p^{-\gamma}$, $q(p) = q_0/(p/Gv)^{+\frac{1}{2}}$

$$Y(p) \rightarrow \frac{3S(p)}{V_0} \propto p^{-\gamma} \quad : p \rightarrow 0 \quad (10a)$$

$$Y(p) \rightarrow \frac{3q(p)S(p)}{V_0} \propto p^{-(\gamma+\frac{1}{2})} \quad : p \rightarrow \infty \quad (10b)$$

with the break around $q(p) = 1$. An approximate solution $Y^*(p)$ (following Kotá and Owens) may be recovered from

$$\frac{\partial}{\partial p} (pY^*(p)) = 0 \Rightarrow 3Y^*(p) \left(\frac{1}{e^q-1} - 1 \right) = \frac{3S_0(p)}{V_0} \quad (11)$$

This solution $Y^*(p)$ 'blows up' for certain low energies at fixed $q_0 < 0$ (infall). The exact solution, equation (9a,b) has the following behaviour for $V_0 < 0$

$$Y(p) \rightarrow \frac{3S_0 p^{-(\gamma-1)}}{|V_0|} + A p^{-3} \quad : p \rightarrow 0 \quad (12a)$$

$$Y(p) \rightarrow \frac{3q(p)S(p)}{|V_0|} \propto p^{-(\gamma+\frac{1}{2})} \quad : p \rightarrow \infty \quad (12b)$$

The term in p^{-3} is part of the homogeneous integral and does not obviously vanish. The particle flux is finite and the choice of A not affected by the boundary condition as $p \rightarrow 0$. It could be that there is some room for injection of particles at the shock. The constant A would be determined by the total energy that could be input from e.g. SN explosions, the depletion of low-energy \bar{p} by ionisation, and the time-dependence in a real Galaxy. An additional "source" term might explain the "bump" in the CR energy spectrum at $\sim 3 \times 10^{14}$ eV, seen by numerous workers (e.g. Watson 1974, Wolfendale 1974 (review)). For the present work, choose $A = 0$. Note that Lerche and Schlickeiser (1980, 1982) never discuss the infall case. Cowsik and Lee (1983) have discussed the high-energy asymptotic solution for the

shock-acceleration of test-particles in the time-independent spherically symmetric case.

Figure 4.6 shows the run of \bar{p} intensity with \bar{p} kinetic energy for a \bar{p} spectrum incident on the Galactic Halo with outflow amounting to $q_0 = 1, \sqrt{2}$ (Jones' best value) and 3; all normalised to the high-energy point of Golden et al. (1979) at ~ 7.3 GeV.

Figure 4.7 shows the \bar{p} intensity escaping from an anti-galaxy with source spectrum $p^{-2.2}$, for values of $q_0 = 0, +1, +\sqrt{2}, +3$ and $+10$.

Figure 4.8 shows the \bar{p} intensity on the Galactic plane for a spectrum of the type in Figure 4.8 incident on the Halo. We conclude that even the value for $q_0 = \sqrt{2}$ is not excluded, but that for $q_0 = 3$ is. The combination of $q_0 = +\sqrt{2}$ (our Galaxy) and $q_0 = +\sqrt{2}$ (anti-galaxy) - the most a priori likely solution, is excluded by the data.

4.5.3 Constraints on q . In the theory of Galactic Modulation, (similar to Solar Modulation),

the integral

$$q(p) = \int_0^d V(z) dz / K(z, p) \quad (13)$$

is important. Constraints on q are available from the:

- (1) Distribution and mean grammage traversed by CR nuclei.
- (2) CR positron spectrum (Protheroe 1981).
- (3) Estimation of $V_0, D, K(z, p)$ from mass-loss, observed gas scale-height, mean gas density, CR diffusion.

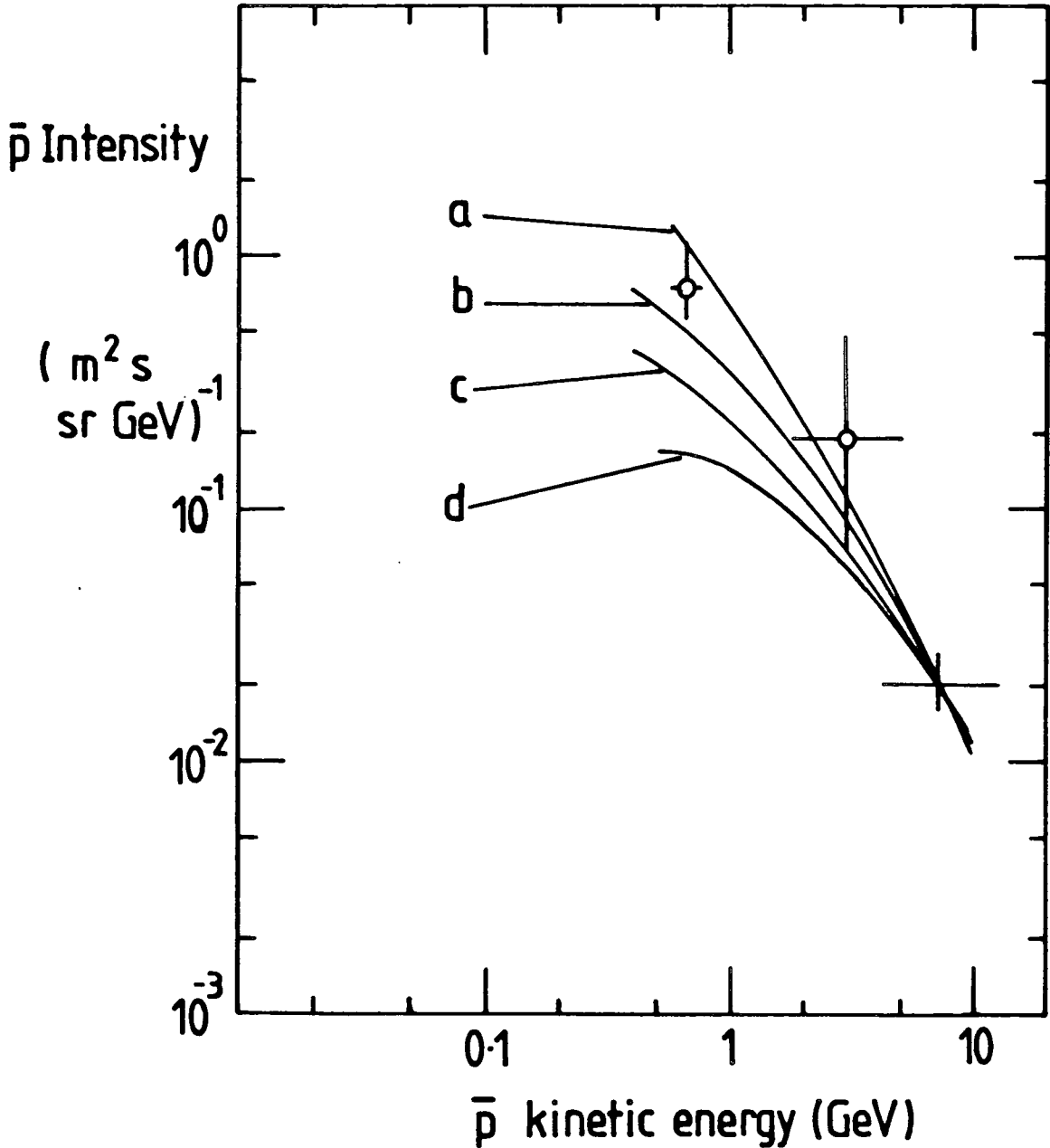


Fig. 4.6 Predictions of \bar{p} intensity v \bar{p} kinetic energy for a model in which Extragalactic primary \bar{p} 's (power law rigidity spectrum $\propto (R/\text{GV})^{-2.2}$) are partially excluded by an outwards directed Galactic Wind, whose strength is indicated by energy-loss parameter $q = q_0 (R/\text{GV})^{1/2}$. Curves a,b,c,d refer to values of q_0 : 1, 2, 3 respectively. The curves are normalised to the high-energy point of Golden et. al. (1979) and compared with the most likely demodulated \bar{p} flux ($\Phi = 600 \text{ MeV}$) as reported by Buffington et. al. (1981).

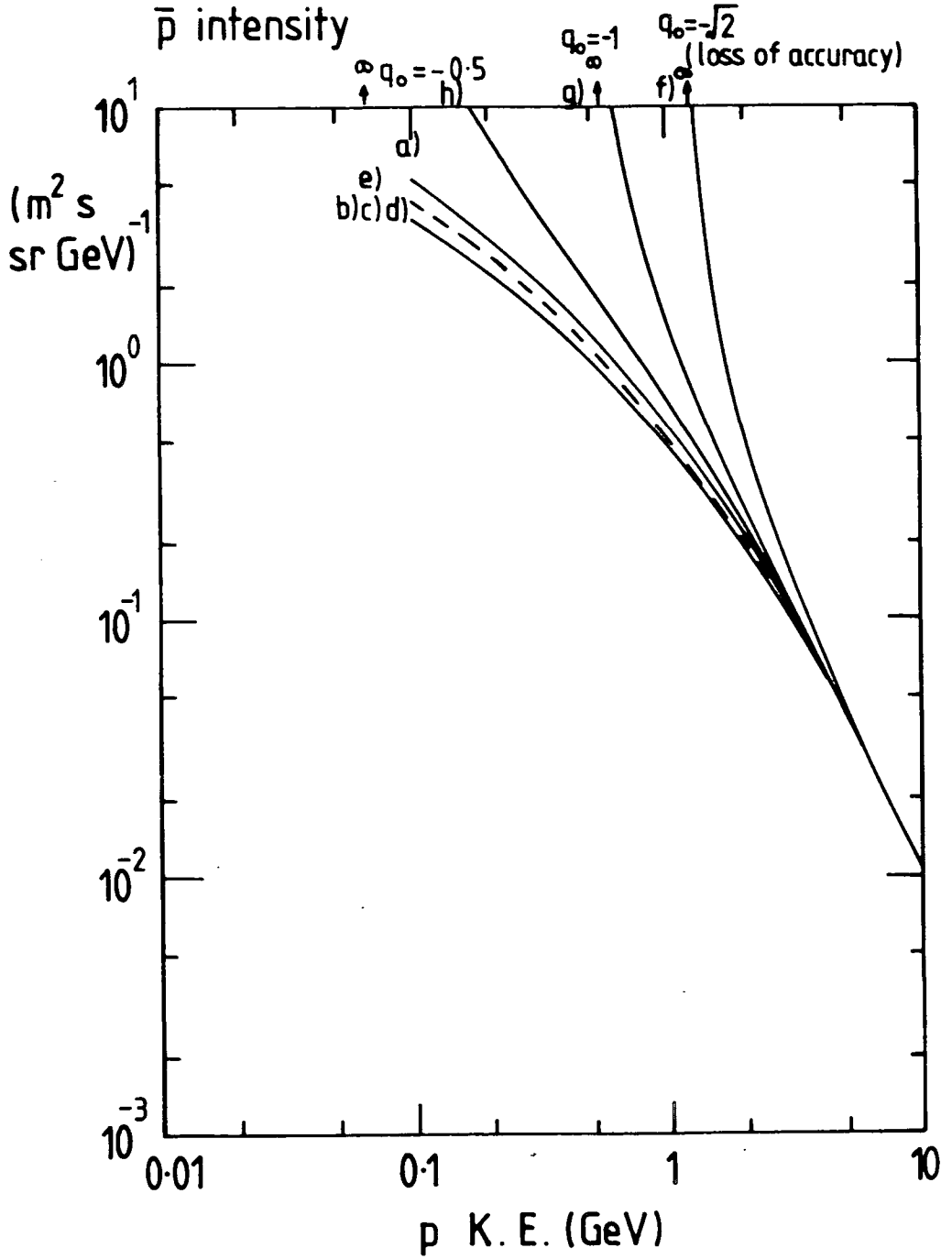


Fig. 4.7 Escaping antiproton spectra for various conditions:

(a) $R^{-2.2}$, (b) $R^{-2.2}$, $q_0 = 1$, (c) $R^{-2.2}$, $q_0 = 2$,

(d) $R^{-2.2}$, $q_0 = 3$, (e) $R^{-2.2}$, $q_0 = 10$.

(f) $q_0 = -1$, (g) $q_0 = -2$ (h) $q_0 = -0.5$.

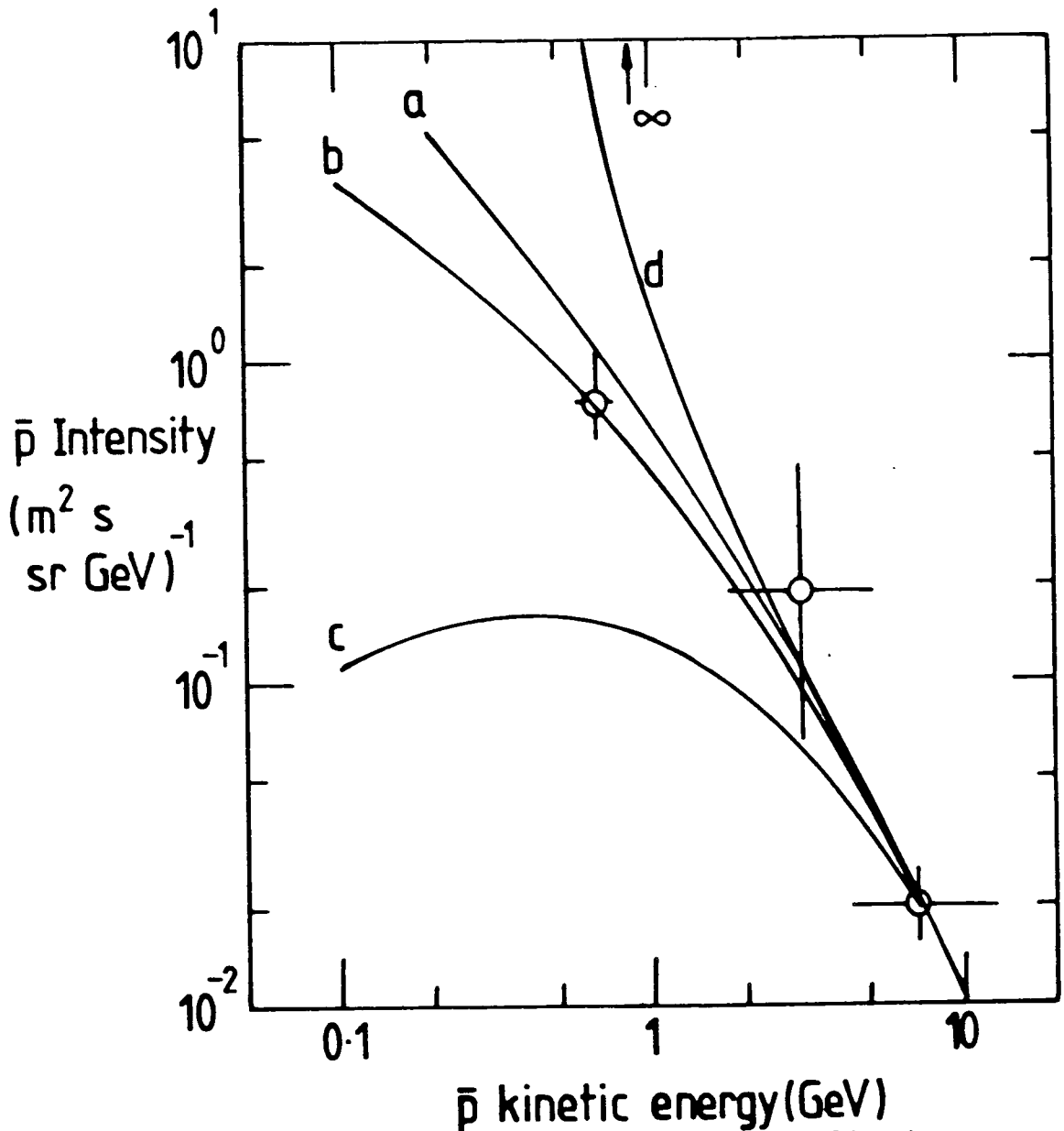


Fig. 4.8 Predictions of \bar{p} intensity v \bar{p} kinetic energy for a model in which Extragalactic primary \bar{p} 's (rigidity spectrum $\propto (R/\text{GV})^{-2.2}$) escaping from anti-galaxies with winds of strength q_{ex} , are modulated by a Galactic Wind of strength q_{gal} , for several pairs of values $(q_{\text{gal}}, q_{\text{ex}})$.

Curve $a, (0,0)$; $b, (0, \sqrt{2})$; $c, (\sqrt{2}, \sqrt{2})$; $d, (-1,0)$.

The Y-approximation (in text) is used here.

the direction perpendicular to the Galactic plane is

- (4) Other constraints already mentioned. Taking each case in turn: (a) the grammage indicated by the surviving fraction of ^{10}Be ($f_s = 0.14 \pm 0.07$) is in the range 0.1 to 0.3 for a diffusion coefficient in the range few $10^{28} - 10^{29} \text{ cm}^2\text{s}^{-1}$ at $\beta = 0.65$. The column density ρ_0 is uncertain by a factor of about two. Jones et al. cover the range $1 < q_0 < 3$. Freedman et al. cover the range (depending on f_s) 0.6 to 0.9. The range 0.6 to 3 with best value $\sqrt{2}$ covers the range of plausible values: (b) from a study of the positron spectrum (Orth et al and Buffington 1974, Giler 1977) and the L/M nuclei secondary/primary ratio, Protheroe (1981) suggests that the turnover of the primary spectrum starts at $q_0^2 = 4$ ($q_0 = 2$ being a reasonable choice).
- (5) The mass exchange between the mechanically-heated HISM and the Halo could amount to several $M_\odot\text{y}^{-1}$ (Chevalier and Oegerle 1979, Cox 1981).

Consider the motion of a fluid 'blob' (mass m_0) ejected from the Galactic plane with velocity v_0 . The potential energy V increases with distance from the Galaxy up to height ~ 10 kpc. Figure 4.9 (taken from Spitzer 1978) shows the variation of $V_g(z)$ with z , above the Solar position. The equation of motion is

$$m_0 \frac{dV(t)}{dt} = -G \frac{dV_g(z)}{dz} = -F \quad (14)$$

where red-giant stars principally contribute to $V_g(z)$. The force F per unit mass, exerted by the Galaxy, in the direction perpendicular to the Galactic plane is

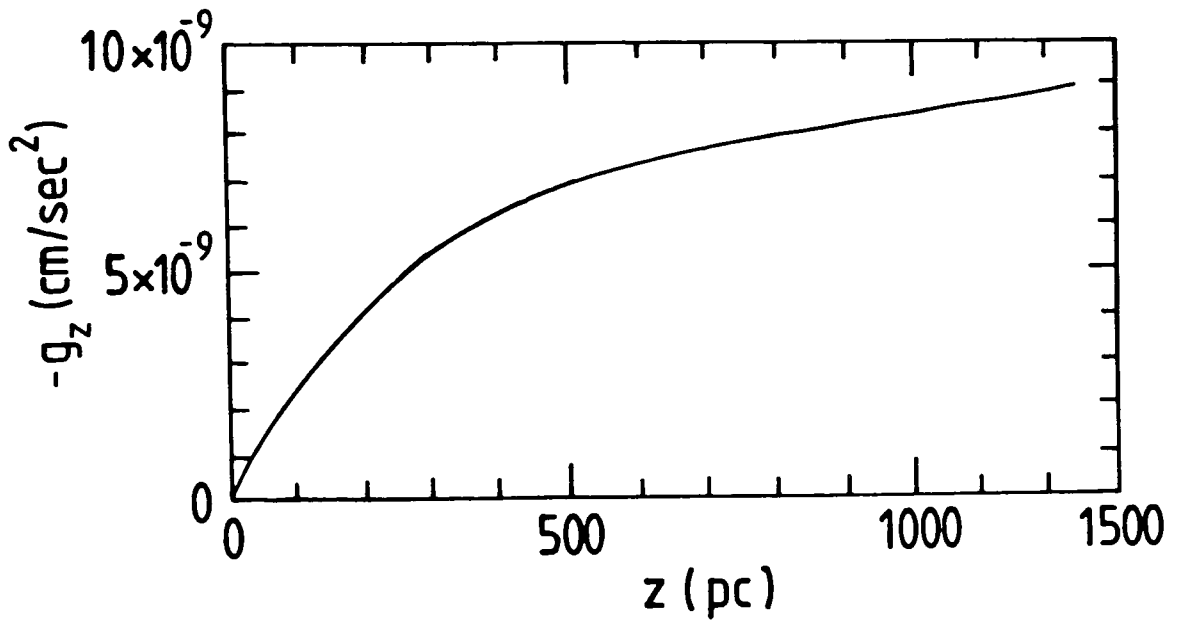


Fig. 4.9 Gravitational acceleration perpendicular to the galactic plane.

The curve shows values of $-g_z$ (referred to as $V_g(z)$ in this text) in cm s^{-2} as a function of z , the height above the galactic plane in pc, deduced from the measured distribution of K giant stars with z .

(from Spitzer 1978)

given by

$$F \sim -0.3 \times 10^{-10} \text{ cm s}^{-2} \text{ pc}^{-1} \quad (15 \text{ a})$$

where $v \sim 340 \text{ km s}^{-1}$ (e.g. Axford 1981a, review) for distances 15 kpc above the plane. Hence velocity V at time t

$$V(t) \sim V_0 t + \frac{1}{2} F t^2 \quad (15 \text{ b})$$

If the hot intercloud phase ($T \sim 10^4 \text{ K}$, $n_H \sim 0.03 \text{ cm}^{-3}$) is ejected with speed $(1 \text{ to } 2) \times 10^2 \text{ km s}^{-1}$ into the Halo, the maximum height reached will be $\sim 10 \text{ kpc}$.

The CR observed in the Disc have, on average, not penetrated more than $D/q(p)$ into the Halo. Thus the observed nuclear and \bar{p} spectrum is not obviously affected by conditions further out. If sufficiently numerous, the CR may make their own waves, streaming at V_A^* forward with respect to the gas.

4.6 Modulation of Galactic Spectra by Galactic Wind

These calculations may be applied to the modulation of a source of anti-protons by a Galactic Wind.

Adopting the secondary source spectrum of Tan and Ng 1981, the spectrum seen in the Disc for $q_0 = 0 \pm 1$ is shown in Figure 4.10 together with the modulation of the primary proton (Figure 4.11), electron (Figure 4.12) and positron spectrum (Figure 4.13) they predict.

Note a possible test for anti-matter. If a Galactic origin \bar{p} spectrum $\sim p^{-2.7}$ continues to higher energies, the spectrum will eventually steepen to $\sim p^{-3.2}$ due to diffusion.

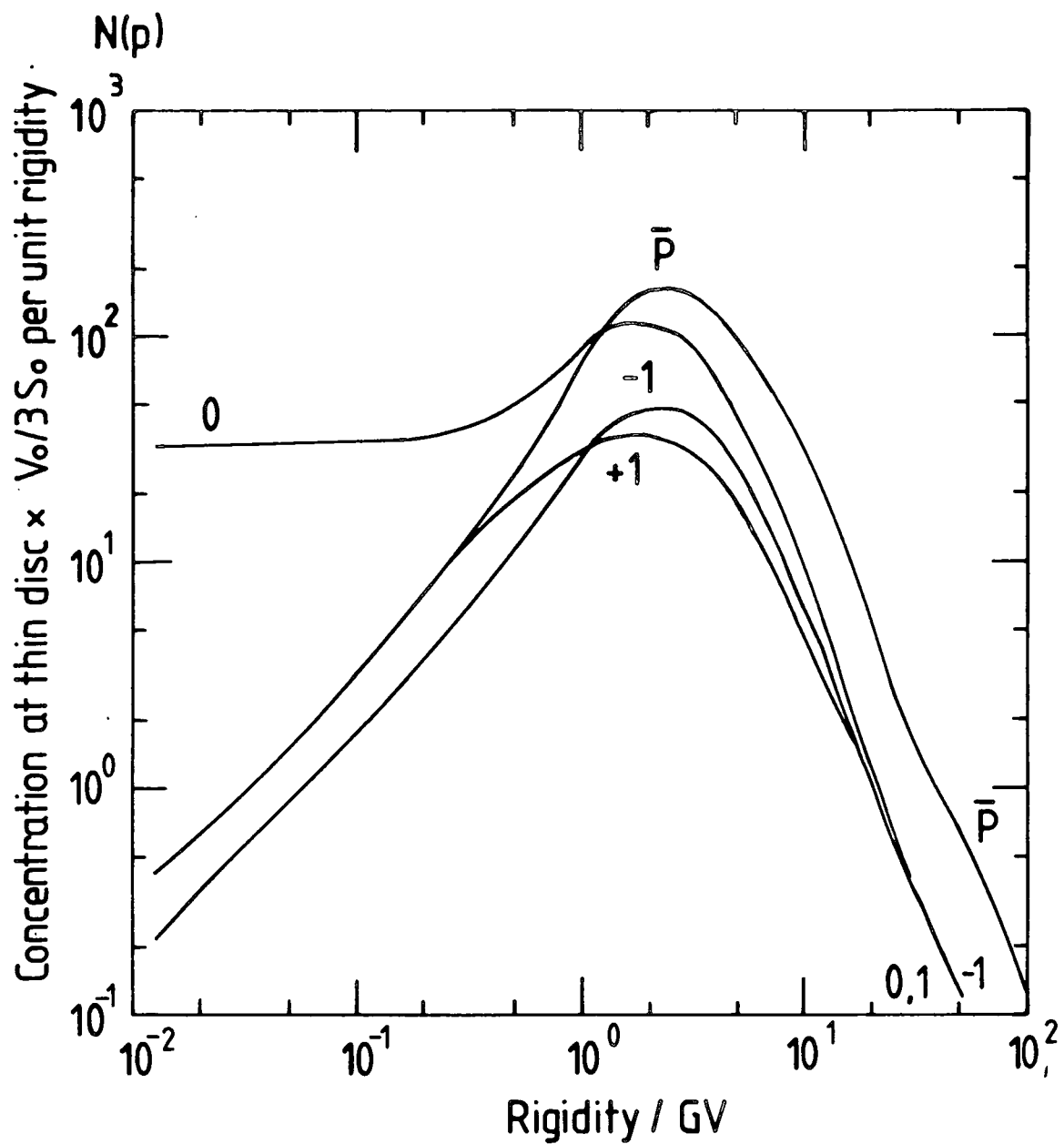


Fig. 4.10 Adiabatic deceleration/acceleration of Galactic secondary \bar{p} by Galactic winds of strength $q_0 = 1, -1, 0$. The quantity plotted for '0' is $S(p)/p^{\frac{1}{2}}$.

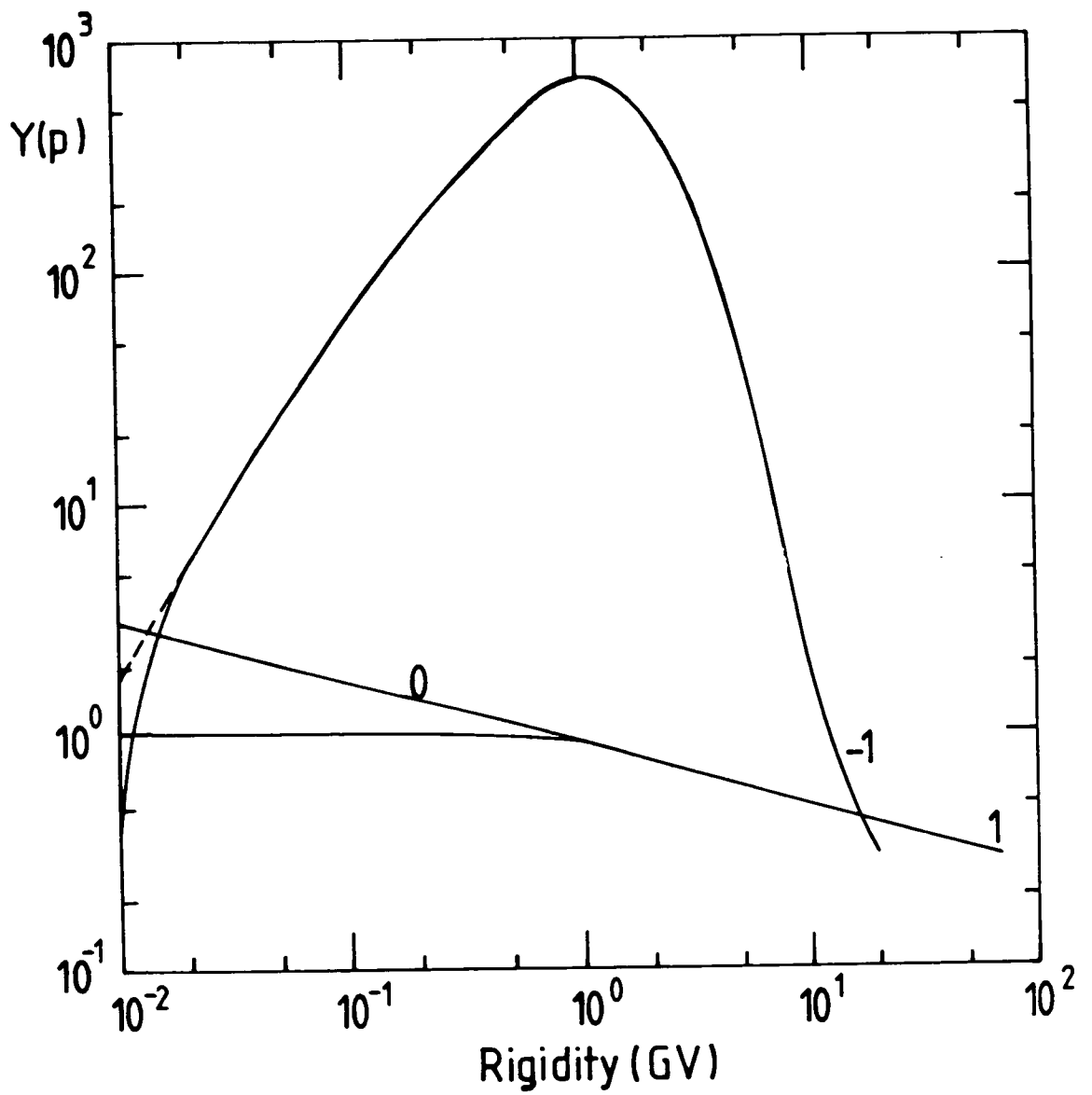


Fig. 4.11 Modulation of Galactic protons by Galactic winds of strength $q_0 = \pm 1$.

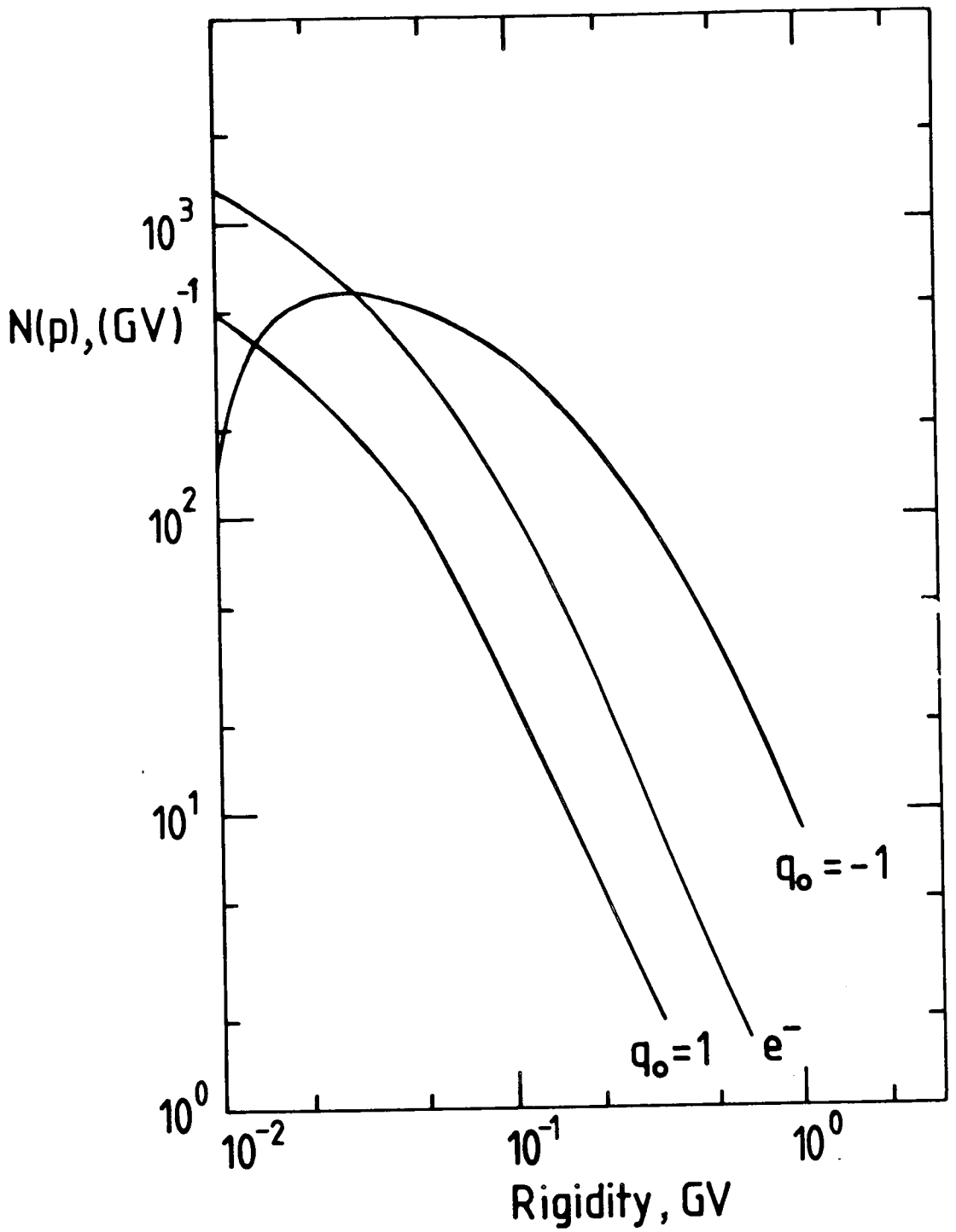


Fig. 4.12 Adiabatic deceleration/acceleration of Galactic secondary electrons by Galactic winds of strength $q_0 = \pm 1$.

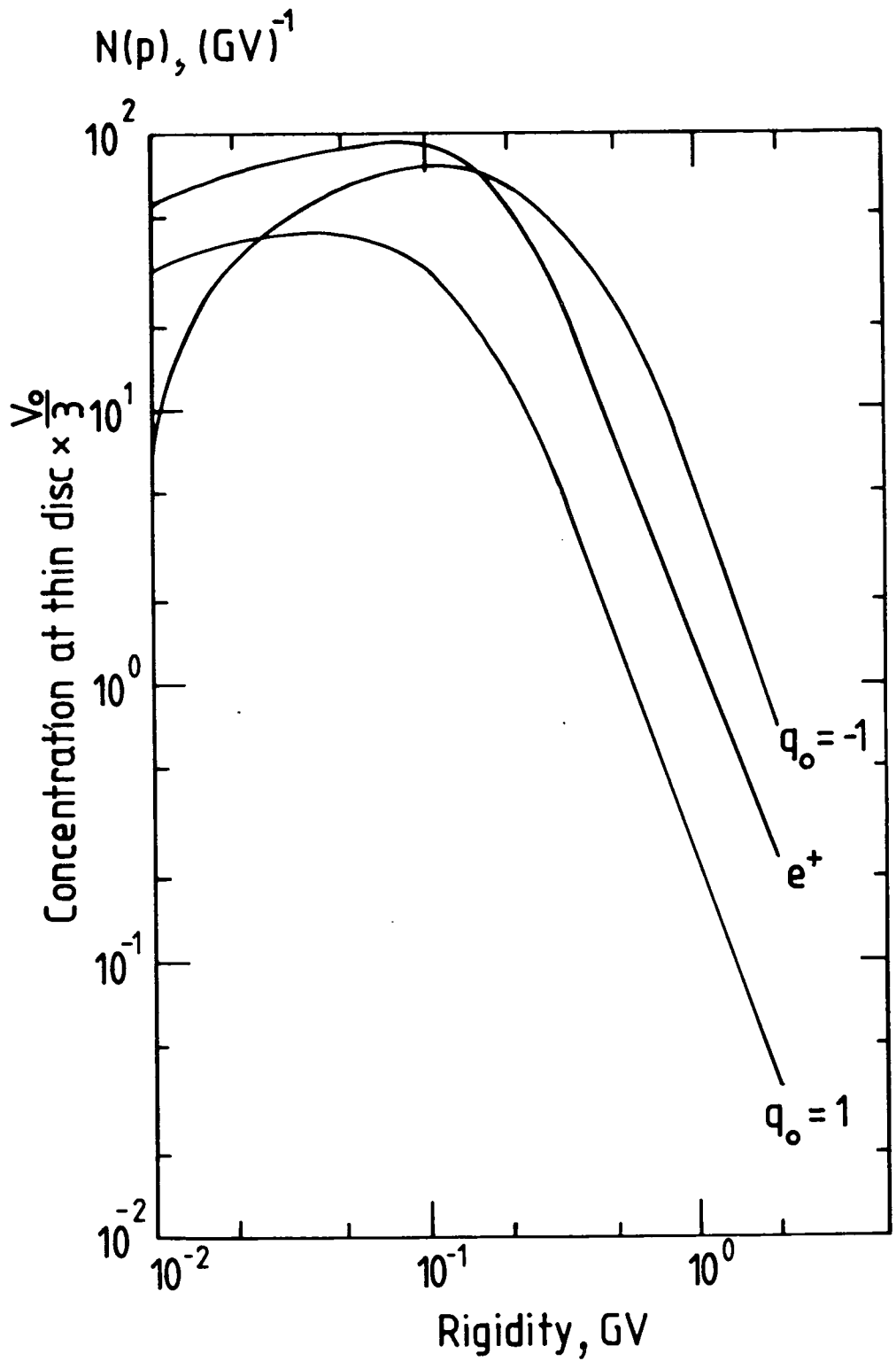


Fig. 4.13 Adiabatic deceleration/acceleration of Galactic secondary positrons by Galactic winds of strength $q_0 = \pm 1$.

4.7 Acceleration of High Energy Particles at Galactic Wind Terminal Shock?

Figure 4.14 shows a model of a Galactic Wind recently proposed by Jokipii and Morfill (1985), hereafter JM.

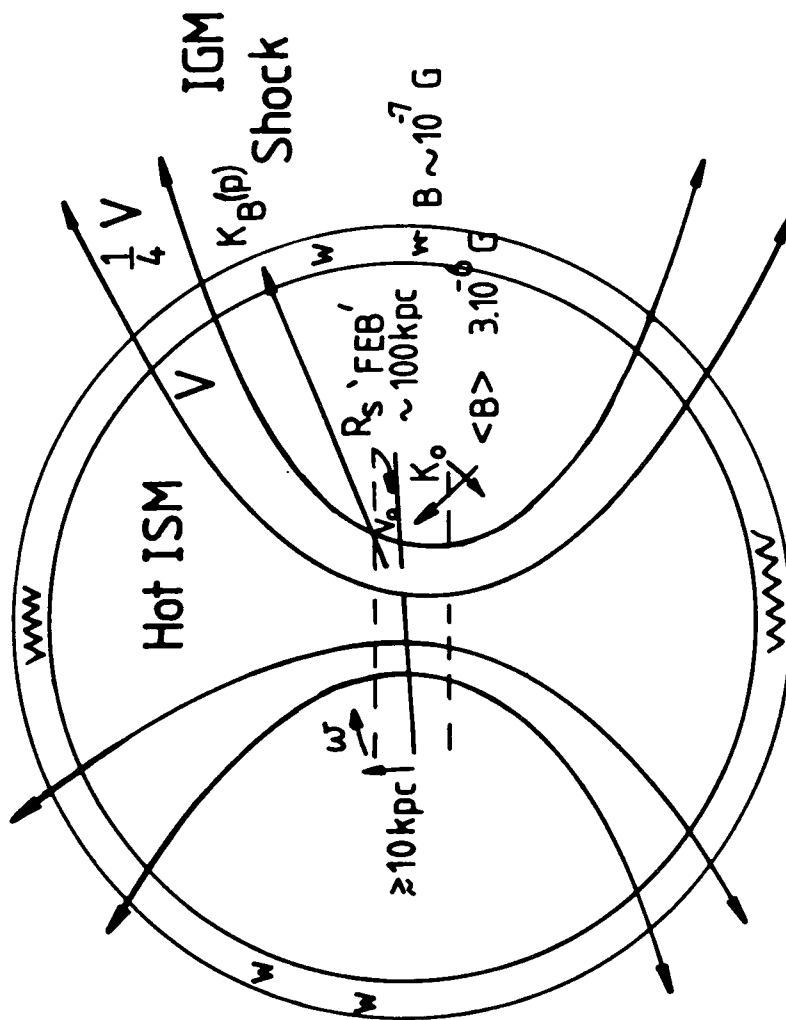
As stated in that paper, a mixture of gas, magnetic field and cosmic rays (CR's) similar to the hot phase of the interstellar medium (HISM) is expected to form a Galactic Wind (e.g. Johnson and Axford 1971, Ipavich 1975, Jokipii 1976, McKee and Ostriker 1977, Cox 1981).

The energy dependence of the CR composition (e.g. $^{10}\text{Be}/^{7+9}\text{Be}$) suggests a general energy-dependent outflow of CR from the Galactic disc (e.g. Jones 1979, Ormes and Protheroe 1983). This has been ascribed to either:

- (1) a CR diffusion coefficient which turns over to constant value in the rigidity interval (1-3)GV (the question of rigidity v. kinetic energy as organiser of the CR data has been investigated by e.g. Webber and Lezniak (1981) and other workers), or
- (2) a Galactic Wind which transports CR out of the Galaxy.

An upper limit to the steady (net) speed of convection of CR nuclei (esp. ^{10}Be) from the Galaxy at (low) energy (~ 280 MeV/nucleon) is $\sim 14 \text{ km s}^{-1}$ (Freedman et al. 1979, with thesis, see also Češarsky 1980, review). This speed is only slightly dependent on the assumed gas column density in the disc, applies at least up to the assumed free-escape boundary (~ 10 kpc above the Galactic plane) for a one-dimensional model, and

Fig. 4.14 The Galactic Halo model of Jokipii and Morfill (1985).



hardly affects the source power required to maintain the energy density of CR.

However, it may be that supernova (SN) shock waves run up and strengthen in the Halo above ~ 10 kpc, causing a much faster outflow of material which escapes from the Galaxy ($\sim 2 M_{\odot}/\text{year}$, 500 km s^{-1}). The sound speed in a low density, high temperature, CR filled, coronal gas is $\sim 200 \text{ km s}^{-1}$. Perhaps this outflow terminates in a large (~ 100 kpc), old (perhaps $\sim 10^9$ to 10^{10} years) strong shock; pressure balance, possible intracluster wind and infalling gas streams will all play a part. This type of Halo is advocated by e.g. Bregman (1981) or Axford (1981a, review). According to JM, the wound-up magnetic field is supposed to be $\sim 10^{-7}$ Gauss at 100 kpc from the Galaxy. The (fastest possible) acceleration of CR to $\sim 10^{16} - 10^{17} \text{ eV}$ in such a shock probably implies non-linear acceleration, $\delta B \sim B$, with corresponding energy density of the magnetic field $B^2/8\pi \sim 2.5 \times 10^{-4} \text{ eV cm}^{-3}$. The CR diffusion coefficient K_B is given by

$$K_B = \frac{1}{3} \cdot 10^{15} \left(\frac{\text{pc}}{\text{eV}} \right) \text{ cm}^2 \text{ s}^{-1} \quad (r_g(B=10^{-7}) \sim 3.3 \times 10^4 \left(\frac{\text{pc}}{\text{eV}} \right) \text{ cm}) \quad (15)$$

and the condition that the shock is locally plane

$$\frac{VL}{K_B(\omega)} \gg 1 \Rightarrow \left(\frac{\text{pc}}{\text{eV}} \right) \ll 4.5 \times 10^{16} \text{ eV} \quad (16)$$

If acceleration proceeds for the cosmological time $\sim 10^{10}$ years (without cosmological deceleration), the maximum rigidity reached is $\sim 6 \times 10^{17} \left(\frac{\text{pc}}{\text{eV}} \right) \Big|_{t=0}$ if shock remains steady. The plasma is probably a high beta plasma, $\beta = 8\pi P_{\text{CR}}/B^2 \gtrsim 1$ (or the wind would not

continue to expand) so CR may stream freely from the shock after building up to equipartition energy density with the waves, $(\delta B)^2(k)/8\pi$ (k = wave number = $1/r_g(B)$), which may well have a steeply falling spectrum (e.g. Kolmogorov : $\gamma = -3/2$).

Cosmic rays which escape from our Galaxy will suffer little change of spectral shape or intensity (strong inelastic collision losses negligible over confinement time) up to height ~ 10 kpc. The bulk flow probably diverges (see Figure 4.14) up to a height ~ 100 kpc. If the CR energy generation rate is $\sim 6 \times 10^{40} \text{ erg s}^{-1}$ denoted by S_0 , (e.g. JM; others) the supply rate to the shock in the absence of external sources (and the presence of adiabatic deceleration) is approximately

$$\left(\frac{10}{100}\right)^4 S_0 (P/\text{GV})^{-\gamma} H \left[10^4 - \frac{P}{\text{GV}}\right] \text{ cm}^3 \text{ sr}^{-1} \text{ s}^{-1} \quad (P \geq P_0) \quad (17)$$

where $P_0 \sim 10^4 \text{ GV}$ and H represents the Heaviside function.

The spectral shape at source (γ) is probably $p^{-2.4}$ for rigidity

$< 18 \text{ GV}$, $p^{-2.0}$ above this value (e.g. Ormes and Protheroe 1981). The shell of CR will be of width $\langle K(p) \rangle / V_0$

$\sim 1.5 \text{ Mpc}$ at 10^{19} eV (see Drury 1983, review).

Very high CR ($> 10^{18} \text{ eV}$) are subject to additional losses by interaction with the 3K relict radiation.

- (a) pair production of e^+ and e^- ,
- (b) photoproduction of hadrons and
- (c) photo-disintegration of nuclei via the Giant Dipole Resonance.

Particles accelerated for nearly cosmological times will be much decelerated in the 'expanding Universe'. The source power to supply enough seed particles to produce the observed flux of very high energy particles ($> 10^{18}$ eV) at earth would be $\sim 10^{43}$ erg s $^{-1}$, much too high for conventional Supernovae. If the total flux of very high energy particles observed at earth were accelerated at this shock, the p spectrum could extend back to ~ 10 MeV (say), implying a Metagalactic p Origin Model, quite inconsistent with observation. The observed 'isotropic' radio background at 408 MHz is 3.2 K, of which ~ 1.7 K is not accounted for by presently known radio galaxies (excluding evolution) (J.L. Osborne, personal communication). The synchrotron radio emission at 408 MHz, by electrons, of the directly-detected ambient intensity (i.e. not the low-energy radio-observed component) in a magnetic field B amounts to $1.7 \text{ K kpc}^{-1} \times (\text{electron intensity/ambient}) \times (B/3 \mu \text{ Gauss})^2$. The electrons involved would either be secondaries to the production of the high energy CR particles, or low-energy electrons which have survived due to the γ^2 factor in the synchrotron or Compton loss rate. It seems very unlikely that the radio Halo could be this large; or that the shock only contains very high energy particles (unless seed particles were supplied slower than depleted by acceleration, loss, or convection through the shock). Note that diffusion is a poor approximation for very high energy particles

above $\sim 10^{15}$ eV. A single-particle trajectory-tracing approach would be more correct (Schlickeiser 1983, rapporteur paper). The modulation of such particles would be severe only if

$$\frac{V_0 h}{K_B(p)} \gtrsim 1$$

As (correctly) stated by JM, low energy particles, $E_p < 10^{14}$ eV do not leak back to the Disc.

The measured anisotropy (\sim few 10% at 10^{18} eV) seems large for such a model. Approximating the shock as an off-centre spherical shell (JM say the shock is pushed closer to Galaxy by motion towards Northern latitudes), the predicted anisotropy δ (without CR scattering) is approximately

$\delta \approx a_1/(a_1 + a_2)$ where a_1, a_2 are the 'semi-minor and major' axes respectively. More probably, particles are continuously re-accelerated by random supersonic motions high in the Halo (above the FEB). Such particles should exhibit an increasing energy with age but enter the Disc rarely. The momentum-diffusion time-scale

$t_2 \gtrsim K_B/V_A^{*2}$, where V_A^* is the Alfvén speed in the ionised part of the plasma. This Alfvén speed is as nearly

as high as the overall sound speed; particles may rapidly be accelerated from high energy ($\sim 10^{14}$ eV) to $\sim 10^{20}$ eV,

without being confined in the Halo. Some of those particles may leak back to earth.

4.7.1 Implications for Extragalactic \bar{p} Origin. If

this model of the Galactic Wind is true

- (1) High energy antiprotons which have survived the journey from external anti-superclusters (Stecker 1981, Kiraly et al. 1982) may be decelerated through

$$\phi \sim [V_0 L / 3 K_B(\rho)] E_p \text{ eV for } \left| \frac{V_0 L}{K_B(\rho)} \right| \lesssim 1$$

- (1) Low energy (e.g. $< 10^{14}$ eV) extragalactic antiprotons will be excluded to the extent of $\exp(-V_0 D / K_B)$.

The extragalactic hypothesis for the origin of the low energy antiprotons observed at earth would be even less likely than before. This would pose the problem of matter-antimatter asymmetry. An additional argument can be adduced against the EG \bar{p} Origin model. The abundance of He (or $\bar{\text{He}}$) appears uniform between observed galaxies or quasars. If they belonged to domains with different baryon/photon ratio, the Helium abundances should differ. Thus it appears improbable that observed Extragalactic objects belong to a domain different from ours. Hence only domains unobservably distant might reasonably be strong \bar{p} sources.

4.7.2 Implications for the model of the Galactic

Wind. If the copious production of CR's in the convective Halo is a necessary consequence of a Galactic Wind, and the gamma-ray etc. data do not permit it, then we must return to the diffusion CR transport model.

4.8 Summary and Conclusions

- * No antiproton origin model is fully consistent with all the data.
- * The Extragalactic \bar{p} origin model is excluded by the (likely) putative Galactic Wind - especially if external antigalaxies also have outflowing winds.

* A downdraft of scattering centres can accelerate and trap low-energy Galactic secondary particles as well as alter the secondary/primary ratio at low energies.

* Acceleration of particles of highest energies observed in our Galaxy from its terminal wind shock is unlikely. If that hypothesis were true, the Extragalactic hypothesis for the origin of the low energy antiprotons observed at earth would be even less likely than before.

CHAPTER 5

The main results and conclusions of each chapter were summarised at each chapter end.

In conclusion,

- (a) It is reassuring that the models developed in Chapter 2 and 3 show that a typical GMC shows ECRI only under unusual circumstances.
- (b) The ECRI models can just account for the brightest observed enhancement (Carina Nebula) in >100 MeV γ -rays, if k is (reasonably) small.
- (c) The proportion of the ambient CR flux due to collapsing clouds is hard to estimate as it depends sensitively on the details of star formation. Not more than a few percent of the total flux may originate this way. As for Galaxy Formation, it is hard to see more than a few percent of the flux below 10^{15} eV/nucleon (10^{21} eV/nucleon for maximum scattering) originating this way.
- (d) The high matter traversal by a small proportion of CR in clouds crushed in Supernova shells may help towards the explanation of (i) the paucity of short pathlengths, (ii) the \bar{p} spectrum observed.
- (e) The Blandford and Cowie (1982) solution for the enhancement of relativistic particles by secondary cloud sub-shocks may now be bounded above by cloud rotation ($n_H^{1/3}$ factor) and below by CR escape, using formulae developed in Chapter 2 and 3. Note, in passing, that a $\simeq 40\%$ enhancement of CR intensity over the last 10^6 years is feasible even with the solution reviewed by Axford

(1981a); there is a mistake in the right-hand scale of his Figure 10. Without cloud-crushing, the $E^{-0.35}$ energy-dependence of the L/M ratio found by HEAO-3 would mean that only very young small shocks would have been effective in accelerating the observed CR, not in itself an unreasonable conclusion. But the new model increases the proton flux and maximum energy somewhat by 'prompt' re-acceleration.

(g) Cloud collapse can either be mediated or inhibited by shocks in which CR are accelerated.

(h) CR's may be excluded from T-Tauri stellar wind cavities, to the extent of $\exp(-VR_s/K_{rr})$.

(i) No current \bar{p} origin model explains all the data.

In conclusion, I hope the work presented in this thesis proves useful to other workers in this growing field.

5.1 Suggested Future Work

(i) Continue improvements to SNR shock-acceleration CR model,

(ii) Look for HV clouds as soon as detectors capable of $10^{-7} \text{ cm}^{-2} \text{ } \gamma (> 100 \text{ MeV}) \text{ s}^{-1}$ become available (GRO...),

(iii) Check whether the luminosity maximum is from the GMC or H-II region in the Carina Nebula,

(iv) Search for 'holes' in the gamma-ray sky with improved detectors and longer observing times.

APPENDIX A

Release of Gravitational Energy During Cloud Contraction

When a homogeneous spherical gas cloud (mass M , radius R_0) contracts uniformly and isotropically to radius R , the gravitational energy changes by

$$\Delta E_g = -\frac{3}{5} G M^2 \left(\frac{1}{R} - \frac{1}{R_0} \right) \quad (A1)$$

(G = gravitational constant). If the initial and present cloud densities are $n_H(0)$ and $n_H(t)$ cm^{-3} at time t after the start of the contraction

$$\Delta E_g = -\frac{3}{5} G \left(\frac{4\pi m_p}{3} \right)^{\frac{1}{3}} \cdot M^{5/3} \left[n_H(t)^{\frac{1}{3}} - n_H(0)^{\frac{1}{3}} \right] \quad (A2)$$

(m_p = proton rest mass).

If the mass is $M_5 \times 10^5$ solar masses and the radius $R_1(t)$ parsecs, equation (A2) becomes

$$\Delta E_g = -5.2 \times 10^{48} \cdot M_5^{5/3} \left[n_H(t)^{1/3} - n_H(0)^{1/3} \right] \text{ erg} \quad (A3)$$

and the radius R at time t is given by

$$R(t) = 99 \left(\frac{M_5}{n_H(t)} \right)^{\frac{1}{3}} \text{ parsec} \quad (A4)$$

APPENDIX B

Solution of the time-dependent transport equation

Solutions of the steady-flow test-particle transport equation with energy losses have been given by Ginzburg and Syrovatskii (1969) and others; including Freedman et al. (1979, 1980) Lerche and Schlickeiser (1980, others) and Volk (1980). Solutions of the steady-flow transport equation with losses and time-dependence have been given by Syrovatskii (1957, loss-time method), for three-dimensional flow and Axford (1981a, review) for one-dimensional flow.

The case of unsteady flow and time-dependence has been considered by Volk and Bogdan (1982), also Axford and Moraal (1982), without energy loss. The case of unsteady flow, spherical symmetry and arbitrary time-dependence has been treated by a perturbation method for an expanding flow (Drury 1982, review), and for a special flow ($\frac{1}{2}R \dot{R}/k(t) = \text{constant}$) by Prishchep and Ptuskin (1982). Cowsik and Lee (1983) have considered steady accretion in the spherically-symmetric case, for test-particles.

I know of no solution published to date describing acceleration of cosmic rays at an unsteady accretion shock, including the particle pressure and energy loss.

The solution above, using the approximate instantaneous spectral index deduced from Cowsik and Lee's (1983) paper, is a reasonable starting point. The spectrum may be further softened by loss cf. Volk (1980). A numerical solution could be obtained by Monte-Carlo simulation.

APPENDIX C

When does magnetic flux-freezing hold?

Maxwell's equations for an homogeneous isotropic conducting fluid in any inertial coordinate frame (CGS)

$$4\pi \underline{j} + \frac{\partial \underline{E}}{\partial t} = c \nabla \times \underline{B} \quad (1)$$

$$\frac{\partial \underline{B}}{\partial t} = -c \nabla \times \underline{E} \quad (2)$$

$$\nabla \cdot \underline{E} = 4\pi \delta \quad (3)$$

$$\nabla \cdot \underline{B} = 0 \quad (4)$$

imply flux-freezing when the electrical conductivity is sufficiently high. This may be shown by two methods:

(1) Following Longair (1981, monograph);

First study the changes in a stationary resistanceless current loop, in a changing magnetic field. Although the external magnetic flux may change, a current is induced which exactly cancels the change in external flux. Secondly consider the coil moving, expanding; the increased area links more flux, cancelling the current produced by the movement in the external field.

(2) Following Parker (1969, monograph);

$$\frac{\partial \underline{B}}{\partial t} = \nabla \times (\underline{v} \times \underline{B}) + \eta \nabla^2 \underline{B} - \nabla \eta \times (\nabla \times \underline{B}) \quad (5)$$

($\eta = c^2/4\pi\sigma$)

$$\text{If } \sigma \rightarrow \infty, \frac{\partial \underline{B}}{\partial t} \rightarrow \nabla \times (\underline{v} \times \underline{B}) \quad (6)$$

Hence $\int_C \underline{dS} \cdot \underline{B} = \text{constant}$, where C is any simply-connected surface enclosing \underline{B} . Hence the condition that $R_m \gg 1$ is necessary for flux-freezing. In the opposite case a variety of effects (magnetic buoyancy, diffusion of magnetic field ...) operate. For sufficiently rapid variation in magnetic field so that the neglected displacement current becomes important, flux-freezing does not hold.

Magnetic reconnection (e.g. Parker 1969, monograph) may also invalidate flux-freezing. This may occur in a collapsing rotating magnetized cloud (e.g. Dorfi 1982). There is some debate about the density at which flux-freezing breaks down (often thought to be 10^{14}cm^{-3} , but see Scalo (1977) who recommends densities as low as 10^8cm^{-3}).

The 'ambipolar diffusion' mechanism operates, the magnetic stress acceleration on the thermal electrons exceeding that on the ions due to lower mass. The cloud may expand until the magnetic field is sufficiently reduced (e.g. Spitzer 1978).

This point has been briefly considered by Bignami, Forman and Morfill (1984).

ACKNOWLEDGEMENTS

It is a pleasure to acknowledge the friendly hospitality of the Durham Theoretical Astrophysics Group where this work was supervised by Prof. A.W. Wolfendale 1979-82, and on the author's return in 1985.

The Cambridge Institute of Astronomy are also thanked for friendly hospitality during June-August 1985 when the work was completed.

The SERC are thanked for a Research Training Award (1979-82), also travel expenses for the following venues:

- (1) Herstmonceux - RGO Introductory Meeting.
- (2) London - The Royal Society Discussion meeting.
- (3) Palermo (Sicily) - Discussion on gamma-ray pulsars.
- (4) Katlenburg-Lindau (FRG) - "Cosmic ray transients in collapsing clouds", presented at X.-Lindau Symposium on the Origin of Galactic Cosmic Rays.

Mrs. Margaret Chipchase is thanked for her careful typing of this thesis, and Mrs. Pauline Russell who drew the illustrations skillfully.

REFERENCES

- Achterberg, A., Blandford, R.D., and Periswal V., (1984), *Astron. Astrophys.*, 132, 97.
- Ahlen, S.P. et al. (1982), *Ap. J.* 260, 20.
- Alfvén, H., (1939), *Nature* 143, 435.
- Alfvén, H., (1954), *Tellus* 6, 232.
- Alfvén, H., and Carlqvist, P., (1978), *Ap. Sp. Sci.* 55, 487.
- Alfvén, H., (1982), *Cosmic Plasma* (Reidel : Dordrecht).
- Allen, C.W., (1973), *Astrophysical Quantities* (Athlone: London).
- Apparao, K.M.V., Durgaprasad, N., Stephens, S.A., and Biswas, S., 1983, *Proc. 18th Int. Cosmic Ray Conf.*, 2, 75.
- Axford, W.I., and Gleeson, L.J., (1968), *Ap. J.* 154, 1011.
- Axford, W.I., (1981a), MPAE-W-100-81-83 (Max Planck Institut für Aeronomie, Garching bei München, FRG).
- Axford, W.I., (1981b), *Proc. X. Texas Symp. on relativistic astrophysics*, Baltimore, *Ann. N.Y. Acad. Sci.* 375, 297.
- Axford, W.I., (1981c), *Proc. Int. School and Workshop on Plasma Astrophysics*, European Space Agency SP-161, 425.
- Axford, W.I., and Moraal, H., (1982), *Astron. Astrophys.* 125, 204.
- Baade, W., and Zwicky, F., (1934), *Phys. Rev.* 45, 138.
- Badhwar, G.D., et al. (1975), *Ap. Sp. Sci.* 37, 383.
- Baldo-Ceolin, M., (1984), *AIP Conf. Proc. (USA)* 114, 36 (Proc. of the Mini-conference on low-energy tests of conservation laws in particle physics).
- Bardeen, J.M., (1981), *Phys. Rev. Lett.*, 46, 382.
- Bell, A.R., (1978a), *MNRAS* 182, 147.
- Bell, A.R., (1978b), *MNRAS* 182, 443.
- Bennett, K., et al. (1977), in *Recent Advances in Gamma Ray Astronomy*, ESA SP-124.
- Bennett, W.H., (1934), *Phys. Rev.* 45, 890.

- Bhat, C.L., et al. (1984), submitted to Nature, 1984.
- Bignami, G.F., (1984), in press.
- Black, J.H., and Fazio, G.G., (1973), Ap. J. Lett. 185, L7.
- Black, D.C., and Bodenheimer, P., (1976), Ap. J. 206, 1388.
- Blandford, R.D., and Cowie, L.L., (1982), Ap. J. 260, 625.
- Blandford, R.D., and Ostriker, J.P., (1980), Ap. J. 237, 793.
- Blitz, L., and Shu, F.H., (1980), Ap. J. 238, 148.
- Bloemen, J.B.G.M., et al., (1984a), Ap. J. 279, 136.
- Bloemen, J.B.G.M., et al., (1984b), Astron. Astrophys. 135, 12.
- Bodenheimer, P., and Sweigart, A., (1969a), Ap. J. 152, 515.
- Bogdan, T.J., and Volk, H.J., (1983), Astron. Astrophys. 122, 129.
- Bogomolov, E.A., et al., (1979), 16th ICRC, 1, 330 (Japan: Kyoto 1979).
- Bothe, W., and Kolhorster, W., (1914), Phys. Z. 56, 751.
- Bregman, J.N., et al., (1981), Nature, 293, 714.
- Bowen, T., Jenkins, E.W., Jones, T.J., Pifer, A.E., and Sembroski, G.H., (1983), Proc. 18th Int. Cosmic Ray Conf., 2, 96.
- Buffington, A., Orth, C.D., Smoot, F.G., (1974), Phys. Rev. Lett., 33, 34.
- Buffington, A., and Schindler, S.M., (1981a), Ap. J. Lett., 247, L105.
- Buffington, A., Schindler, S.M., and Pennypacker, C.R., (1981b), Ap.J. 248, 1179.
- Cameron, A.G.W., (1973), Sp. Sci. Rev. 15, 121.
- Carr, B.J., (1976), Ap. J. 206, 8.
- Cassé, M., (1980, in Origin of Cosmic rays, IAU Symp. 94 (Setti, G., Spada, G., and Wolfendale, A.W., eds). (Reidel: Dordrecht 1981).

- Cassé, M., and Paul, J.A., (1980), *Ap. J.* 237, 136.
- Césarsky, C.J., (1980), *Ann. Rev. Astron. Astrophys.* 18, 289.
- Césarsky, C.J., and Volk, H.J., (1978), *Astron. Astrophys.* 70, 367.
- Césarsky, C.J., and Lagage, P.A., (1981), *OG 4-31 9*, 17th ICRC, p.250.
- Chevalier, R.A., and Oegerle, W.R., (1979), *Ap. J.* 227, 498.
- Chin, L., and Wentel, D.G., (1972), *Ap. Sp. Sci.* 16, 465.
- Clay, J., (1932), *Kon. Akad. Wet.* 35, 1282.
- Clayton, D.D., (1968), *Principles of stellar evolution and nucleosynthesis*, (McGraw-Hill: New York 1968).
- Cowling, T.G., (1945), *Proc. Roy. Soc. London A* 183, 453.
- Cowsik, R., and Lee, M.A., (1983), *Phil. Trans. Royal Soc. A* 383, 409 (London: 1983).
- Cox, D.P., (1981), *Ap. J.* 245, 534.
- Crouch, M.F., et al. (1978), *Phys. Rev. D.*, 18, 2239.
- Cummings, A.C., et al. (1975), 13th ICRC, 1, 340.
- Davies, R.D., (1982), *Phil. Trans. Royal Soc.*, A303, 581.
- Dennison, B., (1980), *Ap. J.* 239, L93.
- Dodds, D. et al., (1975), *Mon. Not. R. astr. Soc.*, 171, 569.
- Dogiel, V.A., Freedman I., Kiraly, P., and Wolfendale, A.W., (1983), 18th ICRC, OG 2, 292.
- Dorfi, E., (1982), *Astron. Astrophys.* 114, 151.
- Drury, L. O'C (1983), *Rep. Progress in Physics* 46, 972.
- Duley, W.W., and Williams, D.A., (1984), *Mon. Not. R. astr. Soc.* 211, 97.
- Eichler, D., (1981), *Ap. J.* 247, 1089.
- Eichler, D., (1982), *Nature*, 295, 391.
- Elmegreen, B.G., (1980), in *Giant Molecular Clouds in the Galaxy* (Solomon, P., Edmunds, M.G., eds). *Proc. 3rd Gregynog Astrophysics Workshop* (Pergamon: New York 1980).

Evenson, P., Garcia-Munoz, M., Meyer, P., and Simpson, J.A., 1983, Proc. 17th Int. Cosmic Ray Conf., 3, 246.

Fermi, E., (1949), Phys. Rev. 75, 1169.

Fichtel, C.E. et al., (1975), Ap. J. 198, 163.

Fisk, L.A., (1969), Ph.D. Thesis, University of California, San Diego.

Freedman, I., Giler, M., Kearsey, S., and Osborne, J.L., (1979), 16th ICRC, OG 2, 131.

Freedman, I., Giler, M., Kearsey, S., and Osborne, J.L., (1980), Astron. Astrophys. 82, 110.

Gaisser, T.K., and Maurer, R.H., (1973), Phys. Rev. Lett. 30, 1264.

Garcia-Munoz, M., Mason, G.M., and Simpson, J.A. (1975), Ap. J. 201, L141.

Garcia-Munoz, M., Mason, G.M., and Simpson, J.A., (1977), Ap. J. 217, 859.

Garcia-Munoz, M., Simpson, J.A., and Wefel, J.P., (1983), 18th ICRC, OG 2, 210

Garmston, H.J., and Watson, A.A., (1972), Nature Phys. Sci. 237, 39.

Gerola, H., and Glassgold, A.E., (1980), in Giant Molecular Clouds in the Galaxy, op cit.

Gibson, A.I., et al., (1982), Nature 296, 833.

Giler, M., Wdowczyk, J., and Wolfendale, A.W., (1980), Astron. Astrophys. 84, 44.

Giler, M., et al., (1977), J. Phys. A10, 843.

Ginzburg, V.I., and Syrovatskii, S.I. (1969), Origin of Cosmic Rays, (Pergamon: New York 1969).

Golden, R.L. et al. (1979), Phys. Rev. Lett. 30, 1264.

Gombosi, T., et al., (1975), Nature 255, 687.

Gordon, M.A., and Burton, W.B., (1980), in Giant Molecular Clouds in the Galaxy, op. cit.

Hartquist, T.W., and Dalgarno, A., (1980), in Giant Molecular Clouds in the Galaxy, op. cit.

- Hawking, S.W., (1974), *Nature* 248, 40.
- Hayakawa, S., (1972), *Ap. Sp. Sci.* 16, 238.
- Heiles, C., Troland, T., and Stevens M., (1982a), *Ap. J.* 252, 179.
- Heiles, C., Troland, T., and Stevens, M., (1982b), *Ap. J.* 262, 135.
- Hermesen, W., (1981), Ph.D. Thesis, University of Leiden.
- Hess, V.F., (1912), *Phys. Z.* 13, 1004.
- Hillas, A.M., (1968), *Can. J. Phys.* 46, S623.
- Hillas, A.M., (1972), *Cosmic Rays* (Pergamon: Oxford 1972).
- Hillas, A.M., (1984), *Nature*, 312, 50.
- Hillier, R., (1984), *Gamma Ray Astronomy* (Oxford Studies in Physics 1984).
- Holman, G.D., Ionson, J.A., and Scott, J.S., (1979), *Ap. J.* 228, 576.
- Houston, B.P., and Wolfendale, A.W., (1982), *Ir. Astron. J.* 15, 182.
- Houston, B.P., and Wolfendale, A.W., (1984), *J. Phys. G*, 10, 1587.
- Houston, B.P., Wolfendale, A.W., and Young, E.C.M., (1984), *J. Phys. G* 10, L147.
- Hunter, C., (1977), *Ap. J.* 218, 834.
- Hunter, C., (1960), *J. Fluid Mech.*, 8, 241.
- Ipavich, F.M., (1975), *Ap. J.* 196, 107.
- Issa, M.R., and Wolfendale, A.W., (1981a), 17th ICRC, OG 1, 150 (Paris: 1981).
- Issa, M.R., and Wolfendale, A.W., (1981b), *Nature* 292, 430.
- Johnson, H.E., and Axford, W.I., (1971), *Ap. J.* 165, 381.
- Jokipii, J.R., (1968), *Ap. J.* 152, 799.
- Jokipii, J.R., (1976), *Ap. J.* 208, 900.
- Jokipii, J.R., (1971), *Rev. Phys. Geophys.* 9, 28.
- Jokipii, J.R., and Kopriva, (1979), *Ap. J.*, 234, 384.
- Jones, F.C., (1979), *Ap. J.* 229, 747.

Khazan, Y.M., and Ptuskin, V.S., (1977), 15th ICRC, 2, 4. (Hungary: Plovdiv 1977).

Kiraly, P., Szabelski, J., Wdowczyk, J., and Wolfendale, A.W., (1981), *Nature*, 293, 120.

Kiraly, P., (1982), in *Progress in Cosmology*, Proc. Oxford Int. Symp. held in Christ Church, Oxford 1981 (Wolfendale, A.W., ed.), (Reidel: Dordrecht 1982).

Klein, O., (1966), *Nature* 211, 1337

Kota, J., and Owens, A.J., (1980), *Ap. J.* 237, 814.

Kraushaar, W.L., et al., (1972), *Ap. J.* 177, 341.

Kolhorster, W., (1914), *Deutsch. Phys. Gesell. Verh.* 16, 719.

Kulsrud, R.M., and Pearce, W.P., (1969), *Ap. J.* 156, 445.

Landau, L.D., and Lifshitz, E.M., (1959), *Fluid Mechanics*, Vol. 6 of *Course of Theoretical Physics* (Pergamon: Oxford 1959).

Lang, K.R., (1978), *Astrophysical Formulae* (Springer-Verlag: Berlin 1978).

Larson, R.B., (1969a), *Mon. Not. R. astr. Soc.*, 145, 271.

Larson, R.B., (1969b), *Mon. Not. R. astr. Soc.*, 145, 297.

Larson, R.B., (1969c), *Mon. Not. R. astr. Soc.*, 145, 405.

Larson, R.B., (1972), *Mon. Not. R. astr. Soc.*, 156, 437.

Larson, R.B., (1973), *Ann. Rev. Astron. Astrophys.*, 11, 219.

Lequeux, J., (1974), in *The interstellar medium*, IAU Symp. (Pinkau K., ed) (Reidel: Dordrecht 1974).

Lequeux, J., (1977), in *Star Formation*, IAU Symp. 75 (T. de Jong and A. Maeder, eds.) (Reidel: Dordrecht 1977).

Lerche, I., and Schlickeiser, R., (1980), *Ap. J.* 239, 1089.

Lerche, I., and Schlickeiser, R., (1982), *Astron. Astrophys.* 116, 10.

Leventhal, M., McCallum, C.J., and Stang, P.D., (1978), *Ap. J.* 225, L11.

Li, T.P., and Wolfendale, A.W., (1981), *Astron. Astrophys.* 103, 19.

Linsley, J., (1980), in *Origin of Cosmic Rays*, IAU Symp. 94, op. cit.

- Linsley, J., and Watson, A.A., (1983), Proc. 18th Int. Cosmic Ray Conf. 12, 135.
- Longair, M.S., (1981), High Energy Astrophysics, (CUP: Cambridge).
- Mayer-Hasselwander, H.A., et al., (1982), Astron. Astrophys. 105, 164.
- McIvor, I., (1975), 14th Int. Cosmic Ray Conf., 3, 624.
- McKee, C.F., and Ostriker, J.P., (1977), Ap. J., 218, 148.
- Meegan, C., and Earl, J.A., (1976), Ap. J. 197, 219.
- Mestel, L., (1965), Quart. J. R., astr. Soc., 6, 161.
- Mestel, L., (1966), Quart. J. R. astr. Soc., 133, 265.
- Meyer, P., (1974), in Origin of Cosmic Rays, Proc. NATO Adv. Study Institute, Durham 1974 (Reidel: Dordrecht 1975).
- Meyer, P., (1978), Nature 272, 675.
- Meyer, P., (1980), in Origin of Cosmic Rays, IAU Symp. 94, op. cit.
- Michel, J.C., (1981), Ap. J. 247, 664.
- Millikan, R.A., and Bowen, I.S., (1926), Phys. Rev. 27, 353.
- Millikan, R.A., and Cameron, G.H., (1926), Phys. Rev. 28, 851.
- Millikan, R.A., and Otis, R.M., (1926), Phys. Rev. 27, 645.
- Mohapatra, R.N., and Marshak, R.E., (1980), in Recent developments in High Energy Physics, Proc. Orbis Scientiae, Coral Gables, FL, USA 14-17 Jan. 1980 (Plenum: New York 1980).
- Montmerle, T., (1981), in Gamma ray astronomy, op. cit.
- Morfill, G.E., (1982), Mon. Not. R. astr. Soc. 198, 583.
- Morfill, G.E., and Scholer, M., (1977), Ap. Sp. Sci., 46, 73.
- Morfill, G.E., Forman, M., and Bignami, G.F., (1984), Ap. J. 284, 856.

- Mouschovias, T.Ch., (1976a), Ap. J. 206, 753.
- Mouschovias, T.Ch., (1976b), Ap. J. 207, 141.
- Mouschovias, T.Ch., and Paleologou, E.V. (1979), Ap. J. 230, 204.
- Nagano, M. et al., (1984), J. Phys. G. Nucl. Phys. 10, 1295.
- Nakano, T., and Tadamaru, E., (1972), Ap. J. 173, 87.
- Ormes, J.F., and Protheroe, R.J., (1983), Ap. J. 272, 756.
- Omnes, R., (1969), Phys. Rev. Lett., 23, 38.
- Orth, C.D., and Buffington, A., (1976), Astrophys. J. 206, 312.
- Owens, A.J., and Jokipii, J.R., (1977a), Ap. J. 215, 677.
- Owens, A.J., and Jokipii, J.R., (1977b), Ap. J. 215, 685.
- Parker, E.N., (1969), Cosmical Magnetic Fields (Pergamon: New York 1969).
- Penston, M.V., (1969a), Mon. Not. R. astr. Soc. 144, 159.
- Penston, M.V., (1969b), Mon. Not. R. astr. Soc., 145, 457.
- Peters, B., and Westergaard, N.J., (1977), Ap. Sp. Sci. 18, 21.
- Piddington, J.H., (1977), Cosmic Electrodynamics (Wiley: New York 1969).
- Prishchep, V.L., and Ptuskin, V.S., (1981), Sov. Astron. 25, 446.
- Protheroe, R., (1981), 17th ICRC, 2, 198.
- Ptuskin, V.S., (1981), Ap. Sp. Sci. 76, 265.
- Raisbeck, G.M., and Yiou, F., (1977), 15th ICRC, 2, 203 (Hungary: Plovdiv ;1977).
- Rana, N.C., and Wolfendale, A.W., (1984), Inst. Physics Conf. Series No. 73: Section 4, presented at VII Eur. Symp. on Antiproton Interactions, Durham 1984, 235.

Reeves, H., (1974), in Origin of Cosmic Rays, NATO Adv. Study Institute, op. cit.

Reeves, H., (1980), in Origin of Cosmic Rays, IAU Symp. 94, op.cit.

Rozycka, M., and Tscharnuter, W.M., (1980), Astron. Astrophys. 81, 347.

Samorski, M., and Stamm, W., (1983), 18th ICRC, 1, 135.

Scalo, J.M., (1977), Ap. J. 213, 705.

Schlickeiser, R., (1983), 18th ICRC, Rapporteur paper, 14, (India: Bangalore 1983).

Schlickeiser, R., (1984), Proc. 18th Int. Cosmic Ray Conf., 12, 193.

Scott, E.H., and Black, D.C., (1980), in Giant Molecular Clouds in the Galaxy, op. cit.

Scoville, N.Z. et al. (1984), Ap. J. 276, 182.

Shu, F., (1977), Ap. J. 214, 488.

Shull, J.M., (1978), Ap. J. 226, 858.

Sivaram, C., and Krishnan, V., (1982), Nature, 299, 427.

Skilling, J., (1975a), Mon. Not. R. astr. Soc. 172, 557.

Skilling, J., (1975b), Mon. Not. R. astr. Soc. 173, 245.

Skilling, J., (1975c), Mon. Not. R. astr. Soc. 173, 255.

Skilling, J., and Strong, A.W., (1976), Astron. Astrophys. 53, 253.

Spitzer, L., (1978), Physical Processes in the Interstellar Medium (Wiley: New York 1978).

Stecker, F.W., (1981) (private communication).

Stecker, F.W., Protheroe, R.J., and Kazanas, D., (1983), Ap. Sp. Sci. 96, 171.

Stecker, F.W., and Wolfendale, A.W., (1984), Nature 309, 37.

Steigman, G., (1976), Ann. Rev. Astron. Astrophys. 14, 339.

- Stephens, S.A., and Mauger, B.G., (1984), Proc. 18th Int. Cosmic Ray Conf., 2, 69.
- Strong, A.W., (1981), 17th ICRC, OG 2, 248.
- Suga, K. et al., (1981), Phys. Rev. Lett. 27, 1604.
- Swanenburg, B.N. et al., (1981), Ap. J. 243, L69.
- Syrovatskii, S.I., (1957), Sov. Astron., 3, 22.
- Szabelski, J., Wdowczyk, J., and Wolfendale, A.W., (1981), Nature 285, 386.
- Tamman, G., (1977), in Supernovae and Supernova remnants, IAU Symp. Special Session (Reidel: Dordrecht).
- Tan, L.C., and Ng, L.K., (1981), J. Phys. G7, 123.
- Tan, L.C., and Ng, L.K., (1983), Ap. J., 269, 751.
- Tipler, F.J., (1980), Phys. Rev. Lett. 45, 949.
- Tokar, S., and Povinec, P., (1983), 18th ICRC, 2, 381.
- Tscharnutter, W.M., (1975), Astron. Astrophys. 39, 207.
- Urch, J.H., and Gleeson, L.J., (1973), Ap. Sp. Sci. 20, 177.
- Valtaoja, E., (1984), Astron. Astrophys. 135, 141.
- Volk, H.J., (1980), preprint Max Planck Institut fur Kernphysik (Heidelberg, FRG).
- Volk, H.J., and Bogdan, T.J., (1982), Astron. Astrophys. 122, 129.
- Volk, H.J., and Forman, M., (1981), MPI-H 1981 V22 (Max Planck Institut fur Kernphysik Heidelberg, FRG).
- Volk, H.J., and McKenzie, (1982), Astron. Astrophys. 116, 191.
- Watson, A., (1974), in Origin of Cosmic Rays, NATO Adv. Study Institute, op cit.
- Wdowczyk, J., and Wolfendale, A.W., (1976), J. Phys. A., 9, 1399.
- Wdowczyk, J., and Wolfendale, A.W., (1984a), J. Phys. G., 10, 1453.

Wdowczyk, J., and Wolfendale, A.W., (1984b), J. Phys. G., 10, 1599.

Webb, G.M. et al. (1981), Ap. J. 80, 323

Webb, G.M., Axford, W.I., and Forman, M.A., (1983), 18th Int. Cosmic Ray Conf., 2, 263

Webb, G.M., Drury, L.O'C., and Biermann, P. (1984), Astron. Astrophys. 137, 185.

Webber, W.R., Damle, S.V., and Kish, J., (1972), Ap. Sp. Sci. 15, 245.

Webber, W.R., and Lezniak, J.A., (1974), Ap. Sp. Sci. 30, 361.

Wentzel, D.G., (1974), Ann. Rev. Astron. Astrophys., 12, 71.

Wolfendale, A.W., (1974), in Origin of Cosmic Rays, NATO Adv. Study Institute, op. cit.

Wolfendale, A.W., (1981), in Origin of Cosmic Rays, op cit.

Wolfendale, A.W., (1982), Q. Jl. R. astr. Soc., 23, 325.

Wolfendale, A.W., (1983), Q. Jl. R. astr. Soc., 24, 226.

Wolfendale, A.W., (1984), in press.

Wolfendale, A.W., (1985), in press.

Zweibel, E.G., and Shull, J.M., (1982), Ap. J. 259, 859.

PUBLICATIONS

1. Freedman, I., Giler, M., Kearsey, S., Osborne, J.L., (1980), Astron. Astrophys., 82, 110; Proc. 16th Int. Cosmic Ray Conf., 2, 181 (Japan : Kyoto 1979).
2. Dogiel, V., Freedman, I., Kiraly, P., Wolfendale, A.W. (1983), Proc. 18th Int. Cosmic Ray Conf., OG2, 292 (India : Bangalore 1983).

SEMINARS

1. University of Palermo (Sicily), Instituta dei Cosmica Fisica (1982) "Upper limit to the high-energy gamma-ray flux from pulsars".
2. Max Planck Institut fur Aeronomie (FRG), "Cosmic ray transients in collapsing clouds".

Please note the corrections to the formulae on
pages 116, 117 and 119 of this paper.

Derivation of the Age Distributions of Cosmic Rays in a Galaxy with a Convective Halo

I. Freedman¹, M. Giler², S. Kearsy¹, and J. L. Osborne¹

¹ Department of Physics, University of Durham, South Road, Durham DH1 3LE, England

² Institute of Physics, University of Lodz, ul. Uniwersytecka 5, 90-950 Lodz 1, Box 447, Poland

Received March 20, 1979

Summary. A model of cosmic ray propagation in the Galaxy is considered in which the sources are uniformly distributed in the disk. The cosmic rays diffuse into a halo where diffusion is combined with outward convection. The propagation equation has been solved analytically to give the distributions of total age and disk-age, and the surviving fraction of radioactive ^{10}Be , f_s , in terms of 4 propagation parameters. A knowledge of the grammage, X , traversed by cosmic rays and of f_s sets lower limits, but no upper limits, to the mean age of cosmic rays at the earth and the extent of the halo. Provided that $f_s \leq 1/3$ an upper limit of $\sim 16 \text{ km s}^{-1}$ to the outward convection velocity in the halo is set by the value of X .

Key words: cosmic ray propagation – galactic halo – ^{10}Be survival – convection velocity

1. Introduction

Observations of the composition of cosmic rays incident on the top of the earth's atmosphere allow deductions to be made about their propagation and confinement in the Galaxy. The proportion of the spallation products, Li, Be, and B, indicate the amount of interstellar matter traversed by the parent C, N, O and heavier nuclei (the "grammage"). The amount of the radioactive isotope ^{10}Be is related to the mean age of these parent particles. The form of this relationship depends on the type of galactic propagation model assumed. Measurements of the abundance of ^{10}Be have been interpreted predominantly in terms of the simplest steady state homogeneous or "leaky box" model in which the cosmic ray intensity, source power, interstellar gas density and probability of escape are uniform throughout the confinement volume. Prischep and Ptuskin (1975) considered the simplest heterogeneous model in which the cosmic ray sources and the main part of the interstellar gas are distributed uniformly in a disk region of infinite lateral extent and the particles diffuse into an outer region, the halo, from the boundaries of which they freely escape. This model would approximate to reality if the lateral gradient of cosmic ray source intensity in the disk were small and the extent of the halo were appreciably less than the radius of the Galaxy. It was shown that the mean age of cosmic rays deduced from the surviving fraction of a secondary radioactive isotope for this model is the same as that for the homogeneous model only for isotopes with mean lifetimes much greater than the escape time for the Galaxy. Although there remains some controversy about whether the distribution of galactic synchrotron radiation over the sky indicates the existence of a quasi-spherical halo confinement region for cosmic ray electrons there is no doubt that the confinement region for electrons (and, by implication, for nuclei) is at least several times broader than the gaseous disk of the Galaxy (see e.g., Brindle et al., 1978). This, together with the mean time spent in the galactic disk, deduced from the grammage, indicates that the above condition is not satisfied for ^{10}Be . A heterogeneous model must therefore be used in interpreting the ^{10}Be data.

The possibility of propagation by outward convection in the halo in addition to diffusion was discussed by Jokipii (1976). The outward streaming cosmic rays can generate hydromagnetic waves coupling them to the gas. The gas may thus be driven outward in a galactic wind. Owens and Jokipii (1977) considered the one-dimensional transport equation for the cosmic ray density with inclusion of a convective term in the halo to represent this wind. Noting that the analytical solution was not easily obtained, they used a Monte Carlo technique to find how the amount of matter traversed and the age distribution of the cosmic rays depend upon the parameters of propagation.

The primary aim of this paper is to present the analytical expressions for the observable quantities relating to such a model. For the corresponding parameters the Monte Carlo results agree well with our analytical solutions. We regard the conclusions that can be drawn regarding the parameters of propagation as being tentative at present however. This is largely due to the uncertainty in the observed abundance of ^{10}Be . The constraints on the propagation parameters that we do obtain differ somewhat from those of Owens and Jokipii, due to our treating the ^{10}Be abundance rather than the total mean age of cosmic rays (derived from the ^{10}Be abundance using the homogeneous model) as the given quantity. Approximate analytical expressions for the grammage and the ^{10}Be abundance have been given recently by Jones (1979). We show how they approach our results in the limit that the halo thickness is very much greater than the disk thickness.

Send offprint requests to: J. L. Osborne

Fig. 1. The simple model of the Galaxy

The plan of the paper is as follows. In Sect. 2 the simple model of the Galaxy is given and the propagation parameters are defined. Section 3 gives a brief summary of the cosmic ray observations. The main parts of the paper are Sect. 4 containing the expressions for the mean disk age and total age and their distributions, and Sect. 5 with the expressions for the surviving fraction of radiative isotope. The derivations of these expressions are given in appendixes. Section 6 contains some conclusions and considers the possibility that a more complex model may be required to account for all of the cosmic ray observations.

2. A Simple Model of the Galaxy

We adopt a simple model similar to that of Owens and Jokipii (1977) in which the galactic disk is uniform and all quantities vary only with distance z from the mid-plane of the Galaxy (Fig. 1). The interstellar gas density ρ , measured in units of atomic mass units (a.m.u.) per unit volume, is taken to be constant in the disk, which extends to $|z| = a$, and to be zero in the halo. As will be shown it is primarily the column density of the disk, ρa , that appears in the expressions so that the step-function approximation to the density distribution is a reasonable one. Similarly the source function of cosmic rays, S particles per unit volume per unit time per unit energy interval, is assumed uniform throughout the disk and is zero elsewhere. For comparison with the ^{10}Be observations it is necessary to consider the production and propagation of particles with velocity $\beta < 1$ and in this case we take $S = \beta S_0$ where $S_0 \propto T^{-1}$, T being the particle kinetic energy.

The propagation model envisages particles diffusing throughout the disk of the Galaxy, suffering convection and diffusion in the halo and escaping freely from the halo boundary at $|z| = D$. Taking the diffusion mean free path as independent of energy, the diffusion coefficient in the disk is $\kappa = \beta\kappa_0$. One might expect the diffusion coefficient to increase with distance from the galactic plane. In order to approximate this behaviour we take $\kappa = F\beta\kappa_0$ in the halo where F is a constant ≥ 1 .

Following Owens and Jokipii we take the outward convection velocity to be $V = V_0$ in the halo and $V = 0$ in the disk. From the results derived below it is apparent that for a halo size, D , at least several times greater than the disk size, a , it is the net change in V between $z = 0$ and $|z| \geq a$ that is important rather than the form of its variation.

The cosmic ray observations give constraints on the parameters V_0 , κ_0 , D , and F . We regard the parameters a and ρ as being, at least in principle, independently determined. The density of the interstellar medium is far from uniform in the disk of the Galaxy; the hydrogen occurs in at least three forms; dense clouds of molecular hydrogen, less massive clouds of atomic hydrogen and a warm, partially ionised intercloud (or circumcloud) medium. If the cosmic rays can freely penetrate each of these the effective gas density, ρ , is simply the overall mean density. A number of separate observations allow estimates to be made of ρ and a . From the study by Radhakrishnan et al. (1972) of H I clouds in 21 cm emission and absorption one can obtain values of $1.5 \cdot 10^{20}$ and $1.3 \cdot 10^{20}$ atom cm^{-2} for the column densities of hydrogen in the form of H I clouds and intercloud medium respectively. From Lyman α observations Bohlin et al. (1978) obtain a value of $0.86 \text{ atom cm}^{-3}$ for the mean density of atomic hydrogen in the galactic plane. Taken with the column densities this implies an equivalent halfwidth of atomic hydrogen $a_{\text{H I}} = 105 \text{ pc}$. The same authors derive a mean density of molecular hydrogen in the solar neighbourhood of $0.29 \text{ atom cm}^{-3}$ while Burton and Gordon (1976) give $a_{\text{H}_2} = 63 \text{ pc}$ within 10 kpc of the galactic centre. Combining these quantities, the weighted equivalent half width of the interstellar hydrogen is $a = 95 \text{ pc}$. We follow Garcia-Munoz et al. (1977a) in assuming a solar system composition for the interstellar gas. The hydrogen density of $1.15 \text{ atom cm}^{-3}$ then implies a total gas density $\rho = 1.53 \text{ a.m.u. cm}^{-3}$.

The value that we have for the column density, ρa , is $4.5 \cdot 10^{20} \text{ a.m.u. cm}^{-2}$. The column density adopted by Jones (1979) is $3.2 \cdot 10^{20}$ hydrogen atoms cm^{-2} , other elements being ignored, while Owens and Jokipii (1977) take $\rho a = 9.3 \cdot 10^{20} \text{ a.m.u. cm}^{-2}$. These differences are not of great importance in the context of the present large uncertainty in the ^{10}Be abundance but should nevertheless be borne in mind.

3. A Summary of the Cosmic Ray Observations

Jones (1979) has given an account of the observations on cosmic ray composition relevant to the present propagation model. We summarise these observations here.

3.1. The Surviving Fraction of ^{10}Be

A quantity that can be predicted from the propagation model is the surviving fraction, f_s , of ^{10}Be , i.e. the ratio of the actual abundance of ^{10}Be to that which would be observed if ^{10}Be were a stable isotope. This cannot be measured directly; the quantity that is measured is

the ratio $^{10}\text{Be}/^9\text{Be}$. Raisbeck and Yiou (1977) predict the ratio of abundance of ^{10}Be without decay to that of ^9Be to be 0.6. This value is determined primarily by the relative cross-sections for production and interaction of the two isotopes. It depends only weakly on the mean grammage traversed and even less on the precise form of the distribution of grammage about that mean. One can therefore obtain f_s by dividing the observed ratio $^{10}\text{Be}/^9\text{Be}$ by 0.6.

The experiments performed up to now can be broadly divided into two groups both with regard to the vehicle used for the detection and the results obtained. The University of Chicago detectors on the IMP-7 and IMP-8 satellites give $f_s = 0.14 \pm 0.07$ (Garcia-Munoz et al., 1977a) for nuclei with mean kinetic energy 80 MeV/nucleon. At these low energies the effects of solar modulation are important. The authors conclude that an energy loss of 220 MeV/nucleon occurs in traversal of the solar cavity. The propagation model predicts the abundances in interstellar space so that the appropriate kinetic energy is 300 MeV/nucleon and the velocity is $\beta = 0.65$.

The other determinations of f_s were made using detectors flown in balloons (Webber et al., 1977; Hagen et al., 1977 and Buffington et al., 1978). These all give significantly higher values of f_s than the satellite measurements. The mean energy of the detected particles is also higher; the highest, that of Buffington et al., is 500 MeV/nucleon at the earth. The higher energy cannot, however, account for the difference in f_s . One can show that the energy dependence of f_s predicted for the homogeneous model is practically the same as for our disk-halo model (see Sect. 5). Using this energy dependence we have converted the surviving fractions from the balloon experiments to those that would be obtained for a 300 MeV/nucleon interstellar energy. The weighted mean of all the converted balloon values is $f_s = 0.27 \pm 0.07$. In view of the large, mainly statistical, errors the balloon and satellite measurements are not in strong disagreement. It is shown, however, in Sect. 5 that the range of f_s from the one standard deviation lower limit of the satellite value of 0.07 to the upper limit of 0.34 of the balloon value is such that at present f_s , in itself, provides a not very significant constraint upon the propagation parameters.

3.2. The Grammage Traversed

From the ratio of abundances of spallation products to primary nuclei in the cosmic ray flux the mean amount of matter that would be traversed by non-interacting cosmic rays in units of g cm^{-2} , the grammage, X , can be inferred. Values have been obtained as a function of energy from the 300 MeV/nucleon interstellar kinetic energy of Garcia-Munoz et al. (1977a) up to 100 GeV/nucleon. At the former energy a value $X = 6 \pm 0.5 \text{ g cm}^{-2}$ was obtained. Between 500 MeV/nucleon and 2 GeV/nucleon X appears to be approximately constant with a value between 7 and 9 g cm^{-2} . Beyond 5 GeV/nucleon there is definite evidence for a decrease of X ; if a power law of the form $X \propto T^{-\alpha}$ is fitted in this region then $\alpha = 0.4_{-0.1}^{+0.2}$ but the data may be equally well fitted by X decreasing more rapidly to about 2 g cm^{-2} at 20 GeV/nucleon and then remaining constant (Fontes et al., 1977).

The homogeneous propagation model gives an exponential probability distribution of grammage. In the following section it is shown that the distribution for the disk-halo model approximates closely to an exponential form provided that the halo is several times larger than the disk. In principle a detailed study of the abundances of secondary elements having different interaction mean free paths would enable the grammage distribution to be determined. In practice the uncertainties in the abundances and spallation cross-sections are such that only a relatively crude check on the distribution can be made. Garcia-Munoz et al. (1977b), from a study of the abundances of the elements from Si to Ni, conclude that, although a pure exponential distribution of grammages is not excluded, a distribution truncated by a linear rise from 0 to 1 g cm^{-2} clearly gives closer agreement with the experimental values. Possible implications of such a deficit in short path lengths are discussed in Section 6.

4. The Age Distributions of Cosmic Rays

4.1. The Disk-age Distribution

As, in our model, the matter in which the grammage is built up is confined to the galactic disk the quantity that is of interest in determining the grammage is the time spent in the galactic disk. We refer to this as the disk-age, t_D . When a particle crosses the disk-halo boundary the chance of its returning to the disk rather than escaping across the outer boundary of the halo is independent of its previous history and depends only upon the size of the halo and the convection velocity and diffusion coefficient in it. It should thus be possible to regard the probability of return as a reflection coefficient.

The age distribution in a disk with partially reflecting boundaries and a given spatial distribution of continuously emitting sources is easily obtained. It corresponds to the solution of the time dependent diffusion equation after an instantaneous input of particles at time $t_D = 0$ following this source distribution.

One requires the solution of

$$\frac{\partial N}{\partial t} = \beta \kappa_0 \frac{\partial^2 N}{\partial z^2} \quad (4.1)$$

The boundary conditions are, at $z=0$ for a symmetric source distribution, $dN/dz=0$ and at $z=\pm a$

$$\frac{\kappa_0}{v} \frac{1}{N} \left| \frac{dN}{dz} \right| = \frac{1-r}{1+r}. \quad (4.2)$$

The reflection coefficient is r and for one dimensional diffusion $\kappa_0 = v\lambda_D/2$, λ_D and v being the effective mean z -components of the scattering mean free path and the velocity of an ultra-relativistic particle. Then

$$N(z, t) = \sum_{n=1}^{\infty} B_n(\alpha_n) \cos\left(\alpha_n \frac{z}{a}\right) \exp\left(\frac{-\alpha_n^2 \beta \kappa_0 t}{a^2}\right) \quad (4.3)$$

are the roots of the eigenvalue equation

$$= \varepsilon/\alpha \quad (4.4)$$

$$\left(\frac{1-r}{1+r} \right) \quad (4.5)$$

case that the sources are uniformly distributed across the disk one takes as the initial condition that $N=1$ for all $|z| < a$ giving

$$\frac{4 \sin(\alpha_n)}{2\alpha_n + \sin(2\alpha_n)} \quad (4.6)$$

at $z=0$, writing t_D for the disk-age

$$= \sum_{n=1}^{\infty} \frac{4 \sin(\alpha_n)}{2\alpha_n + \sin(2\alpha_n)} \exp\left(-\frac{\alpha_n^2 \beta \kappa_0 t_D}{a^2}\right). \quad (4.7)$$

6 we consider the possibility of a gap in the source distribution for $|z| < b$; then

$$\frac{\sin(\alpha_n) - \sin(b\alpha_n/a)}{2\alpha_n + \sin(2\alpha_n)}. \quad (4.8)$$

pression (4.7) gives the age distribution normalised to unity at $t_D=0$. The age distribution at $z=0$ expressed as probability per e is given by

$$\frac{2\varepsilon\beta\kappa_0}{a^2(2+\varepsilon)} N(0, t_D). \quad (4.9)$$

can disk-age determined from (4.7) is

$$\frac{a^2 \sum_{n=1}^{\infty} \alpha_n^{-4} \sin(\alpha_n)/(2\alpha_n + \sin(2\alpha_n))}{\beta\kappa_0 \sum_{n=1}^{\infty} \alpha_n^{-2} \sin(\alpha_n)/(2\alpha_n + \sin(2\alpha_n))}. \quad (4.10)$$

be shown that this reduces to

$$\frac{a^2}{\beta\kappa_0} \left(\frac{1}{\varepsilon} + \frac{1}{3} + \frac{\varepsilon}{24+12\varepsilon} \right). \quad (4.11)$$

ective reflection coefficient, and hence ε , remains to be determined. It is shown in Appendix A that

$$\left(\left[1 - \exp\left(-\frac{(D-a)V_0}{\beta F \kappa_0}\right) \right]^{-1} + \frac{\Gamma-1}{3} \right) \quad (4.12)$$

otation as in Sect. 2. If one lets $V_0 \rightarrow 0$, i.e. no convection then

$$\frac{F}{(D-a)}. \quad (4.13)$$

other hand, if $V_0 \rightarrow \infty$ then $\varepsilon \rightarrow \infty$ and

$$\frac{5}{12} \frac{a^2}{\beta\kappa_0}$$

ponding to a disk with free escape at the boundary.

Appendix B the disk-age distribution is obtained using an alternative approach. An artificial decay term is added to the equation and the age distribution follows from an inverse Laplace transformation of its solution.

the observed quantity, the grammage, is given by $X(\beta) = \beta c \rho m_H \langle t_D \rangle$ thus

$$c \rho m_H \frac{a^2}{\kappa_0} \left(\frac{1}{\varepsilon} + \frac{1}{3} + \frac{\varepsilon}{24+12\varepsilon} \right). \quad (4.14)$$

quantities a , ρ and Γ are independently known, Eqs. (4.12) and (4.14) give the relation between κ_0 , V_0 , F , and D required to fit the ed grammage. With $X(\beta=0.65)=6 \text{ g cm}^{-2}$ the relation between κ_0 , V_0 , and D is as shown in Fig. 2 for the case $F=1$ and $\Gamma=2.5$. lower limit to κ_0 , from the grammage alone, corresponds to free escape at the disk boundary. Values are given in the figure up to 0 kpc but the one-dimensional model becomes progressively less applicable to the real Galaxy at dimensions beyond 15 kpc. If κ_0

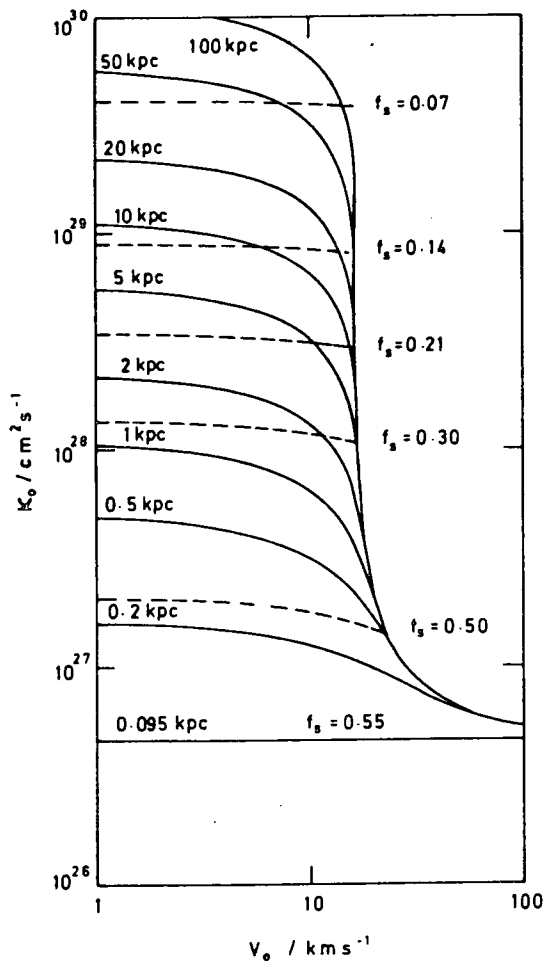


Fig. 2. The values of diffusion coefficient, κ_0 and convection velocity, V_0 allowed, for the case $F = 1$, by the observed grammage, X and surviving fraction, f_s , of ^{10}Be at $\beta = 0.65$. The solid lines show the variation of κ_0 with V_0 for various assumed halo sizes, D that leads to $X = 6 \text{ g cm}^{-2}$. The dashed lines show the restriction on the ranges of κ_0 , V_0 , and D imposed by a given f_s .

is constrained to be $\geq 3 \times 10^{27} \text{ cm}^2 \text{ s}^{-1}$ it is apparent that $V_0 \lesssim 17 \text{ km s}^{-1}$. In Sect. 5 it is shown that the observed surviving fraction of ^{10}Be gives an indication that this is indeed the case.

For the non-convective case ε , and hence X , is independent of the particle velocity β ; the mean path length in the disk does not depend on the velocity at which it is traversed. This is not true for the more general case given by Eq. (4.12) where ε decreases and X increases with β . For example if $V_0 = 10 \text{ km s}^{-1}$, $D \gg a$, and κ_0 and F are chosen to give $X = 6 \text{ g cm}^{-2}$ at $\beta = 0.65$ then, at $\beta = 1$, $X = 7.1 \text{ g cm}^{-2}$. If $V_0 = 15 \text{ km s}^{-1}$ the increase is from 6 to 8.2 g cm^{-2} . To the extent that the observed grammages exhibit this behaviour there is support for some appreciable convective transport. Jones (1979) has taken this further. In order to reproduce the observed decrease of grammage for energies above 5 GeV/nucleon he proposes that $\kappa_0 \propto R^{1/2}$ where R is the particle rigidity. If this rigidity dependence continues to the lowest rigidities the fact that the grammage passes through a broad maximum at about 1 GeV/nucleon has to be accounted for by the effect of convection. He obtains the best fit to the energy dependence of the grammage with $\rho a m_H c / V_0 = 20 \text{ g cm}^{-2}$. With our best estimate of ρa this implies $V_0 = 11 \text{ km s}^{-1}$. The expression for the grammage given by Jones corresponds to that given by Eqs. 4.12 and 4.14 for the case $F = 1$ in the limit $D \gg a$.

When $\varepsilon \lesssim 0.5$ the first term in the series in Eq. 4.7 predominates and the disk-age distribution is practically exponential. For the non-convective case the age distribution has a particularly simple form when $D \gg a$ viz.

$$P(t_D) = \frac{\beta \kappa_0 F}{aD} \exp\left(\frac{-\beta \kappa_0 F t_D}{aD}\right). \quad (4.15)$$

4.2. The Mean Total Age of Cosmic Rays

We next consider the total age of cosmic rays as observed at $z=0$. It should first be noted, however, that there are no observable quantities directly related to this age that allow its unambiguous determination. In the one-dimensional approximation, observed values of grammage and surviving fraction of radioactive nuclei give relationships between the propagation parameters κ_0 , V_0 , D , and F but within these relationships V_0 and F may still be varied widely enough to give mean total ages differing by a factor of 10. There is nevertheless, some intrinsic interest in the total age distribution and when considering the validity of the steady state model one should know over what time-scale one is assuming that the cosmic ray sources emit at constant power.

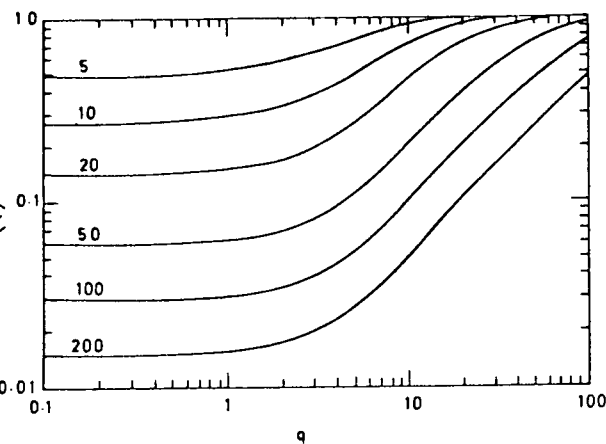


Fig. 3. The ratio of mean disk-age to mean total age for non-interacting, stable cosmic ray nuclei as a function of $q = DV_0/\kappa_0$ for $F=1$ and $\beta=1$. The number on each curve is the value of y , the ratio of halo to disk size

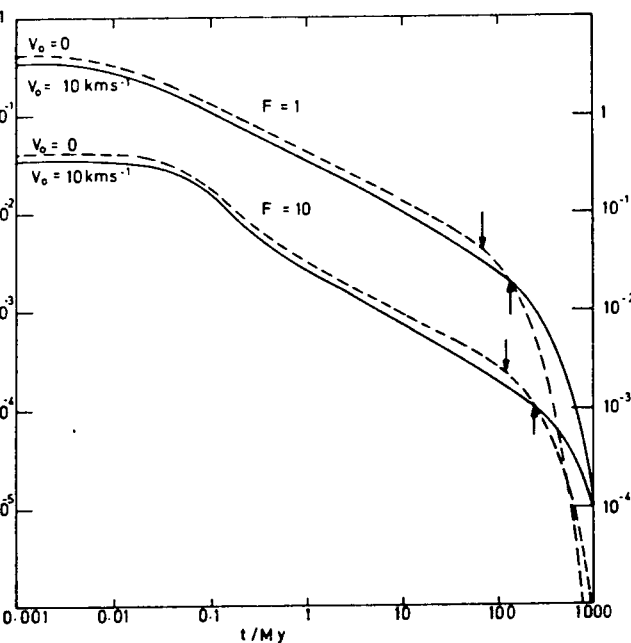


Fig. 4. Examples of total age distributions for sets of propagation parameters, all of which would give the “observed” values, $X=6 \text{ g cm}^{-2}$ and $f_s=0.14$ at $\beta=0.65$. The left hand scale refers to the curves for $F=1$; the right hand scale is for $F=10$. The arrows mark the mean total ages

The expression for the mean total age derived in Appendix B is

$$= \frac{a^2}{\beta\kappa_0} \left\{ \left[\frac{1}{\varepsilon} + \frac{1}{3} + \frac{\varepsilon}{24+12\varepsilon} \right] + \frac{F \left[2g^2 \left(1 - \frac{\varepsilon(y-1)}{F} \right) + g \left(\frac{1+2\Gamma}{3} \right) \left(\frac{2\varepsilon(y-1)}{F} - 1 \right) - \frac{\varepsilon(y-1)}{2F} \left(\left(\frac{1+2\Gamma}{3} \right)^2 - 1 \right) \right]}{\varepsilon^3 \left[\frac{1}{\varepsilon} + \frac{1}{2} \right]} \right\} \quad (4.16)$$

where the following dimensionless parameters are used

$$\frac{D}{a}, \quad g = \frac{\varepsilon\beta y}{q} \quad \text{and} \quad q = \frac{DV_0}{\kappa_0}. \quad (4.17)$$

last, introduced by Owens and Jokipii, expresses the importance of convection relative to diffusion in the propagation. For no convection $q=0$ and (4.16) reduces to

$$= \frac{a^2}{\beta\kappa_0} \left\{ \left[\frac{1}{\varepsilon} + \frac{1}{3} + \frac{\varepsilon}{24+12\varepsilon} \right] + \frac{F}{3\varepsilon^3 \left[\frac{1}{\varepsilon} + \frac{1}{2} \right]} \right\} \quad (4.18)$$

$\varepsilon = F/(y-1)$. The ratio $\langle t_D \rangle / \langle t \rangle$ is a function of β , F , y , and q . In Fig. 3 the variation of the ratio with y and q is shown for $F=1$ and $\beta=1$.

The Total Age Distribution

The derivation of the total age distribution at $z=0$ is also given in Appendix B. The distribution, normalised to unity at $t=0$ is

$$P(t=0, t) = \sum_{n=1}^{\infty} B_n \exp\left(-u_n^2 \frac{\beta \kappa_0}{a^2} t\right). \quad (4.19)$$

where

$$B_n = \frac{2 \sin(u_n)}{u_n + \sin(u_n) \cos(u_n) + u_n \cos^2(u_n) (y-1) [\operatorname{cosec}^2(\omega_n) - \cot(\omega_n)/\omega_n]} \quad (4.20)$$

$$u_n = \frac{(y-1)}{F} \left(F u_n^2 - \frac{q^2}{4 y^2 \beta^2} \right)^{1/2}. \quad (4.21)$$

where u_n are the roots of

$$u_n = \frac{q}{u_n y \beta} \left(\frac{1+2\Gamma}{6} \right) + \frac{F \omega_n}{(y-1) u_n \tan(\omega_n)}. \quad (4.22)$$

Examples of this age distribution for various values of the propagation parameters are given in Fig. 4. Each set of parameters is chosen to give a grammage $X = 6 \text{ g cm}^{-2}$ and $f_s = 0.14$ for ^{10}Be at $\beta = 0.65$. For ages between the characteristic time for diffusion out of the disk, a^2/κ_0 , and the mean age, $\langle t \rangle$, the probability of a cosmic ray particle having age t decreases as $t^{-1/2}$; for $t > \langle t \rangle$ the first term in the series dominates and the probability decreases exponentially.

The Surviving Fraction of Radioactive Nuclei

Before considering the surviving fraction of radioactive nuclei as predicted for our propagation model let us recall the results of the homogeneous model. In this there is a uniform input of the radioactive nuclei at a rate βS_r , and a constant probability per unit time of nuclei being removed by escape, radioactive decay or interaction. The equilibrium density can be expressed as

$$n_r = \frac{S_r}{c \varrho m_H} \left(\frac{1}{X} + \frac{1}{\Lambda_i} + \frac{1}{\Lambda_r} \right)^{-1}. \quad (5.1)$$

where ϱm_H is the, uniform, gas density in the propagation region; X is, as before, the mean column density in g cm^{-2} of the gas traversed by stable, non-interacting particles before escape; Λ_i is the interaction mean free path of the radioactive nuclei; Λ_r is the column density of gas traversed at velocity βc by a radioactive nucleus during its time dilated mean life $\gamma \tau$.

Thus

$$n_r = \varrho m_H \beta \gamma \tau. \quad (5.2)$$

The surviving fraction, f_s , is obtained by dividing n_r by the density obtained for $\Lambda_r \rightarrow \infty$ i.e.

$$f_s = \frac{\Lambda_r (X + \Lambda_i)}{X \Lambda_r + \Lambda_i \Lambda_r + X \Lambda_i}. \quad (5.3)$$

In the homogeneous model the only adjustable parameter is ϱ . Thus for example for ^{10}Be , $\Lambda_i = 9.3 \text{ g cm}^{-2}$ (Hagen et al., 1977), and the values $f_s = 0.14$ and $X = 6 \text{ g cm}^{-2}$ measured by Garcia-Munoz et al. require $\varrho = 0.2 \text{ amu cm}^{-3}$. The time for a particle to traverse 6 g cm^{-2} at this density is 19 My.

The surviving fraction for the present heterogeneous model can be obtained from the solution of the propagation equation including "decay" given in Appendix B, when the following substitutions are made. In the disk

$$\beta c \varrho m_H \left(\frac{1}{\Lambda_i} + \frac{1}{\Lambda_r} \right) \quad (5.4)$$

and in the halo

$$\equiv \beta c \varrho m_H / \Lambda_r. \quad (5.5)$$

Making these substitutions in (B.6) the equilibrium density of radioactive nuclei at $z=0$ is

$$n_r = \frac{S_r \Lambda_i \Lambda_r}{c \varrho m_H (\Lambda_i + \Lambda_r)} \left\{ 1 - \left[\cosh(\Lambda_i) + y \frac{\Lambda_i}{\Lambda_r} \sinh(\Lambda_i) \right]^{-1} \right\} \quad (5.6)$$

where

$$j(\epsilon) = \left[\frac{X}{j(\epsilon)} \left(\frac{1}{\Lambda_i} + \frac{1}{\Lambda_r} \right) \right]^{1/2}, \quad j(\epsilon) = \left(\frac{1}{\epsilon} + \frac{1}{3} + \frac{\epsilon}{24 + 12\epsilon} \right)$$

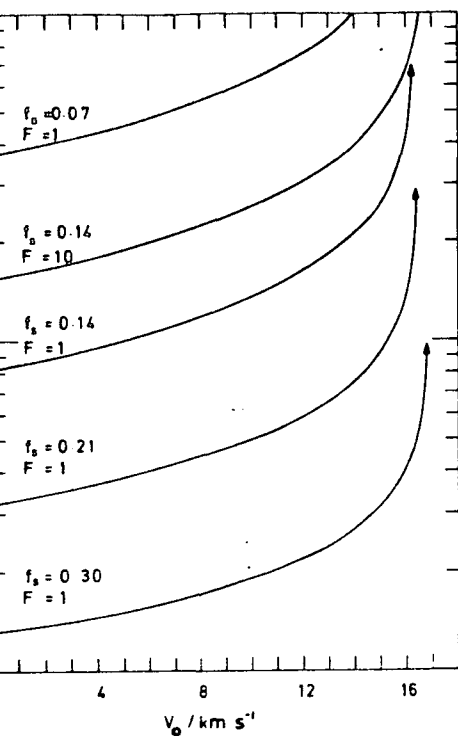


Fig. 5. The ratio of halo to disk size, y , which gives the observed grammage and a fixed surviving fraction, f_s , of ^{10}Be , as a function of the convection velocity in the halo. The value of y depends also upon the ratio of the halo and disk diffusion coefficients, F

$$\frac{+2\Gamma}{6} \frac{q}{\beta} + yF \left\{ \frac{X}{jA_r} + \left(\frac{q}{2\beta F y} \right)^2 \right\}^{1/2} \coth \left\{ (y-1) \left[\frac{X}{jA_r} + \left(\frac{q}{2\beta F y} \right)^2 \right]^{1/2} \right\}.$$

g (5.6) by the particle density obtained for $A_r \rightarrow \infty$ gives

$$A_r \frac{1 - \left[\cosh(A_1) + y \frac{A_1}{A_2} \sinh(A_1) \right]^{-1}}{+ A_i \frac{1 - \left[\cosh(A_3) + \frac{A_3}{\epsilon} \sinh(A_3) \right]^{-1}}}{(5.7)}$$

$$\frac{X}{jA_i} \left[\frac{1}{2} \right]$$

umed in deriving the expression that the source function of ^{10}Be is uniform throughout the disk. The approximation is justified endix C.

surviving fraction is a function of three adjustable propagation parameters. If F is chosen, the value of y (the ratio of halo to disk required to give the observed f_s can be found as a function of q from (5.7). The parameter q expresses the relative importance of ion to diffusion in the propagation. It is perhaps of more direct interest to determine the value of y required as a function of V_0 . his Eqs. (5.7) and (4.14) have to be taken together; for a given V_0 the pair of values of y and κ_0 required to fit simultaneously the d values of f_s and X are obtained by an iterative procedure. Figure 5 shows examples of how y varies with V_0 . The required halo eases with V_0 , at first relatively slowly but then more rapidly as V_0 approaches 16 km s^{-1} . Above some limiting velocity, V_{max} , at greater than 16 km s^{-1} it is impossible simultaneously to obtain $X = 6 \text{ g cm}^{-2}$ and the given value of f_s no matter how large o. From Eqs. (5.7) and (4.14) V_{max} can be found; for $f_s \rightarrow 0$ it is simply

$$\frac{\beta c \rho a m_H}{X(\beta)} \left(\frac{3}{\Gamma + 2} \right) = 16.2 \text{ km s}^{-1}.$$

ue of V_{max} at first increases only slowly with f_s and F : e.g. for $f_s = 0.4$ and $F = 10$ $V_{\text{max}} = 20.4 \text{ km s}^{-1}$. Eventually, however, as f_s es its limiting value of 0.55, corresponding to free escape at the disk boundary, $V_{\text{max}} \rightarrow \infty$. As the expression for V_{max} involves q s a product only, our approximating the gas density distribution in the disk to a uniform slab will have had only a minor effect. values of κ_0 , for the case $F = 1$, required to give observed values of f_s and X are shown as a function of V_0 by the dashed lines in For a given f_s , κ_0 does not depend strongly upon V_0 even as the latter approaches its maximum allowed value. expression for f_s given by Jones (1979) gives a value close to that given by (5.7) when $y \gtrsim 100$.

The energy dependence of f_s enters primarily as the factor $\beta\gamma$ in A_s . The variation of f_s with energy predicted by (5.3) is very close to that predicted by (5.7). The present heterogeneous propagation model does not therefore help to explain the apparently much stronger observed variation with energy.

6. Discussion

The conclusions that can be drawn regarding cosmic ray propagation, in the context of the model considered here, must be regarded as tentative at present due mainly to the uncertainty in the surviving fraction of ^{10}Be . The aim of this paper has been to derive expressions relating the observable quantities to the propagation parameters that appear in the simplest heterogeneous model of the Galaxy in anticipation of an improvement in the accuracy of the data. Some general remarks can, nevertheless, be made and, if one regards the bulk of the evidence on the ^{10}Be abundance as indicating a surviving fraction, $f_s \lesssim 0.33$ at an interstellar energy of 300 MeV/nucleon one quantitative conclusion can be drawn.

Even if f_s and the grammage, X , were perfectly well known they would give no upper limit to the size of the halo confinement region for cosmic rays or to their mean total age. The required halo size can be made arbitrarily large by assuming a convection velocity approaching V_{\max} as shown in Fig. 5. Similarly the deduced mean total age can be increased by increasing the value of F , the ratio of the diffusion coefficient in the halo to that in the disk. The converse of this is that a lower limit to the halo size and total age is obtained under the assumption that there is no convection and $F = 1$. The four different total lifetime distributions shown in Fig. 4 are for sets of propagation parameters that all give $f_s = 0.14$ and $X = 6 \text{ g cm}^{-2}$. The minimum required halo size and mean total age are 7.8 kpc and 19 My respectively. The latter can be compared with the value of 19 My deduced using the homogeneous model.

From Fig. 2 it can be seen that, for a given grammage and value of F , what f_s does determine is the value of κ_0 , the effective diffusion coefficient in the disk. For example, for $f_s = 0.14$, $\kappa_0 \approx 9 \cdot 10^{28} \text{ cm}^2 \text{ s}^{-1}$ if $F = 1$; if $F = 10$, $\kappa_0 \approx 1.7 \cdot 10^{28} \text{ cm}^2 \text{ s}^{-1}$. Correspondingly the grammage determines the maximum allowed convection velocity. Provided that $f_s \lesssim 0.33$, $V_{\max} \approx 16 \text{ km s}^{-1}$ independent of any assumptions concerning F . It must be borne in mind, however, that V_{\max} is proportional to the column density of the galactic disk which is not known with great precision.

A quantity of interest when considering the origin of cosmic rays is the source power required to maintain their density in the galactic disk. If one defines a confinement time t_{con} as the ratio of equilibrium density at $z=0$ to source power, Eq. (B.7) gives

$$t_{\text{con}} = \frac{a^2}{\kappa_0} \left(\frac{1}{\varepsilon} + \frac{1}{2} \right). \quad (6.1)$$

It is closely related to the disk age, in fact

$$\frac{t_{\text{con}}}{\langle t_D \rangle} = \frac{\left(\frac{1}{\varepsilon} + \frac{1}{2} \right)}{\left(\frac{1}{\varepsilon} + \frac{1}{3} + \frac{\varepsilon}{24 + 12\varepsilon} \right)}. \quad (6.2)$$

Thus the ratio of confinement time to disk-age is practically independent of the propagation parameters; it varies from 1.0 when $\varepsilon \rightarrow 0$, corresponding to a very large halo, to 1.2 when $\varepsilon \rightarrow \infty$, corresponding to free escape at the disk boundary. The confinement time is essentially fixed by the observed grammage, regardless of the variation of any single propagation parameter. It might seem, for instance, that a larger convection velocity would require a greater source power but this is not so; an increase in V_0 demands an adjustment to κ_0 and y to keep the grammage as observed and there is practically no change in the source power requirements.

Before concluding one must consider whether a more complex propagation model than the one considered here is needed to explain all of the observed properties of the cosmic ray flux. In Sect. 3 it was mentioned that there is evidence for a truncation of the distribution of grammages for values $< 1 \text{ g cm}^{-2}$. The present model gives a distribution close to a simple exponential. There are essentially two ways to account for the absence of low grammages. The first is that the first 1 g cm^{-2} is built up within the sources themselves or in regions surrounding the sources that must be traversed by the cosmic ray particles before they enter the general interstellar medium. This would involve only a minor change to the present propagation model, i.e. the value of X , the mean grammage in the interstellar medium, should be reduced from 6 to 5 g cm^{-2} .

The second explanation requires the nearest source of cosmic rays to be at some appreciable distance from the sun. The present model has a continuous distribution of cosmic ray input in the disk but the sources could be discrete provided that the distance to the nearest source were small compared to the disk thickness. The assumption of more sparsely distributed sources destroys the symmetry upon which the one-dimensional propagation equation is based. An approximate result can be obtained by considering that a gap in the source distribution in the disk for $|z| < b$ corresponds to the nearest discrete source being at distance b from the sun. From Eq. (4.8) the disk-age probability distribution is found to be zero at $t_D = 0$, to rise to a maximum at $t_D \sim b^2/\kappa_0$ and then to decrease exponentially. Consideration of Eq. (4.11) for the case $V_0 = 0$, $F = 1$ shows that if the most probable grammage is to be 1/6 of the mean then

$$b^2 \approx \frac{a^2 y}{6}. \quad (6.3)$$

Since in this picture b cannot be greater than a , one requires $D < 600 \text{ pc}$. The source gap affects the ^{10}Be surviving fraction very little as the source function for secondary nuclei follows the equilibrium distribution of the parents. Such a small halo is clearly inconsistent with $f_s \approx 0.14$. The discrepancy is greater for a convective halo having a higher diffusion coefficient than the disk. In order that the source gap

distribution is

$$n(z, v) = \int_0^{\infty} P(z, t) \exp(-vt) dt \quad (\text{B.1})$$

because $\exp(-vt)$ is the probability that a particle which takes time t to reach z will survive. From this one can see that $n(z, v)$ is the Laplace Transform of $P(z, t)$. One can find the Inverse Laplace Transform of $n(z, v)$ by treating v as a complex variable.

First, the density distribution $n(z, v)$ is to be obtained. In the steady state

$$\frac{\partial^2 n}{\partial z^2} - V \frac{\partial n}{\partial z} - n \frac{\partial V}{\partial z} + \frac{1}{3} \frac{\partial V}{\partial z} \frac{\partial (Tn)}{\partial T} - nv + S = 0. \quad (\text{B.2})$$

With the values of κ , V , and s in the disk and halo as assumed in Sect. 2 this becomes

$$\frac{\partial^2 n}{\partial z^2} - \frac{nv}{\beta} + S_0 = 0 \quad |z| < a \quad (\text{B.3})$$

$$\text{and} \quad (\text{B.4})$$

$$\kappa_0 \frac{\partial^2 n}{\partial z^2} - \frac{V_0}{\beta} \frac{\partial n}{\partial z} - \frac{\mu nv}{\beta} = 0 \quad a < |z| < D.$$

Here, in order that the solution may have more general use later, the decay probability in the halo is taken to be μv ; for the disk-age calculation $\mu = 0$. As $\partial V / \partial z = V_0 \delta(z - a)$ and $n \propto T^{-\Gamma}$ there is a boundary condition

$$\kappa_0 \left(\frac{\partial n}{\partial z} \right)_{z=a-\Delta} = F \kappa_0 \left(\frac{\partial n}{\partial z} \right)_{z=a+\Delta} - \frac{n V_0}{\beta} \left(\frac{2+\Gamma}{3} \right) \quad (\text{B.5})$$

where Δ is an infinitesimal increment in z , in addition to the conditions that n is continuous at $z = a$ and $n = D$. Note that, for $\beta < 1$, $n \propto T^{-\Gamma}$ would be strictly true only for $V_0 = 0$. For a better approximation at $\beta = 0.65$ replace Γ in (B.5) by $\Gamma - 0.3$. The solution for $z < a$

$$n(z, v) = \frac{S_0 \beta}{v} \left\{ 1 - \frac{\left[\left(\frac{1+2\Gamma}{6} \right) \frac{V_0}{\beta \kappa_0} + F \xi \coth(\xi(D-a)) \right] \cosh \left(\left(\frac{z^2 v}{\beta \kappa_0} \right)^{1/2} \right)}{\left[\left(\frac{1+2\Gamma}{6} \right) \frac{V_0}{\beta \kappa_0} + \left(\frac{v}{\beta \kappa_0} \right)^{1/2} \tanh \left(\left(\frac{a^2 v}{\beta \kappa_0} \right)^{1/2} \right) + F \xi \coth(\xi(D-a)) \right] \cosh \left(\left(\frac{a^2 v}{\beta \kappa_0} \right)^{1/2} \right)} \right\} \quad (\text{B.6})$$

where

$$\xi = \left[\frac{\mu v}{F \beta \kappa_0} + \left(\frac{V_0}{2 F \beta \kappa_0} \right)^2 \right]^{1/2}.$$

For $v = 0$ this reduces to the steady-state distribution of stable, non-interacting particles,

$$n_0(z) \equiv n(z, v=0) = \frac{S_0 a^2}{\kappa_0} \left(\frac{1}{\varepsilon} + \frac{1}{2} - \frac{z^2}{2a^2} \right). \quad (\text{B.7})$$

With ε defined in Eq. (4.12).

For simplicity we shall obtain the disk-age distribution at $z = 0$. Set $\mu = 0$ in (B.6) then

$$n(0, v) \equiv n(v) = \frac{S_0 \beta}{v} \frac{\left[\frac{\varepsilon}{a} \left(\cosh \left(\left(\frac{a^2 v}{\beta \kappa_0} \right)^{1/2} \right) - 1 \right) + \left(\frac{v}{\beta \kappa_0} \right)^{1/2} \sinh \left(\left(\frac{a^2 v}{\beta \kappa_0} \right)^{1/2} \right) \right]}{\left[\frac{\varepsilon}{a} \cosh \left(\left(\frac{a^2 v}{\beta \kappa_0} \right)^{1/2} \right) + \left(\frac{v}{\beta \kappa_0} \right)^{1/2} \sinh \left(\left(\frac{a^2 v}{\beta \kappa_0} \right)^{1/2} \right) \right]}. \quad (\text{B.8})$$

Writing $v = x + iy$ the Inverse Laplace Transform of $n(v)$ is

$$P(t) = \frac{1}{2\pi i} \int_{x-i\infty}^{x+i\infty} n(v) \exp(vt) dv \quad (\text{B.9})$$

where x is such that the line of integration in the complex plane lies to the right of all poles. The standard technique of contour integration leads to

$$P(t) = \sum_m r_m \exp(v_m t) \quad (\text{B.10})$$

where v_m are the poles of $n(v)$ and r_m are the residues of $n(v)$ at v_m . As $P(t)$ is real and tends to zero as $t \rightarrow \infty$ one requires v_m to be real and < 0 . Thus, setting the denominator of (B.8) to zero and writing $v_m = -\alpha_m^2 \beta \kappa_0 / a^2$ gives the equation for the poles,

$$\tan(\alpha_m) = \varepsilon / \alpha_m. \quad (\text{B.11})$$

values r_m are found from their definition

$$n(v-v_m)n(v) = \frac{4S_0\beta \sin(\alpha_m)}{2\alpha_m + \sin(2\alpha_m)} \quad (\text{B.12})$$

$$\frac{4S_0\beta \sin(\alpha_m)}{2\alpha_m + \sin(2\alpha_m)} \exp\left(-\alpha_m^2 \frac{\beta \kappa_0}{a^2} t\right) \quad (\text{B.13})$$

apart from a constant multiplying factor, is identical to that derived in Sect. 4.1.

In a similar fashion the total age distribution can be derived if $\mu=1$ in Eq. (B.6) so that the “decay” is operative throughout the whole confinement region. Rewriting (B.6) for $z=0$ with $v = -u^2\beta\kappa_0/a^2$

$$\frac{S_0\beta \left[(\cos(u)-1) \left\{ \left(\frac{1+2\Gamma}{6} \right) \frac{q}{y\beta} + \frac{F\omega}{y-1} \cot(\omega) \right\} - u \sin(u) \right]}{v \cos(u) \left[\left(\frac{1+2\Gamma}{6} \right) \frac{q}{y\beta} + \frac{F\omega}{y-1} \cot(\omega) - u \tan(u) \right]} \quad (\text{B.14})$$

where y , and q are as defined in (4.17) and (4.21). It follows that the equation for the poles is (4.22) and the residues are given by

$$\frac{S_0\beta \sin(u_m)}{\sin(u_m) \cos(u_m) + u_m \cos^2(u_m) (y-1) [\operatorname{cosec}^2(\omega_m) - \cot(\omega_m)/\omega_m]} \quad (\text{B.15})$$

From (B.10) the total age distribution is as given in Sect. 4.3. This result can also be obtained via the Green’s Function for the time-dependent propagation equation.

Returning to Eq. (B.1), differentiate it with respect to v , then

$$= - \int_0^\infty t P(z, t) \exp(-vt) dt \quad (\text{B.16})$$

as $v \rightarrow 0$

$$\left. \frac{d}{dv} \right|_{v \rightarrow 0} = \int_0^\infty t P(z, t) dt = \langle t \rangle n_0(z) \quad (\text{B.17})$$

$n_0(z)$ is given by (B.7) and $\langle t \rangle$ is the mean age at z . Using (B.8) one obtains Eq. (4.11) for the mean disk-age at $z=0$ while (B.14) and (B.16) for the mean total age.

Appendix C: The Source Function of Secondary Nuclei

The surviving fraction of radio-active nuclei was calculated assuming a source function, for those nuclei, uniform throughout the disk. The radioactive nuclei are secondaries resulting from the spallation of primary heavier nuclei on the interstellar gas and their distribution is therefore the product of the gas distribution and the equilibrium density distribution of the parent nuclei. We assume the former to be uniform throughout the disk but the density of the latter decreases towards the disk boundaries in a manner dependent upon the propagation parameters adopted. The calculated surviving fraction is therefore not completely consistent with our earlier results. The degree of approximation involved is investigated here.

From Eq. (B.7) it can be seen that the equilibrium density of non-interacting stable nuclei varies across the galactic disk as

$$\frac{2 + \epsilon[1 - (z/a)^2]}{2 + \epsilon} \quad (\text{C.1})$$

If the observed surviving fraction of ^{10}Be is indeed ~ 0.14 then one requires $\epsilon \ll 1$ (the precise value depends on the assumed value of F ; for $F=1$, $\epsilon \sim 0.01$) and the uniform source function is a good approximation.

The maximum variation of the source function occurs for the case of free escape at the disk boundary, corresponding to $\epsilon \rightarrow \infty$ in which case the parent nuclei have a finite interaction length, A_p , and Eq. (B.6), for $D=a$, leads to

$$\frac{\cosh(a/a_0) - \cosh(z/a_0)}{\cosh(a/a_0) - 1} \quad (\text{C.2})$$

where $a_0 = [(A_p \kappa_0)/(c \rho m_H)]^{1/2}$. The parent nuclei of ^{10}Be are mainly C, N, and O for which $A_p \sim 6.3 \text{ g cm}^{-2}$. For a grammage of 6 g cm^{-2} the free escape at the disk boundary $\kappa_0 = 4.6 \cdot 10^{26} \text{ cm}^2 \text{ s}^{-1}$ so that $a_0 \sim 63 \text{ pc}$. Substituting this in (C.2) one obtains a z -distribution close to that for non-interacting particles, i.e. proportional to $[1 - (z/a)^2]$.

With a source function for radioactive nuclei varying with z in this manner and $D=a$ one obtains

$$= \frac{\sum_{n=1}^{\infty} (-1)^{n-1} \left\{ (2n-1)^3 \left[A_r^{-1} + A_i^{-1} + \frac{5}{48X} (2n-1)^2 \pi^2 \right] \right\}^{-1}}{\sum_{n=1}^{\infty} (-1)^{n-1} \left\{ (2n-1)^3 \left[A_i^{-1} + \frac{5}{48X} (2n-1)^2 \pi^2 \right] \right\}^{-1}}$$

which gives $f_s = 0.555$ for $\beta = 0.65$. The value obtained for $D=a$ from (5.7), which assumes a uniform source function, is $f_s = 0.542$. It can be seen that, even in the limiting case, the assumption of a uniform source function for the radioactive nuclei has a negligible effect on f_s .

References

- Ohlin, R.C., Savage, B.D., Drake, J.F.: 1978, *Astrophys. J.* **224**, 132
 Pringle, C., French, D.K., Osborne, J.L.: 1978, *Monthly Notices Roy. Astron. Soc.* **184**, 283
 Ruffington, A., Orth, C.D., Mast, T.S.: 1978, *Astrophys. J.* **226**, 355
 Burton, W.B., Gordon, M.A.: 1976, *Astrophys. J. Letters* **207**, L189
 Montes, P., Meyer, J.P., Perron, C.: 1977, Proc. 15th Int. Cosmic Ray Conf., Plovdiv, **2**, 234
 Garcia-Munoz, M., Mason, G.M., Simpson, J.A.: 1977a, *Astrophys. J.* **217**, 859
 Garcia-Munoz, M., Mason, G.M., Simpson, J.A.: 1977b, Proc. 15th Int. Cosmic Ray Conf., Plovdiv, **1**, 224
 Miller, M., Wdowczyk, J., Wolfendale, A.W.: 1977, *J. Phys. A* **10**, 843
 Miller, M., Wdowczyk, J., Wolfendale, A.W.: 1978, *J. Phys. A* **11**, 199
 Eagen, F.A., Fisher, A.J., Ormes, J.F.: 1977, *Astrophys. J.* **212**, 262
 Jokipii, J.R.: 1976, *Astrophys. J.* **208**, 900
 Jones, F.C.: 1979, *Astrophys. J.* **229**, 747
 Owens, A.J., Jokipii, J.R.: 1977, *Astrophys. J.* **219**, 677
 Trisic, V.L., Ptuskin, V.S.: 1975, *Astrophys. Space Sci.* **32**, 265
 Radhakrishnan, V., Murray, J.D., Lockart, P., Whittle, R.P.J.: 1972, *Astrophys. J. Supp. Ser.* **24**, 15
 Saisbeck, G.M., Yiou, F.: 1977, Proc. 15th Int. Cosmic Ray Conf., Plovdiv, **2**, 203
 Webber, W.R., Lezniak, J.A., Kish, J.C., Simpson, G.A.: 1977, *Astrophys. Letters* **18**, 125

Note added in proof: In Appendix B the fourth term in Eq. (B2) representing convective energy loss is correct only for $\beta \rightarrow 1$. In general T_n should be multiplied by a factor $\alpha = 1 + (1 - \beta^2)^{1/2}$. To take account of this the spectral slope, Γ , in Eqs. (B5), (B6), (4.12), and (4.22) should be replaced by $\alpha(\Gamma - 1) + 1$. When the flattening of the spectrum for $\beta < 1$, mentioned in Appendix B, is also taken into account the net effect is that the value of V_{\max} deduced for $\beta = 0.65$ should be reduced from 16.2 km s^{-1} to 14.2 km s^{-1} .

CAN COSMIC RAYS BE ACCELERATED IN COLLAPSING MOLECULAR CLOUDS?

Y.A. Dogiel, Lebedev Physical Institute, Moscow;
 P. Kiraly, Central Research Institute, Budapest;
 I. Freedman and A.W. Wolfendale, Department of Physics,
 University of Durham.

ABSTRACT

An interesting observation (Wolfendale, 1983) is that with contemporary data on the numbers and masses of giant molecular clouds (GMC) in the Galaxy the gravitational energy given out during collapse is of the order of that required to furnish the observed cosmic ray energy spectrum. Coupled with the fact that some GMC appear to give more γ -rays than would be expected using the ambient cosmic ray intensity there is the possibility that cosmic rays are accelerated during cloud collapse. The present paper examines this probability.

1. Introduction

The relevance of GMC to cosmic ray physics is manifold. As important components of the I.S.M. they should contribute to the grammage if they can be penetrated by cosmic rays (observations on the GMC in Orion, Wolfendale, 1981, Caraveo, 1981 suggest that they can). Cosmic rays might then provide the most important ionizing agents in the dense central parts of the clouds. Gamma ray production by the interactions of CR with the gas in the I.S.M. might then simulate γ -ray sources (e.g. Li and Wolfendale, 1982). Supernova explosions in GMC could contribute to the \bar{p} flux (Eichler, 1982). Finally, there is the possibility, referred to in the Abstract that a significant fraction of the cosmic rays might have received their acceleration in the clouds. It is the last mentioned topic which is of concern here.

2. Cosmic Rays in Collapsing GMC

It is highly likely that star formation occurs as an end result of the collapse of a GMC but the details of the stages in between are the subject of fierce debate. The maximum possible cosmic ray enhancement will occur if we imagine that the particles are trapped when contraction starts (the trapping being due to magnetic fields) and that an implosion caused by an external shock wave, induces the contraction. In this case we might have a 'negative escape velocity' at $t = 0$, i.e. the sum of the kinetic and potential energies is zero.

The motion of the surface of the cloud, assumed spherical, can be written as

2.

$\ddot{R}(t) = -GM/R(t)^2$ where $R(t)$ is the cloud radius at time t and M is the cloud mass. There follows

$\dot{R}(t)^2 = 2GM/R(t) - A$ where A is obtained from the initial condition at time $t = 0$. Here we have $A = 0$ and $\dot{R}(0) = -\sqrt{2GM/R(0)}$, yielding $R(t) = (1-t/t_c)^{2/3} R(0)$; where $t_c = \frac{\sqrt{2}}{3} \sqrt{R(0)^3/GM}$.

Working now in units of mass $M \cdot 2 \cdot 10^{38} \text{ g}$ and distance $R \cdot 10^{20} \text{ cm}$ we have $t_c \approx R^{3/2} M^{-1/2} \cdot 1.3 \cdot 10^{14} \text{ s}$, the cloud density is $\rho = MR^{-3} \cdot 5 \cdot 10^{-23} \text{ g cm}^{-3} \approx 30 MR^{-3} \text{ atoms cm}^{-3}$.

The characteristic grammage for CR propagation obtained from ρ and the collapse time is

$$\lambda = t_c c \rho \approx 200 R^{-3/2} M^{1/2} \text{ g cm}^{-2}.$$

The energy density is $\approx 2.5 M^2 R^{-4} \text{ eV cm}^{-3}$.

The attenuation grammage of cosmic ray nuclei due to nuclear interactions for an energy spectrum of differential exponent $\beta = 2.5$ is $\approx 105 \text{ g cm}^{-2}$ so that for the value of λ given above it is clear that energy losses may well be important.

The extent to which losses are offset by adiabatic gains is not immediately obvious and needs consideration. If losses could be neglected, the total number of CR in the cloud in a specified relativistic energy range would increase by adiabatic compression as $R(t)^{-(\beta-1)}$ i.e. as $R(t)^{-1.5}$ for $\beta = 2.5$. The fractional gain per unit time follows as

$$R(t)^{1.5} \frac{d}{dt} [R(t)^{-1.5}] = 7.7 \times 10^{-15} (1 - t/t_c)^{-2/3} \text{ s}^{-1}$$

for the collapse of a typical cloud ($M = R = 1$). The loss is given by $\frac{c\rho(t)}{\lambda_a} = 1.5 \times 10^{-14} (1 - t/t_c)^{-2} \text{ s}^{-1}$.

The ratio of loss/gain is $\approx 2(1-t/t_c)^{-4/3}$ and increases from 2 as the collapse occurs.

Taken at its face value, the above result indicates that losses predominate over acceleration and the ambient CR intensity falls with time rather than rises. The collapsing cloud hypothesis for CR origin, or as an explanation of γ -ray sources, therefore appears untenable in its present form and major modification is necessary if it is to survive. Modification can be considered in two forms - a minor variant, in which interaction losses are minimised during the acceleration phase and a major variant, in which subsequent further collapse into the star formation phase is included. The latter is considered in a later section.

Returning to the energetics of cloud collapse, Wolfendale (1983) quoted a total gravitational energy liberated in GMC collapse of $\sim 10^{40} \text{ erg s}^{-1}$. Now this is already somewhat less (by $\approx 3-10$) than required to explain the bulk of the cosmic ray energy so that, with the inevitable significant energy losses, it does look as though clouds collapsing to the typical sizes seen do not provide the bulk of the cosmic ray energy. The requirements for some γ -ray sources to be explained in this way are much less severe, however, probably by a factor 100, and the hypothesis may still have value here. The problem is to keep the particles away from the matter in the initial collapse phase - we have so far assumed that the cloud has uniform density - and this appears to be not impossible. Granulation of the material in the clouds is a well known feature of actual clouds and this could play an important part in providing the necessary factor of increase of, say, an order of magnitude in the gain/loss rate for a fraction of the clouds. Further work is necessary on this aspect.

3. Enhanced production of CR in GMC

Some of the gas in GMC continues to collapse and eventually forms stars whereby further gravitational energy is released. Cosmic rays are presumably accelerated in this processes, to some extent, at least.

The gravitational potential energy of a typical cloud of $M = 1$, $R = 1$ is $\sim 3 \times 10^{49} \text{ erg}$ and if 1% of the gas forms stars (a typical value) their potential energy is $\approx 7 \times 10^{51} \text{ ergs}$. Thus, if only a few percent of this energy finds its way into cosmic rays during collapse and if these particles are trapped in the cloud a γ -ray 'source' will result.

A bonus occurs at a later stage when stellar winds are formed and essentially nuclear energy is transformed into mechanical energy. A number of workers have considered the specific cases of Wolf-Rayet stars and OB associations (e.g. Montmerle, 1979, 1981). The energetics here again are of the right order to explain the whole cosmic ray energy generation only if virtually all the mechanical energy is transformed into cosmic rays (Wolfendale, 1983); a much more likely situation, once more, is that a few per cent is thereby transformed leading to a partial contribution to the CR budget but more particularly allowing the explanation of a number of γ -ray sources (e.g. Eta Carina).

Eta Carina itself can be considered in detail, following Montmerle (1981) who identified it with the γ -ray source 2CG 288-00 (one of the 25 sources reported by the COS B collaboration; Swanenburg et al., 1978). This source probably represents the best example at present for the suggested mechanism. Issa et al., (1981) have also examined the source and they estimate that an enhancement in cosmic ray intensity by a factor ~ 12 is needed, if the adopted mass of the complex is correct. Montmerle invokes a rather complex mechanism in which protons are accelerated by stellar winds and then confined by resonant Alfvén-wave scattering in an associated giant HII region. The total mechanical power of the stellar winds for the Carina complex is

estimated by Montmerle to be $P_w \approx 5 \times 10^{38} \text{ erg s}^{-1}$ so that in a typical cloud lifetime of 10^7 y the energy output will be $\approx 10^{53} \text{ erg}$, somewhat higher than the $7 \times 10^{51} \text{ ergs}$ referred to earlier. Montmerle derives a proton acceleration efficiency of 4% for the mechanism concerned and this must be multiplied by the trapping efficiency. The latter is made to be high by invoking the resonant Alfvén-wave scattering referred to and it is seen that we are back to an overall CR efficiency of a percent or so, as required.

A relevant point to note in connection with Montmerle's model is the need to have both strong mass-losing stars and strongly ionizing stars together; the author points out that perhaps only two regions exist in the Galaxy where the necessary conditions prevail. This would again confirm our view that only γ -ray sources - and only a fraction of them, at that, are likely to be due to the invoked mechanism.

Finally, brief mention can be made of supernovae, at least from the standpoint of SN associated with GMC. Two situations, at least, can be invoked - the first where an exterior SN produces a shock which accelerates the collapse of a GMC (see §2) and the second where a SN occurs inside the GMC and CR, accelerated in the shock, or by the associated pulsar, interact with the local gas. There is, as usual, the observation that the total mechanical energy involved is of the order of that required to explain the observed CR energies, and also the fact that acceleration efficiency is probably only $\sim 1\%$. The probability of finding SN within GMC and the behaviour of the shock in such a high density medium is very uncertain but the likelihood of this mechanism too being important, at least for γ -ray sources, is strong.

References

- Caraveo, P., 1981, Phil. Trans. R. Soc. A 301, 569.
 Eichler, D., 1982, Nature, 295, 391.
 Issa, M.R., et al., 1981, Proc. 17th I.C.R.C., 1, 150.
 Li, T.P. and Wolfendale, A.W., 1982, Astron. Astrophys., 116, 95.
 Montmerle, Th., 1979, Ap.J., 231, 95; 1981, Phil. Trans. R. Soc., A301, 505.
 Swanenburg, B.N. et al., 1978, Nature, 275, 298.
 Wolfendale, A.W., 1981, IUPAP/IAU Symp. 94 (Reidel, Dordrecht), 309;
 1983, Milne Lecture, Q. J. Roy. Astr. Soc. (in press).

